



저작자표시-비영리-변경금지 2.0 대한민국

이용자는 아래의 조건을 따르는 경우에 한하여 자유롭게

- 이 저작물을 복제, 배포, 전송, 전시, 공연 및 방송할 수 있습니다.

다음과 같은 조건을 따라야 합니다:



저작자표시. 귀하는 원저작자를 표시하여야 합니다.



비영리. 귀하는 이 저작물을 영리 목적으로 이용할 수 없습니다.



변경금지. 귀하는 이 저작물을 개작, 변형 또는 가공할 수 없습니다.

- 귀하는, 이 저작물의 재이용이나 배포의 경우, 이 저작물에 적용된 이용허락조건을 명확하게 나타내어야 합니다.
- 저작권자로부터 별도의 허가를 받으면 이러한 조건들은 적용되지 않습니다.

저작권법에 따른 이용자의 권리는 위의 내용에 의하여 영향을 받지 않습니다.

이것은 [이용허락규약\(Legal Code\)](#)을 이해하기 쉽게 요약한 것입니다.

[Disclaimer](#)

Dissertation for the Degree of Doctor of Philosophy

Effects of Angiotensin Receptor Blocker and
Dapagliflozin on Blood Pressure Control,
Vascular and Renal Function

Yoon-A Jeon

Department of Veterinary Medicine

The Graduate school

Jeju National University

August 2023

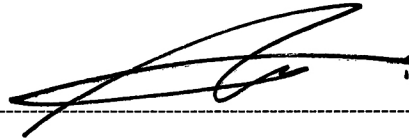
Effects of Angiotensin Receptor Blocker and Dapagliflozin on Blood Pressure Control, Vascular and Renal Function

A dissertation submitted to the graduate school of
Jeju National University in partial fulfillment of
the requirements for the degree of Doctor of
Philosophy in Veterinary Medicine
under the supervision of **Young Jae Lee**

The dissertation for the degree of Doctor of Philosophy
by **Yoon-A Jeon**
has been approved by the dissertation committee.

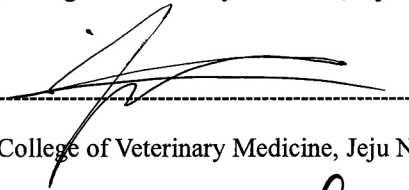
June 2023

Chair



Professor, ChangHwan Ahn, College of Veterinary Medicine, Jeju National University

Member



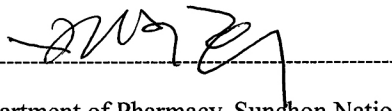
Professor, Gee-Euhn Choi, College of Veterinary Medicine, Jeju National University

Member



Professor, Chang-Hoon Han, College of Veterinary Medicine, Jeju National University

Member



Professor, Soo-Heui Paik, Department of Pharmacy, Sunchon National University

Member



Professor, Young-Jae Lee, College of Veterinary Medicine, Jeju National University

Table of contents

List of Tables.....	viii
List of Figures	ix
List of Supplementary Figures	xiii
ABSTRACT.....	1
INTRODUCTION	4
1. Hypertension and Diabetes	4
1.1. Hypertension.....	4
1.2. Renin-angiotensin-aldosterone system	6
1.3. Diabetes mellitus	8
2. Endothelial dysfunction and inflammation	1 1
3. ARBs and SGLT2 inhibitors	1 5
3.1. Angiotensin receptor type 1 blocker.....	1 5
3.2. SGLT2 inhibitor.....	1 9
4. Objective.....	2 3

Part 1. Enhancement of ARB by Dapagliflozin: Blood Pressure Regulation in SHR.....	2 4
1-1. Materials and methods	2 5
1-1.1. Materials and experimental animals.....	2 5
1-1.2. Blood pressure measurement	2 6
1-1.3. Experimental groups	2 7
1-1.4. Measuring vascular relaxation	2 8
1-1.5. Cell culture.....	2 9
1-1.6. Protein Analysis	2 9
1-1.7. Molecular docking	3 0
1-1.8. Statistical analysis	3 2
1-2. Results.....	3 3
1-2.1. Blood pressure.....	3 3
1-2.2. Interaction with angiotensin receptor type 1	4 0
1-2.3. Vasorelaxation.....	4 2

1-2.4. Combination with hydrochlorothiazide.....	4 5
1-3. Discussion.....	4 9
Part 2. Vascular Protection of ARB and Dapagliflozin	5 5
2-1. Materials and methods	5 6
2-1.1. Materials and experimental animals.....	5 6
2-1.2. Experiment.....	5 6
2-1.3. Measuring vasorelaxation	5 6
2-1.4. Cell culture.....	5 7
2-1.5. Nitrite measurement.....	5 8
2-1.6. Reporter gene assay	5 8
2-1.7. ROS generation.....	5 8
2-1.8. Protein Analysis	5 9
2-1.9. Statistical analysis.....	6 0
2-2. Results.....	6 1

2-2.1.	Endothelium-dependent vasorelaxation	6	1
2-2.2.	NOX/ROS and Nrf2	6	5
2-2.3.	Regulation of Inflammatory Pathways.....	7	4
2-2.4.	Regulation of autophagy	8	6
2-3.	Discussion.....	9	5
Part 3. Enhancement of Dapagliflozin by ARB: Hyperglycemia, SGLT2, and NHE-1.		1	0 4
3-1.	Materials and methods	1	0 5
3-1.1.	Materials and experimental animals.....	1	0 5
3-1.2.	Experiment.....	1	0 5
3-1.3.	Urine and blood analysis.....	1	0 6
3-1.4.	Organ weight.....	1	0 7
3-1.5.	ACHN cells.....	1	0 7
3-1.6.	Protein analysis	1	0 7
3-1.7.	Molecular docking	1	0 8

3-1.8. Statistical analysis	1 0 8
3-2. Results.....	1 0 9
3-2.1. SGLT2.....	1 0 9
3-2.2. NHE-1	1 1 9
3-3. Discussion.....	1 2 5
CONCLUSION	1 3 4
SUPPLEMENTARY DATA.....	1 3 9
REFERENCES.....	1 5 6
국문 초록.....	1 7 5

List of Tables

Table 1. Pharmacokinetic characteristics of ARBs.	1	5
Table 2. Pharmacokinetic characteristics SGLT2 inhibitors.	2	1
Table 3. Binding affinities of angiotensin receptor type 1 with ARBs and dapagliflozin. .	4	1
Table 4. Interactions of angiotensin receptor type 1 with angiotensin-II, ARBs and dapagliflozin.	4	1
Table 5. Binding affinity and interactions of sodium-glucose cotransporter 2 with ARBs and dapagliflozin.	1	1 8

List of Figures

Figure 1. Classification of hypertension stages.....	5
Figure 2. The renin-angiotensin-aldosterone system and target of anti-hypertensive drugs..	7
Figure 3. Interactions of hypertension and diabetes mellitus.....	1 0
Figure 4. Various signaling pathways associated with vascular endothelial dysfunction..	1 4
Figure 5. The distribution and function of renal sodium-glucose cotransporters.....	2 0
Figure 6. The experimental groups and the experimental schedule.	2 7
Figure 7. Myography system for measuring the vascular reactivity.	2 9
Figure 8. Structures of angiotensin receptor type 1 obtained from Protein Data Bank.....	3 1
Figure 9. Structures of dapagliflozin, fimasartan, telmisartan, candesartan, and angiotensin-II obtained from PubChem.	3 1
Figure 10. Effects of dapagliflozin and ARBs on systolic blood pressure of SHR.....	3 6
Figure 11. Effects of dapagliflozin combined administration with ARBs on systolic blood pressure of SHR.	3 9
Figure 12. Effects of vasorelaxation and eNOS activation of ARBs and dapagliflozin.....	4 4
Figure 13. Effects of dapagliflozin, hydrochlorothiazide, and telmisartan on systolic blood pressure and water intake.....	4 8

Figure 14. The anti-hypertensive effects of dapagliflozin and ARBs.	5 4
Figure 15. Effects of ARBs and dapagliflozin on acetylcholine-induced vasorelaxation in the aorta of aged SHR.	6 3
Figure 16. Effects of fimasartan and dapagliflozin on NOX/ROS and Nrf2 in the aorta of aged SHR and L/CM treated EA. hy926 cells.	6 6
Figure 17. Effects of telmisartan and dapagliflozin on NOX/ROS and Nrf2 in the aorta of aged SHR and L/CM treated EA. hy926 cells.	6 9
Figure 18. Effects of candesartan and dapagliflozin on NOX/ROS and Nrf2 in the aorta of aged SHR and L/CM treated EA. hy926 cells.	7 2
Figure 19. Effects of fimasartan and dapagliflozin on inflammatory molecules in the aorta of aged SHR and L/CM treated EA. hy926 cells.	7 5
Figure 20. Effects of telmisartan and dapagliflozin on inflammatory molecules in the aorta of aged SHR and L/CM treated EA. hy926 cells.	7 7
Figure 21. Effects of candesartan and dapagliflozin on inflammatory molecules in the aorta of aged SHR and L/CM treated EA. hy926 cells.	7 9
Figure 22. Effects of fimasartan and dapagliflozin on inflammatory molecules in the Raw264.7 cells.	8 1
Figure 23. Effects of telmisartan and dapagliflozin on inflammatory molecules in the Raw264.7 cells.	8 3
Figure 24. Effects of candesartan and dapagliflozin on inflammatory molecules in the	

Raw264.7 cells.....	8 5
Figure 25. Effects of fimasartan and dapagliflozin on autophagy in aorta of aged SHR and L/CM treated EA. hy926 cells.	8 8
Figure 26. Effects of telmisartan and dapagliflozin on autophagy in aorta of aged SHR and L/CM treated EA. hy926 cells.	9 1
Figure 27. Effects of candesartan and dapagliflozin on autophagy in aorta of aged SHR and L/CM treated EA. hy926 cells.	9 4
Figure 28. The vasoprotective effects of dapagliflozin and ARBs.....	1 0 3
Figure 29. A schematic diagram of the experimental group and the experimental schedule.	1 0 6
Figure 30. Structure of SGLT2 obtained from Protein Data Bank.....	1 0 8
Figure 31. Effects of fimasartan and dapagliflozin on glucose/sodium and SGLT2 in aged SHR.	1 1 1
Figure 32. Effects of telmisartan and dapagliflozin on glucose/sodium and SGLT2 in aged SHR.....	1 1 4
Figure 33. Effects of candesartan and dapagliflozin on glucose/sodium and SGLT2 in aged SHR.....	1 1 6
Figure 34. Effects of fimasartan and dapagliflozin on renal NHE-1 expression and proteinuria in aged SHR.	1 2 0

Figure 35. Effects of telmisartan and dapagliflozin on renal NHE-1 expression and proteinuria in aged SHR.....	1 2 2
Figure 36. Effects of candesartan and dapagliflozin on renal NHE-1 expression and proteinuria in aged SHR.....	1 2 4
Figure 37. The glucose/sodium regulation and renoprotective effects of dapagliflozin and ARBs.....	1 3 3
Figure 38. The effects of ARBs and dapagliflozin on blood pressure control, vascular and renal function.....	1 3 8

List of Supplementary Figures

Supplementary Figure 1. Effects of fimasartan and dapagliflozin on heart rate, body weight, and water intake in SHR.	1 3 9
Supplementary Figure 2. Effects of telmisartan and dapagliflozin on heart rate, body weight, and water intake in SHR.	1 4 0
Supplementary Figure 3. Effects of candesartan and dapagliflozin on heart rate, body weight, and water intake in SHR.	1 4 1
Supplementary Figure 4. The binding interaction of angiotensin receptor type1 and angiotensin-II.....	1 4 2
Supplementary Figure 5. The binding interaction of angiotensin receptor type1 and dapagliflozin.	1 4 3
Supplementary Figure 6. The binding interaction of angiotensin receptor type1 and fimasartan	1 4 4
Supplementary Figure 7. The binding interaction of angiotensin receptor type1 and telmisartan	1 4 5
Supplementary Figure 8. The binding interaction of angiotensin receptor type1 and candesartan	1 4 6
Supplementary Figure 9. Cell viability of ARBs and dapagliflozin treated EA. hy926 cells.	1 4 7
Supplementary Figure 10. Effects of ARBs and dapagliflozin on p38MAPK expression in aged	

SHR.....	1 4 8
Supplementary Figure 11. Effects of ARBs and dapagliflozin on Water intake, food intake and body weight in aged SHR.....	1 4 9
Supplementary Figure 12. Effects of ARBs and dapagliflozin on organ index in aged SHR.	1 5 0
Supplementary Figure 13. The binding interaction of SGLT2 and dapagliflozin.....	1 5 1
Supplementary Figure 14. The binding interaction of SGLT2 and fimasartan.....	1 5 1
Supplementary Figure 15. The binding interaction of SGLT2 and telmisartan.....	1 5 2
Supplementary Figure 16. The binding interaction of SGLT2 and candesartan.....	1 5 2
Supplementary Figure 17. Effects of ARBs and dapagliflozin on SGLT2 and NHE-1 expression in ACHN cells.....	1 5 3
Supplementary Figure 18. Effects of ARBs and dapagliflozin on NHE-1 expression in aorta of aged SHR.....	1 5 4
Supplementary Figure 19. Effects of ARBs and dapagliflozin on NHE-1 expression in heart of aged SHR.....	1 5 5

ABSTRACT

Effects of Angiotensin Receptor Blocker and Dapagliflozin on Blood Pressure Control, Vascular and Renal Function

Yoon-A Jeon

Department of Veterinary Medicine

The Graduate school

Jeju National University

Hypertension and diabetes are chronic conditions that share various complications and frequently cooccur. In clinical stages, monotherapy is insufficient to control blood pressure and blood glucose depending on the severity of symptoms, and combination therapy is used. Nevertheless, numerous challenges exist, including drug-induced disruptions in glucose metabolism or ionic imbalances and vascular and renal dysfunctions that remain unmitigated by controlling blood glucose and blood pressure. Given these unresolved challenges, we investigated the potential of a novel combination: an angiotensin receptor blocker (ARB) used as a primary hypertension treatment and a sodium-glucose cotransporter 2 inhibitor (SGLT2 inhibitor) used in diabetes treatment. Both agents are well known for potent anti-inflammatory and renoprotective effects, and they possibly have the counteraction effects on glucose

imbalance induced by ARBs and elevation of the renin-angiotensin-aldosterone system (RAAS) instigated by SGLT2 inhibition. Therefore, our research aimed to compare the effects of ARBs on blood pressure, vascular function, and renal outcomes when monotherapy and combined with dapagliflozin. Our study measured blood pressure, vascular function, blood glucose levels, and renal injury indices, including sodium-hydrogen exchanger-1 (NHE-1) and urinary protein, following a short-term administration of drugs in spontaneously hypertensive rats (SHR). Furthermore, to elucidate the mechanism underlying the improvement of vascular function, evaluated the expression of molecules associated with inflammation, oxidative stress, and autophagy in EA. hy926 cells exposed to low-grade inflammation and aortic tissue of aged SHR. Consequently, dapagliflozin synergistically enhanced the blood pressure regulatory effects of fimasartan and telmisartan, resulting in a more significant reduction in blood pressure and prolonged maintenance of the achieved levels. The combination of telmisartan with dapagliflozin also exhibited a synergistic effect on glucose and sodium excretion through common inhibition of SGLT2; however, it led to increased renal NHE-1 expression compared to the group treated with telmisartan alone. Fimasartan and candesartan exhibited an augmented acetylcholine response in the aorta by activating autophagy, inhibiting inflammation, and reducing oxidative stress. Moreover, this enhancement was further potentiated through co-administration with dapagliflozin. Fimasartan and candesartan also demonstrated a reduction in NHE-1 expression and proteinuria, indicating the renoprotective effects of these drugs. In summary, the combination of telmisartan with dapagliflozin shows the most pronounced effects in lowering blood pressure and blood glucose levels; however, potential side effects can be exercised when using this combination due to overlapped mechanisms of SGLT2 inhibition. The combination of candesartan and dapagliflozin demonstrated superior vascular and renal protection; however, it exhibited fewer synergies in reducing blood pressure than other ARBs. The combination of fimasartan and dapagliflozin

showed synergistic effects in reducing blood pressure and enhancing vascular and renal protection; these findings indicate the strength of this combination as a multifaceted therapeutic approach for managing hypertension and diabetes. As our results are derived from a short-term preclinical trial, further investigations are required to fully comprehend the interplay between the two drugs and potential side effects. Despite this, results show that the combination of ARB and SGLT2 inhibitors can be used as various selections contingent upon individual characteristics, and it may serve as a novel alternative, providing substantial advantages not only in managing blood pressure and blood glucose but also imparting vascular and renal protection.

INTRODUCTION

1. Hypertension and Diabetes

1.1. Hypertension

Hypertension is a debilitating condition characterized by uncontrolled high blood pressure. Diagnostic criteria for hypertension typically involve a systolic blood pressure (SBP) of 140 mmHg or higher and a diastolic blood pressure of 90 mmHg or higher [1] (Figure 1). Hypertension can be categorized into two types: essential and secondary hypertension. Essential hypertension accounts for over 90% of cases [2]. Hypertension affects approximately 25% of the global adult population, and management is complex due to its multifactorial involving the heart, blood vessels, kidneys, and central nervous system [3]. While the exact cause of hypertension is challenging to ascertain, it is influenced by genetic factors and lifestyle, including a high-salt diet, smoking, alcohol consumption, and stress [4, 5]. In genetics, essential hypertension is strongly associated with the angiotensinogen and angiotensin-converting enzyme (ACE) genes [4, 6]. Initially, hypertension is often asymptomatic. However, management and treatment are highly recommended because as it progresses, it can lead to severe complications such as cardiac hypertrophy, stroke, heart failure, atherosclerosis, renal dysfunction, and diabetes [7, 8].

The treatment of hypertension involves various drug classes, including beta-receptor blockers, calcium channel blockers (CCBs), diuretics, renin-angiotensin-aldosterone system (RAAS) inhibitors, and vasodilators [9, 10]. The drug and dosage selection depends on the individual's heart, kidney, and cerebrovascular disease risk factors. Generally, to minimize the risk of side effects, recommended to initiate treatment with a low dose of monotherapy [9]. However, due to the complexity of hypertension, monotherapy has limitations in controlling the progression

and severity of the condition. Consequently, approximately 75% of patients with stage 2 hypertension require combination therapy involving two or more drugs to achieve the target BP [11].

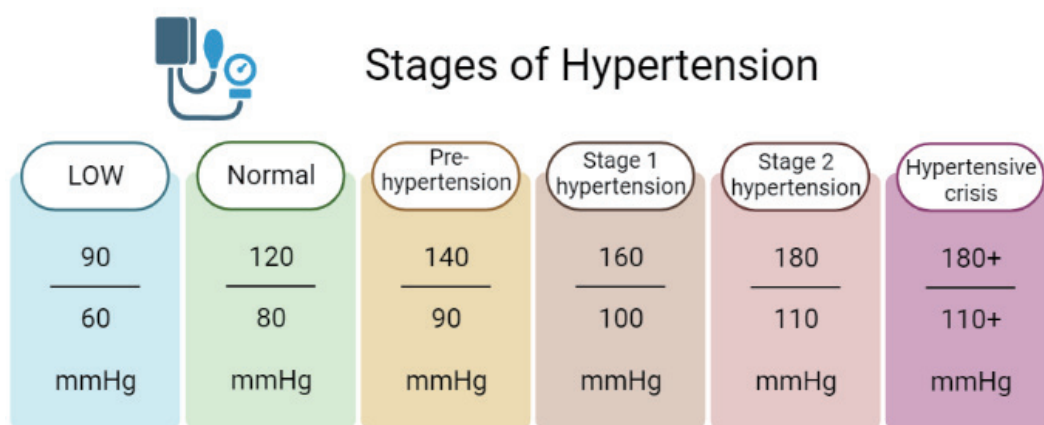


Figure 1. Classification of hypertension stages.

Classification of hypertension stages according to the '2017 Guideline for the Prevention, Detection, Evaluation, and Management of High Blood Pressure in Adults' by 'The American College of Cardiology' (ACC) / 'The American Heart Association' (AHA).

1.2. Renin-angiotensin-aldosterone system

The RAAS is a critical regulatory mechanism that maintains systemic blood pressure by regulating ECV [12, 13] (Figure 2). When the baroreceptors detect a decrease in renal arterial pressure and sodium content, renin secretion is stimulated, leading to the angiotensinogen being cleaved to angiotensin-I (Ang1) [14, 15]. Ang1 is subsequently converted to angiotensin-II (Ang2) by ACE and binds to receptors to exert various functions [16]. The Ang2 receptor is a G-protein-coupled receptor with seven transmembrane domains, and clinically significant isoforms include angiotensin receptor type 1 (AT1) and type 2 (AT2) [17]. Upon binding of Ang2 to AT1 receptors, it induces smooth muscle contraction, stimulates sodium channels in the renal proximal tubule, and stimulates the secretion of aldosterone and vasopressin in the adrenal cortex [18, 19]. Aldosterone promotes sodium reabsorption in the collecting duct, and vasopressin increases blood pressure by preserving body fluid volume through water reabsorption [20, 21]. Like this, RAAS plays a central role in regulating blood pressure; however, excessive activation can lead to hypertension and its severe complications, such as cardiovascular diseases, diabetes, kidney diseases, and even neurodegenerative diseases [22, 23].

Excessive RAAS also associated with chronic inflammation and oxidative stresses. Ang2 stimulates the production of reactive oxygen species (ROS) by increasing the activity of nicotinamide adenine dinucleotide phosphate (NADPH) oxidase (NOX), leading to the generation of inflammatory mediators [22, 24, 25]. Additionally, uncontrolled Ang2 disrupts the physiological regulation of water, sodium, and potassium homeostasis through excessive aldosterone production [26]. Indeed, primary aldosteronism, accompanied by hypokalemia, is the most common cause of secondary arterial hypertension [24, 27]. At the vascular level, excessive aldosterone also stimulates endothelial dysfunction, infiltration of inflammatory

cells, and atherosclerotic plaque development [26, 27]. Consequently, several antihypertensive drugs are being developed to inhibit excessive activation of the RAAS. However, it is essential to note that RAAS inhibitors, including ACE inhibitors, angiotensin receptor blockers (ARB), aldosterone receptor antagonists, and direct renin inhibitors, carry an increased risk of hyperkalemia (serum potassium > 5.5 mmol/L), particularly in patients with chronic Renal failure [28, 29]. The reported incidence rate of hyperkalemia with ACE inhibitors or ARB-treated patients is up to 10% [28]. Therefore, when initiating therapy with a RAAS inhibitor, must be considered to glomerular filtration rate, serum potassium level, and potassium intake level of the patient [29].

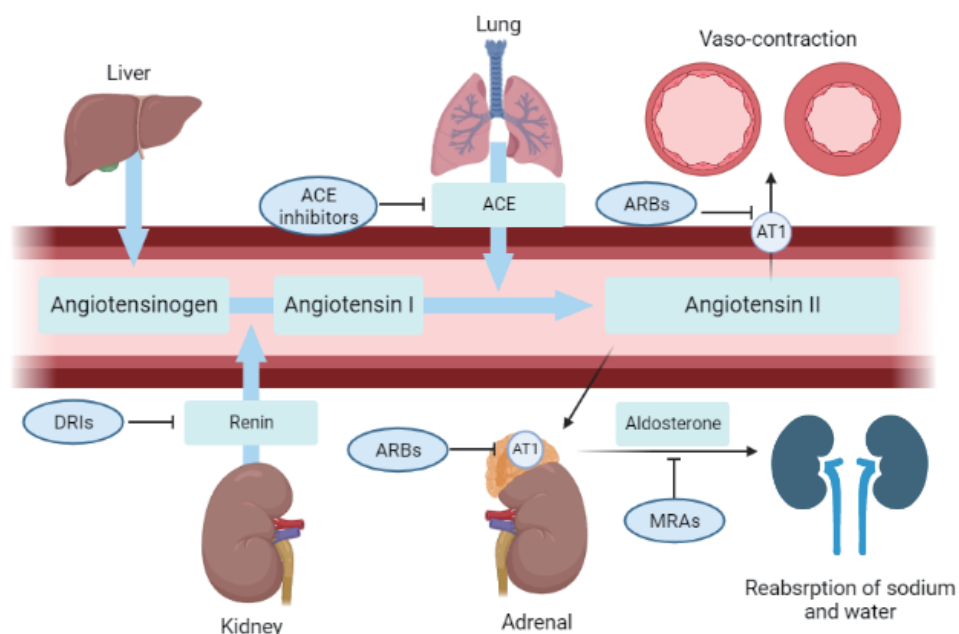


Figure 2. The renin-angiotensin-aldosterone system and target of anti-hypertensive drugs.

ACE, Angiotensin Converting Enzyme; ARB, Angiotensin Receptor Blocker; AT1: Angiotensin Receptor Type 1; DRI, Direct Renin Inhibitor; MRA, Mineralocorticoid Receptor Antagonist.

1.3. Diabetes mellitus

Diabetes mellitus is characterized by chronic hyperglycemia resulting from impaired insulin production [30]. Diabetes global prevalence has been escalating because of aging populations, changes in lifestyle, and obesity. The latest report indicates that diabetes affects over 400 million individuals worldwide [31]. The diagnostic criteria for diabetes, as defined by the ‘American Diabetes Association’, include a fasting plasma glucose level ≥ 126 mg/dl (7.0 mmol/l), a 2-hour plasma glucose level ≥ 200 mg/dl (11.1 mmol/l) during an oral glucose tolerance test, or a Hemoglobin A1c level $\geq 6.5\%$ [32]. Despite advances in therapeutic strategies, diabetes remains a significant cause of severe complications such as kidney, microvasculature, and macro vasculature. Macrovascular complications involve cardiovascular diseases, including coronary artery disease, peripheral arterial disease, and stroke [33]. Microvascular complications, such as retinopathy, nephropathy, and neuropathy, can result in disabilities such as blindness, kidney failure, and non-traumatic lower-limb amputations [34].

Diabetic kidney disease (DKD) is a prevalent microvascular complication of diabetes and a cause of chronic kidney disease (CKD) and end-stage renal disease (ESRD) [35]. DKD is characterized by albuminuria and a progressive decline in glomerular filtration rate (GFR) [36]. DKD burdens patients significantly due to morbidity, mortality, and economic costs associated with dialysis and transplantation. Both type 1 and type 2 diabetes have the risk of DKD, and the risk is notably higher in individuals with impaired glycemic control, hypertension, and specific genetic predispositions [35, 37]. Moreover, DKD is associated with cardiovascular disease, further complicating management and contributing to worse outcomes [38]. Despite efforts to understand the pathophysiology of DKD, it remains only partially understood; hyperglycemia-induced metabolic and hemodynamic changes, inflammation, oxidative stress,

and the activation of RAAS have been implicated [39, 40]. The management of DKD focuses on controlling blood glucose and blood pressure using anti-diabetic agents and RAAS inhibitors [41]. Novel therapeutic strategies targeting inflammation, fibrosis, and other mechanisms are under investigation [41, 42].

Hypertension and diabetes are chronic diseases that coexist and share several underlying causes; they share risk factors such as obesity, insulin resistance, inflammation, and lifestyle, including diet and physical inactivity [43, 44]. Also, as previously described, hypertension and diabetes collaboratively contribute to the progression of their common complications, renal and vascular dysfunction (Figure 3). Upregulation of the RAAS, oxidative stress instigated by the advanced glycation end-product (AGE)/receptor for AGE (RAGE) axis, inflammation, and activation of the immune system mediate these [45, 46]. Inflammation-driven macrovascular dysfunction accelerated in diabetes, and it can lead to myocardial infarction, stroke, and peripheral arterial disease [47]. Moreover, vascular aging, a characteristic of hypertension signified by arterial wall thickening and collagen deposition, also contributes to these changes [48]. Indeed, compared to either disease alone, metabolic disease patients have a significantly increased risk of complications, including coronary artery disease, renal failure, and congestive heart failure [49]. These risk factors also contribute to the aggravation of both diseases; hypertension incidence in individuals with diabetes is twice higher than in non-diabetic individuals [43, 50]. Additionally, essential hypertension is often accompanied by insulin resistance and hyperinsulinemia, which can further exacerbate hyperglycemia [51]. In the United States, approximately 60 million people have hypertension, 10 million have diabetes, and around 3 million individuals have both [50]. To reduce morbidity and mortality, novel blood pressure management guidelines have been developed for diabetic patients, and monitoring of blood glucose and insulin levels is recommended for hypertensive patients.

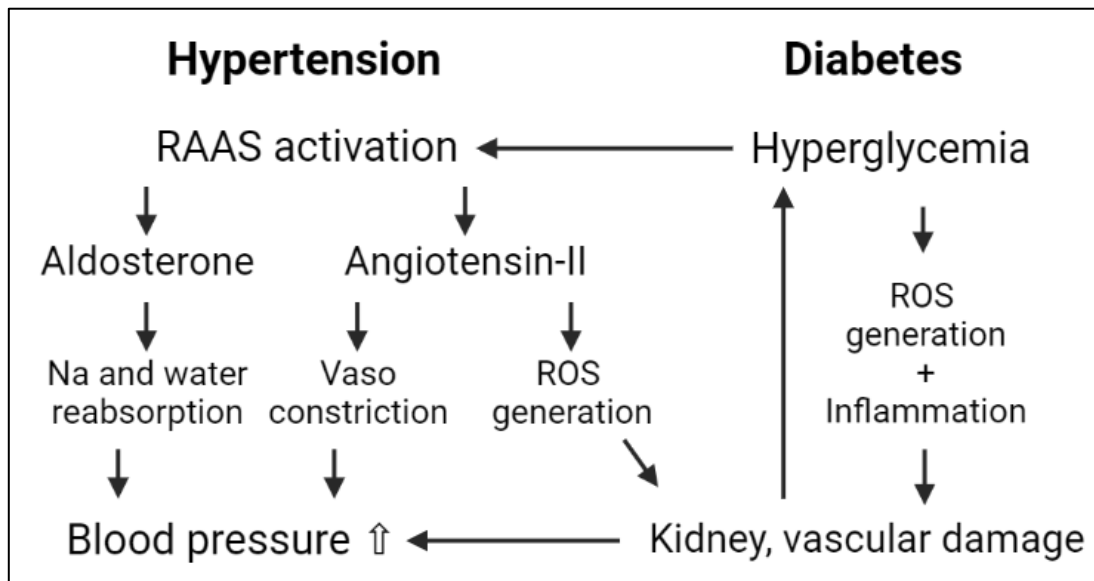


Figure 3. Interactions of hypertension and diabetes mellitus.

2. Endothelial dysfunction and inflammation

The ‘American Society of Hypertension (ASH)’ and the ‘Korean Society of Clinical Hypertension (KSH)’ have recently issued recommendations for chlorthalidone [52, 53]. This recommendation is due to chlorthalidone's benefit in protecting the vascular and decreasing cardiovascular risk [52]. Like this, enhancing vascular function is considered as critical as managing blood pressure when selecting therapeutic options in clinical practice. The vascular system plays a crucial role in preserving homeostasis in the body, mediating essential functions such as blood flow regulation, oxygen delivery, and nutrient exchange [54]. Endothelial cells located within the inner lining of blood vessels significantly regulate vascular tone. These cells release various substances, including endothelin and endothelial-derived relaxing factors, such as nitric oxide (NO), for managing vascular tone [54]. Consequently, disturbances in endothelial function precipitate and accelerate hypertension, along with several cardiovascular and metabolic diseases [55, 56]. During the initiation and progression phases of the immune response, nuclear factor kappa-B (NF- κ B) is released from the inhibitor of NF- κ B (I κ B). It translocates to the nucleus, binds to specific DNA sequences such as the activator protein 1 (AP-1) site, and induces gene expression of various inflammatory molecules [57]. One of them, intercellular adhesion molecule 1 (ICAM-1), is an adhesion molecule that plays essential roles in the recruitment of leukocytes and regulation of adhesion to the endothelium, which is essential for immune surveillance and inflammation [58, 59]. Overexpression of adhesion molecules promotes the adhesion of leukocytes and monocytes to the endothelial surface, resulting in endothelial dysfunction and vascular damage [60]. Furthermore, the accumulation of leukocytes and monocytes on the endothelial surface can lead to pro-inflammatory cytokines, oxidative stress, and further immune system activation, causing vascular damage and inflammation [61].

As another inflammatory factor, inflammasome, a pattern-recognition receptor (PRR), is a protein that regulates innate immune responses and inflammation [59]. Among them, the NOD-like receptor family, pyrin domain-containing protein 3 (NLRP3), is a multimeric protein complex with a relatively well-known structure and function. It is mainly found in immune cells such as macrophages and is activated by various stimuli such as microbial components, stress, and cell damage [62]. Once activated, NLRP3 forms an inflammasome complex and mediates the activation of caspase-1, which promotes the production and release of pro-inflammatory cytokines [63]. NLRP3 activation plays a vital role in the immune response to infection and injury, but excessive or prolonged activation contributes to chronic inflammation and tissue damage [62]. Various studies have shown that NLRP3 inflammasome activation is associated with several chronic inflammatory diseases and metabolic disorders, including obesity, hypertension, diabetes, atherosclerosis, neuroinflammation, retinopathy, stroke, and cancer [64, 65]. It is widely recognized that NLRP3 and NF- κ B exhibit a close, reciprocal relationship in their functional activity and expression levels for the progression of inflammation.

In hypertension, excessive Ang2 reduces the activation of endothelial NO synthase (eNOS) through the AT1/NOX/ROS/PP2A pathway and induces endothelial damage via oxidative stress [22, 23]. Oxidative radicals play an essential role in the development and progression of various cardiovascular diseases, and antioxidants have been reported to reduce atherosclerotic plaques and improve vascular function decline [58, 66]. Simultaneously, the increased production of ROS in endothelial cells sets off inflammatory pathways, amplifying cell damage; it suggests a complex interaction between oxidative stress and inflammation [67]. The inflammatory cascade depletes tetrahydrobiopterin (BH4), an essential eNOS cofactor, and curtails NO bioavailability [68]. This phenomenon also initiates the process of endothelial dysfunction and cell death by inducing damage to organelles such as mitochondria and

membranes. Inflammation also can cause acute or chronic oxidative stress directly or indirectly through ROS sources like NOX and the mitochondrial electron transport chain [69]. These integrated pathways trigger the formation of atherosclerotic plaques and exacerbate vascular dysfunction [68, 70, 71]. Therefore, many researchers focus on inflammation and ROS to mitigate endothelial damage (Figure 4).

Autophagy is a protective cellular mechanism that facilitates the removal of damaged organelles and proteins. Autophagy activation has multiple advantages, such as inhibiting apoptosis in pulmonary arterial hypertension and reducing ischemia/reperfusion-induced endothelial damage [72, 73]. The activation of autophagy in the vascular endothelium can decrease the expression of cell adhesion molecules and the infiltration of monocytes, thereby mitigating excessive inflammation and offering protection against atherosclerosis [74-76]. Indeed, autophagy is well known to be a negative regulator of NLRP3 inflammasome. Meanwhile, impaired autophagy increases cellular stress by exacerbating inflammation and deficient cellular repair mechanisms [75, 76]. For this reason, autophagy has emerged as a target for vascular protection in various chronic diseases, especially diabetes, and hypertension.

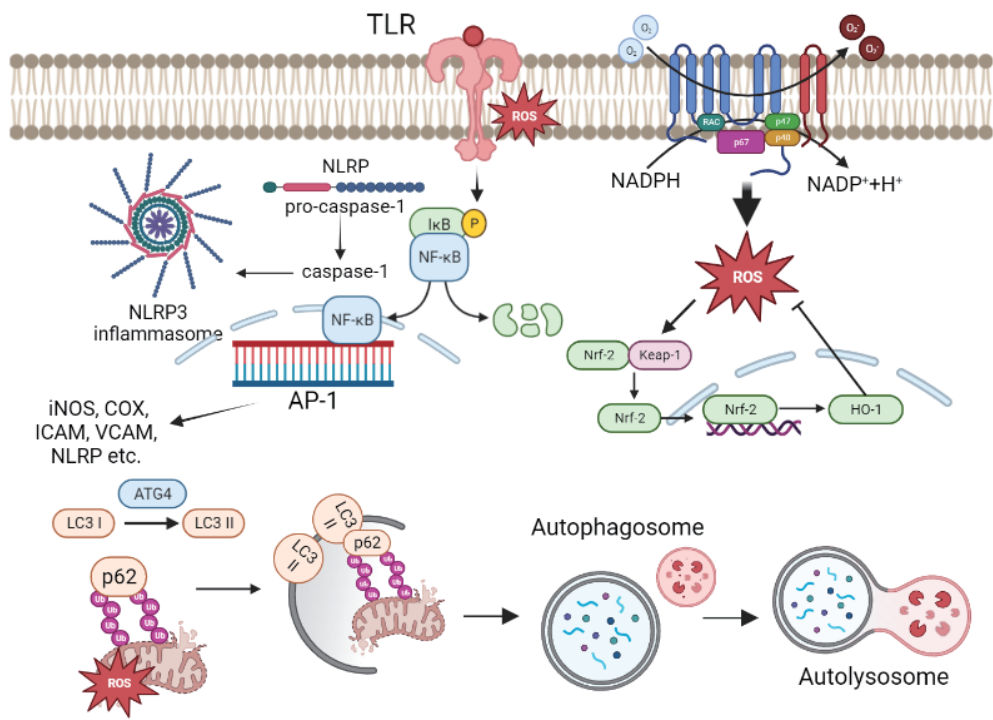


Figure 4. Various signaling pathways associated with vascular endothelial dysfunction.

NADPH, Nicotinamide Adenine Dinucleotide Phosphate; ROS, Reactive Oxygen Species; TLR, Toll-like Receptor; NF-κB, Nuclear Factor Kappa-B; IκB, Inhibitor of NF-κB; AP-1, Activator Protein 1; NLRP3, NOD-Like Receptor Family, Pyrin Domain Containing Protein 3; LC3, Microtubule-Associated Protein 1A/1B-Light Chain 3; ATG4, Autophagy-Regulating Protease 4; P62, Sequestosome-1.

3. ARBs and SGLT2 inhibitors

3.1. Angiotensin receptor type 1 blocker

ARB, a class of RAAS inhibitors, is widely used as a first-line prescription drug. Various ARBs with different molecular structures have been developed [77, 78] (Table 1). ARBs are alternatively used for patients resistant to ACE inhibitors or who experience cough, angioedema, or other side effects; ARBs are known to have excellent tolerability with few side effects. The first ARB developed was losartan, which has been widely used in basic and clinical research since its inception in 1986 [79]. Since then, valsartan, candesartan, telmisartan, eprosartan, and olmesartan have been developed in the 1990s, with fimasartan and azilsartan emerging since the 2000s [80, 81].

Table 1. Pharmacokinetic characteristics of ARBs.

Drugs	Dose (mg)	T _{max} (h) ¹⁾	T _{1/2} (h) ²⁾	Bioavailability (%)	Urinary elimination (%)
Losartan	25, 50, 100	3-4	2	33	35
Valsartan	40, 60, 80, 320	2-4	6-9	10-35	13
Irbesartan	75, 150, 300	1.5-2	11-15	60-80	20
Eprosartan	400, 600	1-2	5-9	13	7
Olmesartan	5, 20, 40	1-2	13	26	35-50
Telmisartan	20, 40, 80	0.5-1	24	42-58	< 1
Candesartan	4, 8, 16, 32	3-4	5-9	15	33-59
Fimasartan	60, 120	0.5-3	7-10	30-40	< 3

¹⁾ T_{max}, time to maximum plasma concentration

²⁾ T_{1/2}, half-life

We selected fimasartan, telmisartan, and candesartan for our research; based on molecular structures, documented efficacy, and pharmacokinetic characteristics. Fimasartan, an oral antihypertensive drug developed by Korea's Boryung Pharmaceutical, is an AT1 selective antagonist approved and used in Korea, China, India, Singapore, and Russia. The recommended daily dose is 60-120 mg, with a T_{max} of 0.5 - 3 hours and a relatively long half-life of 7 - 10 hours [82, 83]. Fimasartan is a derivative of losartan in which the imidazole ring is replaced, a non-biphenyl ARB with a benzimidazole structure, and IUPAC name is 2-[2-butyl-4-methyl-6-oxo-1-[[4-[2-(2H-tetrazol-5-yl)phenyl]phenyl]methyl]pyrimidin-5-yl]-N,N-dimethylethanethioamide [82]. The tetrazole group is a shared characteristic of many ARBs, which binds to AT1, replacing Ang2 [84]. Fimasartan contains a tetrazole group, but unlike the others, it includes a thiocarbonyl group, which is unique to its structure.

Telmisartan is prescribed in 20-80 mg doses once daily and has a 0.5 to one-hour T_{max} . Half-life is 24 hours, the most prolonged among ARBs; it can effectively address the rise in blood pressure in the morning, known to cause acute myocardial infarction and stroke. Telmisartan possesses a biphenyl-imidazole structure, and its IUPAC name is 2-[4-[[4-methyl-6-(1-methylbenzimidazol-2-yl)-2-propylbenzimidazol-1-yl]methyl]phenyl]benzoic acid [85, 86]. Unlike fimasartan, telmisartan has a carboxylic acid group instead of a tetrazole group. Telmisartan is also known to activate peroxisome proliferator-activated receptor gamma ($PPAR\gamma$), a therapeutic target for hyperlipidemia and diabetes; therefore, telmisartan has beneficial for not only hypertension but also diabetes [87, 88].

Candesartan cilexetil is a highly effective orally administered antihypertensive drug that selectively binds to and inhibits the AT1 with high affinity and slow dissociation. It is prescribed at doses ranging from 4 to 32 mg once daily, has a T_{max} of 3 - 4 hours, and a half-life of 5 - 9 hours [89, 90]. By blocking the RAAS, candesartan has significantly reduced

cardiovascular mortality and morbidity in hypertensive patients and is known to prevent heart failure [91]. Candesartan features a biphenyl-tetrazole structure, and IUPAC's name is 1-cyclohexyloxycarbonyloxyethyl 2-ethoxy-3-[[4-[2-(2H-tetrazol-5-yl)phenyl]phenyl]methyl]benzimidazole-4-carboxylate [92]. These structural differences may give rise to differences in pharmacokinetics, pharmacodynamics, and side effect profiles [93, 94].

Although ARBs are drugs with relatively few side effects, hyperkalemia is possible, which is a chronic problem with the RAAS inhibitors, as mentioned above. In addition, overdoses of ARBs typically present symptoms such as hypotension, dizziness, and bradycardia, which could result from parasympathetic stimulation [95]. These drugs are not approved for use in children younger than one year of age and are contraindicated during pregnancy due to their direct action on the RAAS, which could affect the development of immature kidneys [96]. They are also associated with serum aminotransferase elevations [97]. Also, relatively recently, losartan, the 9th most prescribed drug in the US, has been found to contain nitrosamine impurities that are potential carcinogens. Due to these findings, losartan has been subject to widespread recalls since 2018, with the synthesis of its tetrazole ring structure implicated as the likely source of contamination [98]. However, it is worth noting that, unlike valsartan and irbesartan, which also contain tetrazole rings, candesartan, and fimasartan has not been associated with nitrosamine impurities and remains a safe and effective option for hypertension treatment [99, 100].

As mentioned above, 'The Seventh Report of the Joint National Committee (JNC-7)' and 2007 'European Society of Hypertension/European Society of Cardiology (ESH/ESC)' recommend combination therapy of two or more agents in patients with stage 2 or higher hypertension. ARBs are mainly combined with a CCB or a thiazide diuretic. These combinations can provide additive antihypertensive effects and offset some side effects of the individual drugs.

Specifically, CCB excites RAAS and sympathetic nerves along with vasorelaxation to induce reflex vasoconstriction and tachycardia, and ARB inhibits them; therefore, the antihypertensive effect can be increased when combined. [101]. Indeed, combining an ARB and amlodipine can offer substantial blood pressure-lowering effects [102].

Thiazide diuretics are another kind of drug that reduces blood pressure by promoting sodium excretion and reducing fluid volume [103]. Thiazide diuretics have the side effect of exciting the RAAS by increasing sodium excretion and decreasing circulating volume [104]. Since ARB blocks this, the antihypertensive effect is enhanced when combined [105]. In addition, since thiazide diuretics can reduce hyperkalemia, a chronic side effect of ARB, combining the two drugs can improve antihypertensive effects and prevent side effects [106]. Recent studies have confirmed that combining fimasartan with hydrochlorothiazide (HCTZ), a diuretic, shows excellent blood pressure-lowering efficacy, leading to the development and sale of combination preparations [107]. In addition, candesartan, combined with HCTZ and amlodipine, can effectively lower blood pressure in patients with inadequate response to initial therapy and clinical utility as a second-line agent [108, 109]. In some cases, triple therapy (ARB, CCB, and Thiazide diuretics) might be necessary for patients with high cardiovascular risk or with poor dual treatment. These combinations have shown efficacy in lowering blood pressure in numerous clinical trials. Still, studies of these treatments considering their lifestyle, potential for drug interactions, comorbidities, and possible side effects must be investigated more.

3.2. SGLT2 inhibitor

In a healthy adult, the kidneys filter approximately 180 g of glucose and reabsorb daily [110]. Sodium-glucose cotransporter (SGLT) mediates this process in the proximal tubule. SGLT is an ion exchanger that reabsorbs glucose and sodium in a 1:1 ratio and is responsible for 90% of glucose reabsorption at normal blood glucose levels [110, 111] (Figure 5). SGLT1 is distributed in the S2 and S3 segments, and SGLT2 is distributed in the S1 and S2 segments.

SGLT2 inhibitors are antidiabetic agents that reduce blood glucose by inhibiting glucose reuptake by SGLT2 [112]. Clinical studies have demonstrated that SGLT2 inhibitors can decrease Hemoglobin A1c by 0.6-0.9% and fasting blood glucose by 18-36 mg/dL [113]. Furthermore, SGLT2 inhibitors promote weight loss by reducing calories through increased glucose excretion and can lower SBP by 3-5 mmHg through increased sodium and water excretion [114, 115]. In addition to promoting diuresis and reducing blood glucose, SGLT2 inhibitors have been reported to have various protective effects on the cardiovascular and renal systems [116, 117].

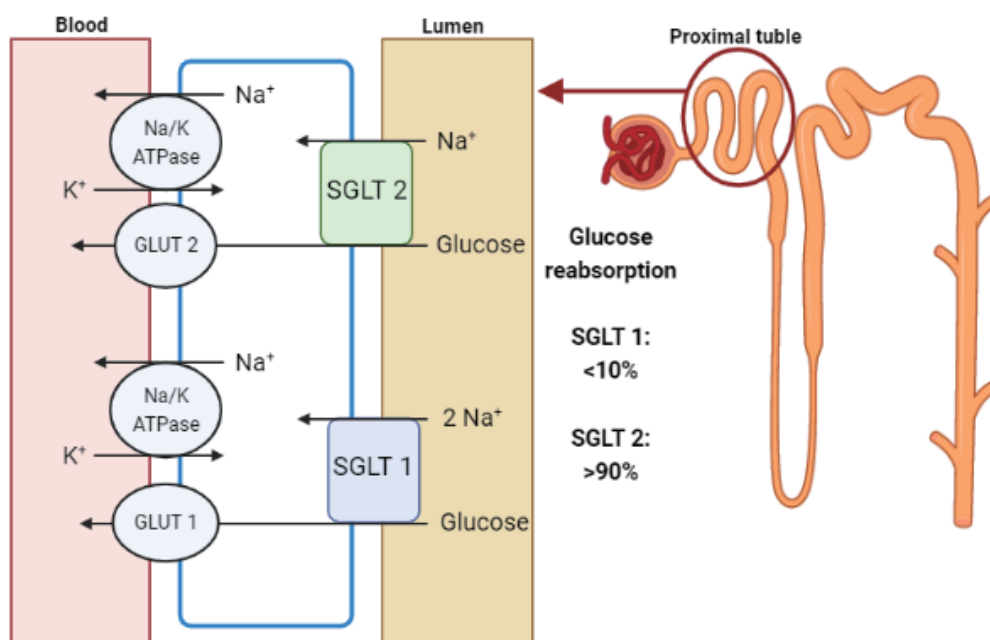


Figure 5. The distribution and function of renal sodium-glucose cotransporters.

GLUT, Glucose Transporter; Na/K ATPase; Sodium–Potassium Adenosine Triphosphatase; SGLT, Sodium-Glucose Cotransporter.

Dapagliflozin is the kind of SGLT2 inhibitor with a T_{max} of 2.5 hours and a half-life of approximately 13 hours (Table 2). Dapagliflozin is a highly potent (inhibitory constant 0.55 nmol/L) and reversible SGLT2 inhibitor that is more selective for SGLT2 than SGLT1 [118]. Dapagliflozin increased the amount of glucose excreted in the urine and reduced fasting and post-prandial plasma glucose levels in patients with type 2 diabetes [119]. Dapagliflozin-induced glucose diuresis in patients with type 2 diabetes was associated with caloric loss, a modest reduction in body weight, mild osmotic diuresis, and transient natriuresis [120]. Dapagliflozin is also known to reduce the risk of kidney failure and prolonged survival in patients with CKD with or without type 2 diabetes [118, 121]. Indeed, patients with stage 4

CKD randomized to dapagliflozin experienced a 27% reduction in the primary composite endpoint [121]. Furthermore, several studies also reported reductions in SBP and cardiovascular morbidity and protection of vascular endothelial cells in dapagliflozin-treated patients [122-125].

Table 2. Pharmacokinetic characteristics SGLT2 inhibitors.

Drugs	Dose (mg)	T _{max} (h) ¹⁾	T _{1/2} (h) ²⁾	Bioavailability (%)	Elimination route (%)
Dapagliflozin	5, 10	2	12.9	78	Feces 21 Urine 75
Empagliflozin	10, 25	1.5	12.4	78	Feces 41 Urine 54
Canagliflozin	100, 300	1-2	13.1	65	Feces 52 Urine 33

¹⁾ T_{max}, time to maximum plasma concentration

²⁾ T_{1/2}, half-life

One of the mechanisms is to reduce the sodium-hydrogen exchanger-1 (NHE-1), independent of SGLT2. NHE-1 is a membrane protein that regulates intracellular ion balance in various tissues; NHE-1 is primarily involved in maintaining intracellular pH [126]. At the same time, in the kidney, it reabsorbs Na⁺ filtered in the proximal tubule and regulates body fluid and electrolyte homeostasis [127, 128]. Several reports have demonstrated that NHE-1 expression and activity are increased in hypertension, and it can induce vasoconstriction by increasing intracellular sodium and calcium concentrations [129-131]. Increased NHE-1 is also shown in diabetic kidneys, which can contribute to diabetic nephropathy by promoting sodium ion

retention and volume expansion, impairing GFR, and increasing proteinuria [132, 133]. Therefore, NHE-1 is a potential target for treating cardiovascular dysfunction and DKD, especially using SGLT2 inhibitors [134, 135].

On the other hand, acute renal damage in patients with end-stage renal disease has been reported when treating SGLT2 inhibitors, including dapagliflozin. Other side effects, such as ketoacidosis, increased genital infection, and decreased bone density, are also known [136]. In addition, natriuresis due to SGLT2 inhibition may cause activation of RAAS, a chronic problem of diuretics. Indeed, dapagliflozin can increase plasma renin, aldosterone, and copeptin levels [137].

In this context, infrequent trials combining SGLT2 inhibitors with ARBs are commencing. This approach hypothesizes that the co-administration of ARBs and dapagliflozin may have advantageous outcomes by counteracting each drug's adverse effects, such as hyperkalemia triggered by ARBs and RAAS activation by dapagliflozin. Indeed, in the DAPA-HF trial, dapagliflozin curtailed the incidence of hyperkalemia among patients concurrently administered mineralocorticoid receptor antagonist (MRA)s [138]. This strategy may also be safe against metabolic disorders such as glucose dysregulation and insulin resistance, which are common side effects of thiazide diuretics. However, there has been a shortage of non-clinical experiments investigating the response to the ARB and dapagliflozin combination, especially in drug interaction and its mechanisms. Additionally, research addressing compensatory reactions, a typical occurrence in the initial stages of patients prescribed antihypertensive and antidiabetic drugs, is virtually non-existent.

4. Objective

Combination therapy is a strategic approach widely adopted for efficient blood pressure management. Hypertension and diabetes commonly coexist, thus leading to investigations on the co-administration of various antidiabetic and antihypertensive treatments. However, investigations into the combination of ARB and SGLT2 inhibitors remain nascent. Therefore, more research is needed to fully understand the unexpected side effects, compensatory reactions, the precise actions and mechanisms of each drug, and the benefits of combining these treatments.

We hypothesized that the co-administration of ARBs and dapagliflozin might have advantageous outcomes by counteracting each drug's adverse effects and offering benefits beyond blood pressure regulation, including blood glucose reduction, diuresis, natriuresis, RAAS inhibition, renal and vascular protection. Therefore, our research investigated the effects of the short-term co-administration of dapagliflozin and ARBs (fimasartan, telmisartan, and candesartan) in spontaneously hypertensive rats (SHR). In particular, we explored the enhancement of dapagliflozin in ARB-induced blood pressure control and the effect of ARBs on dapagliflozin-induced SGLT2 inhibition. We also probed the protective effects and mechanisms of co-administration on the kidney and vascular for identifying the additional benefits.

**Part 1. Enhancement of ARB by Dapagliflozin:
Blood Pressure Regulation in SHR**

1-1. Materials and methods

1-1.1. Materials and experimental animals

The ARBs used in this study, including fimasartan, telmisartan, and candesartan cilexetil, were provided by Dr. Yong-Ha Ji. The SGLT2 inhibitor dapagliflozin, containing 10 mg of the active ingredient, was obtained as Forxiga™ tablets (AstraZeneca, UK), and HCTZ (Merck, Germany) was purchased and used according to the manufacturer's instructions.

SHRs were purchased from Charles River (MA, US) and housed at the Jeju National University animal facility for at least seven days before use in the experiments. Animals were fasted for four hours before drug administration, and water was provided *ad libitum*. The animals were housed under controlled conditions with a temperature of $22 \pm 5^{\circ}\text{C}$, a humidity of $50 \pm 10\%$, and a 12-hour light/dark cycle. All animal experiments were performed under the guidelines of the 'Institutional Animal Care and Use Committee at Jeju National University' (protocol number: 2018-0019).

1-1.2. Blood pressure measurement

Experimental animals were acclimatized at 40°C for 15 minutes for blood pressure measurement, and then tail-cuff and Volume Pressure Recording (VPR) sensors were installed. Blood pressure was measured using the tail-cuff method (Coda, Kent Scientific Co., CT, US). The measurement cycle consisted of five preliminary and ten mains, with a time of 15 seconds per measurement. To get reliable results, values were selected according to the heart rate of rats (250-450 bpm) and standards of the CODA software (tail volume, systolic and diastolic measurement time interval, difference between systolic and diastolic blood pressure).

Experimental animals with SBP over 190 mmHg were selected, and measuring blood pressure once a day for three days before drug administration to acclimate them to the measurement device. At experimental periods, Blood pressure was measured three times a day at three-day intervals during drug administration: one hour before administration (-1 h), one hour after administration (1 h), and three hours after administration (3 h). In addition, blood pressure changes were tracked for seven days after stopping the administration (Re1-7) (Figure 6).

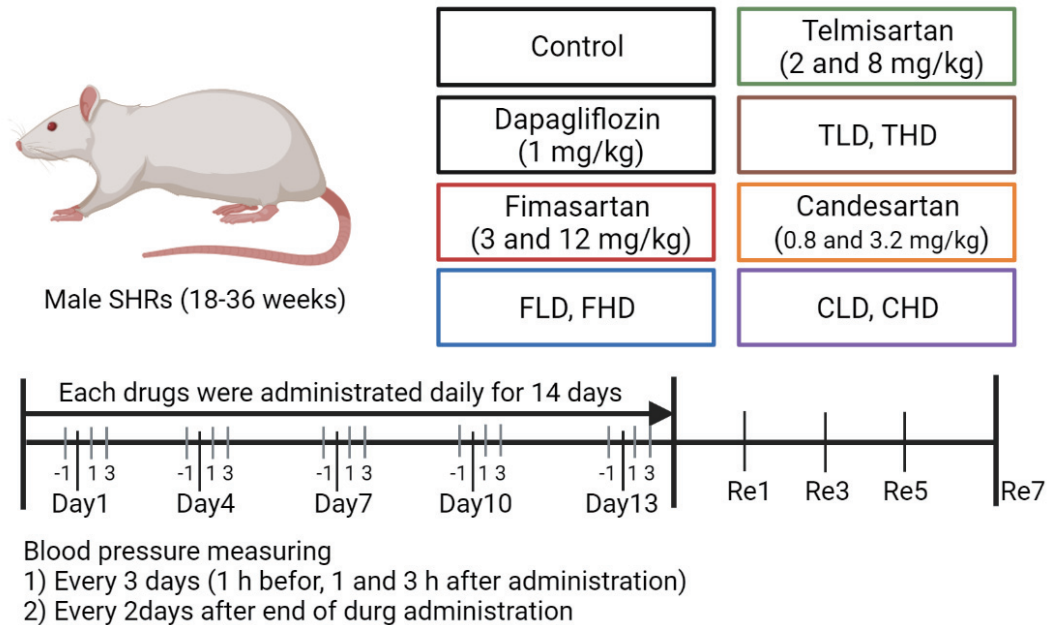


Figure 6. The experimental groups and the experimental schedule.

1-1.3. Experimental groups

(1) Combined Administration of ARBs and Dapagliflozin: Male SHR aged 18-36 weeks, weighing 340-390 g, with a SBP of over 190 mmHg were used. The experimental groups consisted of a control group, a dapagliflozin single administration group, low and high doses of ARB single administration groups, and low and high doses of ARB and dapagliflozin combination groups (Figure 6). All doses were calculated using body surface area conversion factors from FDA, which provides an equivalent dose relative to clinical applications; dapagliflozin 1 mg/kg, fimasartan 3 and 12 mg/kg, telmisartan 2 and 8 mg/kg, and candesartan 0.8 and 3.2 mg/kg. All drugs were dissolved in distilled water and administered orally. The control group received distilled water in the same volume per gram of body weight.

(2) Combined Administration of Telmisartan and HCTZ: Male SHR over 30 weeks,

weighing 360-410 g, with a SBP of over 190 mmHg were used. Experimental groups consisted of a control group, HCTZ single administration group, and telmisartan and HCTZ combination group. HCTZ was administered at 15 mg/kg and telmisartan at 8 mg/kg. All drugs were dissolved in distilled water and administered orally every day. The control group received distilled water at a dose of μL per gram of body weight.

1-1.4. Measuring vascular relaxation

(1) Animals: Wistar Kyoto (WKY) rats were purchased from Charles River and housed at the Jeju National University animal facility for at least seven days before use in the experiments. The animals were housed under controlled conditions with a temperature of $22 \pm 5^\circ\text{C}$, a humidity of $50 \pm 10\%$, and a 12-hour light/dark cycle. All animal experiments were performed under the guidelines of the 'Institutional Animal Care and Use Committee at Jeju National University' (protocol number: 2018-0019).

(2) Measuring vasorelaxation: The thoracic aortas of 20-25 weeks old male WKY rats were harvested immediately after sacrifice using CO_2 gas. The thoracic aorta was prepared into 3-5 mm sections, suspended to metal rings, and mounted to isometric force-displacement transducers (FT03, Grass, AD Instruments, New Zealand). Aortas were placed on the organ bath filled with 37°C Krebs buffer (120 mM NaCl, 4.75 mM KCl, 6.4 mM Glucose, 25 mM NaHCO_3 , 1.2 mM KH_2PO_4 , 1.2 mM MgSO_4 , 1.7 mM CaCl_2), which was adjusted to pH 7.4 while supplying 95% O_2 and 5% CO_2 gas (Figure 7). The tension of the aorta was adjusted to 1.0 g, and stabilized for two hours with solution changes every 20 minutes. After stabilization, the vessels were pre-contracted with 1 μM phenylephrine (PE), and the cumulative concentration of ARBs and dapagliflozin (0-500 μM) were added to measure the level of vascular relaxation. The changes in vascular tone in response to drug treatment were recorded using a physiograph recorder (PowerLab/400, AD instrument) and quantified using the Chart7

program (AD instruments). The levels of vasorelaxation responses by treatment were calculated based on PE-induced contracted tension.

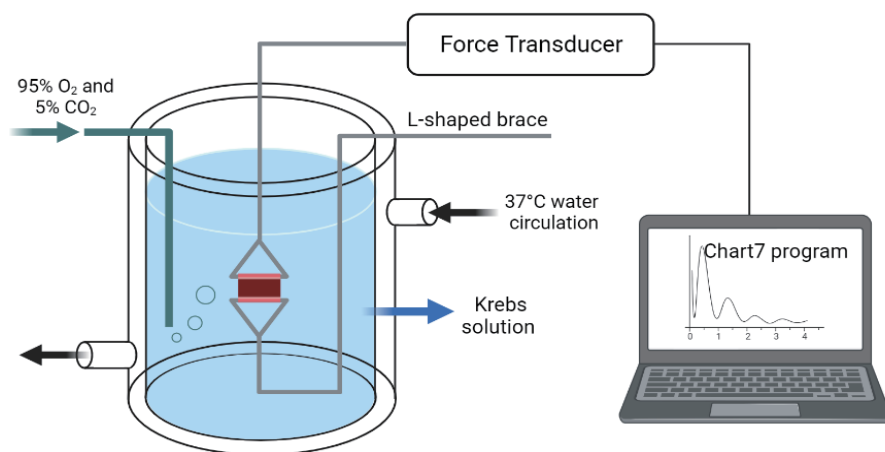


Figure 7. Myography system for measuring the vascular reactivity.

1-1.5. Cell culture

EA. hy926 cells, a hybrid cell line between human umbilical vein endothelial cells (HUVEC) and A549 lung cancer cells, were cultured in Dulbecco's modified Eagle's medium (DMEM, Gibco, MA, US) supplemented with 10% fetal bovine serum (FBS, Gibco) and 100 U/mL Penicillin-Streptomycin (P/S, Gibco). Cells were treated with drugs and collected after 24 hours.

1-1.6. Protein Analysis

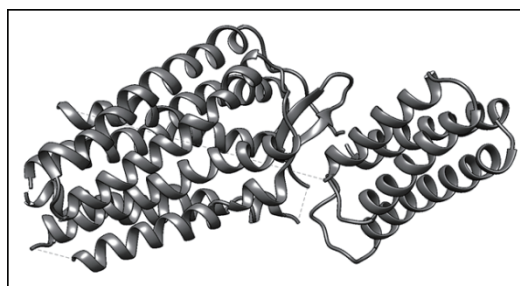
(1) Protein preparation: EA. hy926 cells were washed with phosphate-buffered saline (PBS,

pH 7.4) and then lysed with RIPA buffer (Tech & Innovation, Korea) for 30 minutes on ice. The supernatant was collected after centrifugation at 13,000 rpm, 4°C for 15 minutes. The protein contents of cell lysate were quantified using the Bradford method.

(2) Western blotting: Equal amounts of protein were mixed with sample buffer and denatured at 97°C for seven minutes. 20 µg of protein per well was loaded onto 8-12% SDS-PAGE and electrophoresed at 120-150 V for one hour. The separated proteins were transferred to polyvinylidene fluoride (PVDF, Bio-Rad, CA, US) membranes at 100 V for two hours using wet transfer methods. After washing with TBST (200 mM Tris, 1.37 M NaCl, 0.1% Tween-20), the membranes were blocked with 5% blocking grade buffer (Bio-Rad) for 30 minutes to prevent nonspecific binding. The membranes were incubated overnight at 4°C with anti-eNOS, p-eNOS (Cell Signaling, MA, US), and β-actin (Santa Cruz Biotechnology, CA, US) antibodies. After washing, the membranes were incubated for one hour with a secondary antibody (GeneTex, CA, USA) conjugated with HRP. The protein was visualized using electrochemiluminescence (Amersham Biosciences, UK) and detected using Chemi-Doc molecular imaging system (Fusion Solo S, Vilber Lourmat, France). The expression levels of each protein were obtained using the Evolution Capt software (Vilber Lourmat), normalized by β-actin, and further calculated to relative values based on control. The activation level of eNOS was calculated by the expression level of p-eNOS to the total eNOS protein.

1-1.7. Molecular docking

The structure of AT1 was downloaded in .pdb format from the Protein Data Bank (PDB) (<https://www.rcsb.org/>) (Figure 8) [139]. The structures of compounds were downloaded in .sdf format from PubChem (<https://pubchem.ncbi.nlm.nih.gov/>) (Figure 9).



AT1
(PDBID: 7JN1)

Figure 8. Structures of angiotensin receptor type 1 obtained from Protein Data Bank.

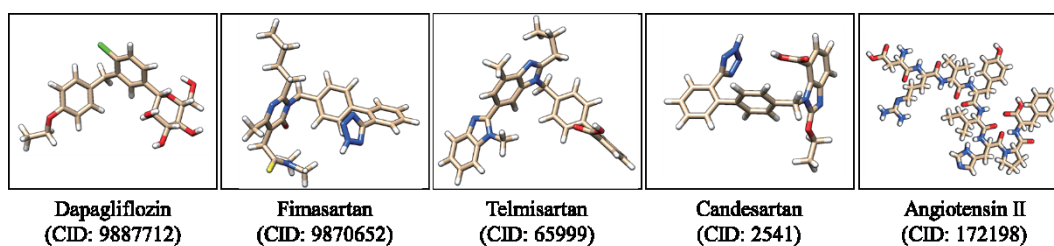


Figure 9. Structures of dapagliflozin, fimasartan, telmisartan, candesartan, and angiotensin-II obtained from PubChem.

To confirm the atomic coordinates of all ligands and the conversion of chemical structures, the PyRx program (OpenEye Scientific Software, US) was used to transform them into pdbqt format. Next, the binding affinity values were obtained using PyRx AutoDock Vina to explore the interaction between the compounds and proteins. The docked forms were then visualized and converted into PDB format using the PyMOL program (Schrödinger, NY, US). Finally, the shape and amino acids of the receptor-ligand interaction site and hydrogen bonds were confirmed using the Discovery studio program (Dassault Systèmes BIOVIA, US) and LigPlot⁺

(European Bioinformatics Institute, UK).

1-1.8. Statistical analysis

All data were presented as mean \pm SEM. Statistical analyses were performed using GraphPad Prism 6 (GraphPad Software Inc, CA, US) program, conducting one-way and two-way ANOVA and using Tukey's post hoc test for significance verification. A p-value of less than 0.05 was considered significant.

1-2. Results

1-2.1. Blood pressure

The effects of three types of ARBs and dapagliflozin on SBP in SHR were as follows. The mean SBP of the dapagliflozin administration group was 222.1 ± 14.54 mmHg, exhibiting no significant differences when compared to 220.4 ± 12.95 mmHg in the control group and 222.7 ± 14.35 mmHg before administration (Figure 10).

The average SBP of administered with the fimasartan alone group was 204.4 ± 16.80 mmHg and 202.9 ± 19.40 mmHg at low (FL) and high (FH) doses, respectively (Figure 10A). The combination group with dapagliflozin demonstrated 201.2 ± 19.13 mmHg and 190.5 ± 21.32 mmHg at low (FLD) and high (FHD) doses, which were lower than the same dose of the erysipelas group. The minimum SBP value was 193.4 mmHg on Day 7 (3 h) and 189.8 mmHg on Day 13 (3 h) in the FL and FH groups, respectively. The FLD and FHD groups showed 185.9 mmHg and 170.4 mmHg, respectively, on Day 13 (3h), which were lower than the same dose of the single group. Remarkably, on Day 4 (1h), and Day 7 (3h), FHD showed 184.4 mmHg and 171.5 mmHg, significantly lower SBP than 206.3 mmHg and 199.7 mmHg of the FH group. Furthermore, FHD exhibited a significant decrease in blood pressure compared to the control group from Day 1 (3 h) ($p < 0.01$). The first significant reduction in the FH group was recorded on Day 7 (1h), signifying that the combination of dapagliflozin induced an earlier decline in SBP. Post-discontinuation of administration, FHD maintained significantly lower SBP than the control group at 191.2 mmHg until Re1. On the same day, FL, FH, and FLD showed an earlier increase of SBP to 215.0 mmHg, 203.0 mmHg, and 209.0 mmHg, respectively. In conclusion, dapagliflozin amplified the blood pressure-lowering effect of fimasartan and extended the response duration.

The mean SBP of the telmisartan alone group was 206.4 ± 19.29 mmHg and 197.3 ± 25.25

mmHg at low (TL) and high (TH) doses, respectively (Figure 10B). Meanwhile, the dapagliflozin combination group demonstrated 192.7 ± 21.97 mmHg and 172.2 ± 25.28 mmHg at low (TLD) and high (THD) doses, respectively, which were lower than the same dose of the erysipelas group. The minimum SBP value was 186.9 mmHg on Day 4 (3 h) and 169.8 mmHg on Day 13 (3 h) in the TL and TH groups. The TLD and THD groups were 171.4 mmHg on Day 4 (3 h) and 143.9 mmHg on Day 13 (1 h), respectively, lower than the same dose of the single group. Mainly, the THD group exhibited significantly lower SBP than the TH group on numerous days; on Day 1 (3 h), Day 4 (1 and 3 h), Day 7 (-1, 1 and 3 h), Day 10 (1 h), and Day 13 (1 and 3 h). The THD group indicated a significant reduction in SBP compared to the control group from Day 1 (3 h) ($p < 0.01$). The first significant decrease in the TH group was recorded on Day 4 (1h), and it was established that the combination of dapagliflozin resulted in an earlier reduction in SBP. After the cessation of administration, THD sustained a significantly lower SBP than the control group at 195.9 mmHg until Re5. On the same day, SBP of TL, TH, and TLD groups were recorded at 216.0 mmHg, 212.7 mmHg, and 213.1 mmHg, respectively, demonstrating an increase earlier. In conclusion, dapagliflozin amplified telmisartan's blood pressure-lowering effect and extended the maintenance period.

The mean SBP of the administered with candesartan alone group was 205.2 ± 166.98 mmHg and 194.8 ± 23.51 mmHg at low (CL) and high (CH) doses, respectively (Figure 10C). The dapagliflozin combination group exhibited 204.0 ± 22.45 mmHg and 191.1 ± 22.21 mmHg at low (CLD) and high (CHD) doses, respectively, analogous to the single group. The minimum SBP value was 190.8 mmHg on Day 4 (3 h) and 175.6 mmHg on Day 7 (1 h) in the CL and CH groups. The minimum SBP of the CLD and CHD groups was 183.3 mmHg on Day 10 (3 h) and 171.9 mmHg on Day 13 (3 h), respectively, marginally lower than the single group. However, no significant difference was observed between the single and combination groups at the same dosage during the experimental period. CH displayed a significant SBP reduction

compared to the control group from Day 1 (3 h) ($p < 0.05$). Conversely, the first decrease in the CHD group was noted on Day 4 (1 h), establishing that the single group achieved a quicker reduction in blood pressure than the dapagliflozin combination group. Post-discontinuation of administration, CH and CHD sustained significantly lower SBP than the control group at 192.5 mmHg and 192.6 mmHg, respectively, until Re1. On the same day, CL and CLD showed an earlier increase than high dose groups at 221.8 mmHg and 210.1 mmHg, respectively. In summation, dapagliflozin tended to partially augment candesartan's blood pressure-lowering efficacy, including diminishing minimum SBP, though the effect was not statistically significant. In part, dapagliflozin was affecting negatively, such as delaying the reduction initiation.

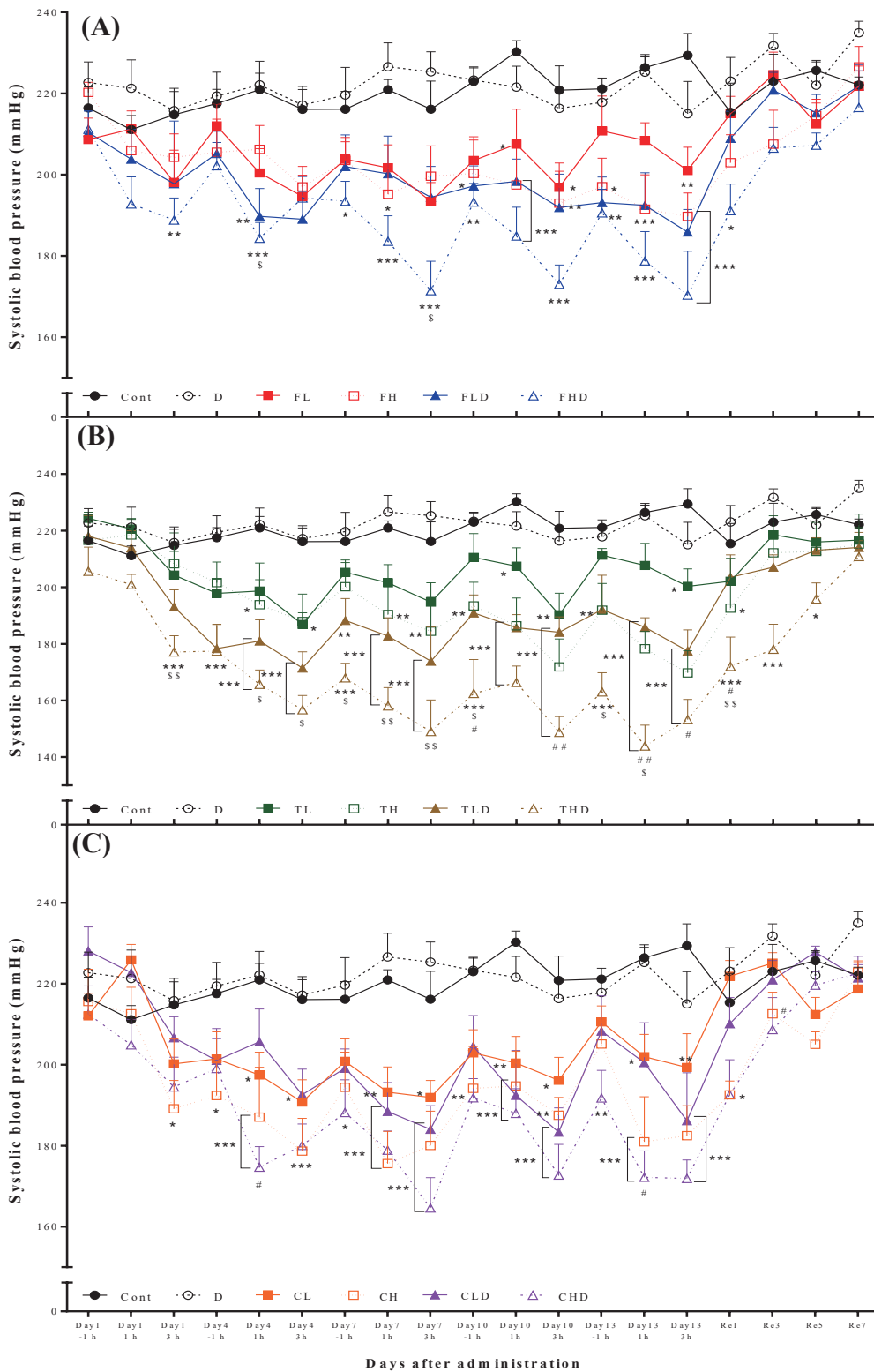


Figure 10. Effects of dapagliflozin and ARBs on systolic blood pressure of SHR.

All experimental animals received the drug orally once a day for two weeks. Systolic blood pressure (SBP) was measured one hour before (-1 h), one hour after (1 h), and three hours after (3 h) administration. SBP was additionally monitored for seven days after the discontinuation of administration to assess blood pressure recovery (Re1-7). (A) SBP of SHR administered individually/combined with fimasartan and dapagliflozin. (B) SBP of SHR administered individually/combined with telmisartan and dapagliflozin. (C) SBP of SHR administered individually/combined with candesartan and dapagliflozin. All data are expressed as mean \pm standard error mean. *, **, *** means a significant difference at the $p < 0.05$, 0.01 , and 0.001 levels compared to the control group. ^S means a significant difference at the $p < 0.05$ and 0.01 levels exist between the same dose of the combined group and single administration group. ^{#, ##} means a significant difference between the low and high concentration groups at the $p < 0.05$ and 0.01 levels. Cont, SHR control group; D, dapagliflozin alone group (1 mg/kg); FL, low-dose fimasartan alone (3 mg/kg); FH, high-dose fimasartan alone group (12 mg/kg); FLD, low-dose fimasartan (3 mg/kg) and dapagliflozin (1 mg/kg) combination group; FHD, high-dose fimasartan (12 mg/kg) and dapagliflozin (1 mg/kg) combination group; TL, low-dose telmisartan alone (2 mg/kg); TH, high-dose telmisartan alone group (12 mg/kg); TLD, low-dose telmisartan (2 mg/kg) and dapagliflozin (1 mg/kg) combination group; THD, high-dose telmisartan (8 mg/kg) and dapagliflozin (1 mg/kg) combination group; CL, low-dose candesartan alone (0.8 mg/kg); CH, high-dose candesartan alone group (3.2 mg/kg); CLD, low-dose candesartan (0.8 mg/kg) and dapagliflozin (1 mg/kg) combination group; CHD, high-dose candesartan (3.2 mg/kg) and dapagliflozin (1 mg/kg) combination group.

The blood pressure-lowering effect was compared between the three types of ARBs co-administered with dapagliflozin (Figure 11). No significant differences in SBP showed between the same-level group of ARBs, which were determined based on the clinical dosages (FL, 206.4±16.80; FH, 202.9±19.40; TL, 206.4±19.29; TH, 197.3±25.25; CL, 205.2±166.98; CH, 194.8±23.51 mmHg). On the other hand, when combined with dapagliflozin, the mean SBP of the low-dose groups were 201.2±19.13 mmHg, 192.7±21.97 mmHg, and 204.0±22.45 mmHg for FLD, TLD, and CLD, respectively, with telmisartan showing minimum level (Figure 11A). The high-dose group also had 190.5±21.32 mmHg, 172.2±25.28 mmHg, and 194.8±23.51 mmHg in the FHD, THD, and CHD groups, respectively, and telmisartan was lowest (Figure 11B). In the case of the low-dose groups, TLD showed a significantly lower SBP value than others, 178.4 and 181.0 mmHg on Day 4 (-1 and 1 h). At the same time, FLD was 181.9 and 190.4 mmHg, and CLD was 201.1 and 205.7 mmHg, respectively (Figure 11A). The high-dose combination groups showed significant differences between drugs in more numerous time points; Day 4 (-1 and 3 h), Day 7 (-1 and 1 h), Day 10 (-1 and 3 h), and Day 13 (-1 and 1 h) (Figure 11B). In addition, the THD group maintained lower blood pressure compared to FHD and CHD at Re3 and 5, at 178.1 and 195.9 mmHg, respectively.

In summary, among the three ARBs, telmisartan showed the best blood pressure reduction when combined with dapagliflozin. In particular, the high-dose group showed an earlier decline and an increase in the maintenance period compared to fimasartan and candesartan.

1-2.2. Interaction with angiotensin receptor type 1

A molecular docking study was conducted to determine whether dapagliflozin's additional blood pressure-lowering effect in combination was due to the interaction with AT1, the target of ARB. The binding affinities of ARBs were determined to be -10.6, -9.7, and -8.7 kcal/mol for telmisartan, candesartan, and fimasartan, respectively (Table 3). The binding affinity of dapagliflozin was -8 kcal/mol. Fimasartan and candesartan formed the same hydrogen bond with THR88 as Ang2 (Table 4). Telmisartan, in contrast, forms hydrogen bonds with TYR35, TYR292, and SER109. Dapagliflozin formed a hydrogen bond with ALA21 and demonstrated van der Waals interactions with THR88 and TYR35, common binding sites of ARB. Notably, all four drugs exhibited pi-pi stacked binding with TRP84. On the other hand, it is noteworthy that when dapagliflozin was pre-bound, the binding affinity of telmisartan to AT1 slightly increased from -10.6 to -10.9 (Table 3). No such change was observed with fimasartan, whereas Ang2 and candesartan demonstrated a slight uptick to -9.4 and -9.8, respectively. In contrast, when the binding of dapagliflozin to the AT1 structure, to which each ARB had already bound, was investigated, the binding affinity did not significantly change from -7.9 to -8 (Table 3). In the structure where fimasartan and telmisartan were combined, hydrogen bonds with TYR184 and ARG167 were observed. In addition, hydrogen bonds with PRO95, ASN98, and GLU1004 were observed in the candesartan-bound structure (Supplementary Figure 5).

In summary, dapagliflozin exhibited a binding form partially similar to ARBs. When dapagliflozin was pre-bound, the binding affinity of telmisartan to AT1 was increased. On the other hand, when AT1 was pre-bound with candesartan, the binding structure of dapagliflozin showed different patterns with other ARBs. In the context of these results, it was substantiated that the enhancement in blood pressure regulation attributable to dapagliflozin could be partially ascribed to interaction with AT1.

Table 3. Binding affinities of angiotensin receptor type 1 with ARBs and dapagliflozin.

	Binding affinity (kcal/mol)		
	AT1	Pre-bonded with dapagliflozin	Pre-bonded with ARBs
Angiotensin-II	-9.3	-9.4	-
Dapagliflozin	-8	-	-
Fimasartan	-8.7	-8.7	-7.9
Telmisartan	-10.6	-10.9	-7.9
Candesartan	-9.7	-9.8	-8

Table 4. Interactions of angiotensin receptor type 1 with angiotensin-II, ARBs and dapagliflozin.

AT1	Hydrogen bond	Hydrophobic interaction
Angiotensin-II	SER16, TRP84, THR88, SER109, ARG167	LEU13, SER15, CYS18, PRO19, ARG23, TYR35, PHE77, LEU81, TYR87, TYR92, VAL108, LEU112, VAL179, ALA181, TYR184, LYS199, TRP253, ASP263, ILE266, GLN267, ASP281, MET284, ILE288, TYR292
Dapagliflozin	ALA21	TYR35, TRP84, TYR87, THR88, TYR92, VAL108, PRO285, ILE288, TYR292
Fimasartan	THR88	PRO19, ALA21, ARG23, ILE31, TYR35, TRP84, TYR87, TYR92, ARG167, ILE172, VAL179, CYS180, PRO285, ILE288
Telmisartan	TYR35, SER109, TYR292	PHE77, LEU81, TRP84, TYR87, THR88, VAL108, LEU112, ARG167, VAL179, ALA181, TRP235, HIS256, THR260, ILE288
Candesartan	THR88, ARG167, CYS180	TYR35, TRP84, TYR87, VAL108, VAL179, ALA181, PHE182, TYR184, ASP281, MET284, PRO285, ILE288

1-2.3. Vasorelaxation

As another mechanism of SBP-control improvement, the vasorelaxation effects of three types of ARBs and dapagliflozin were investigated in the thoracic aorta of WKY rats. Aortas were constricted with 1 μM of PE, and drugs were treated in a concentration-dependent manner. All four drugs showed vasorelaxation effects in the aorta over 50% at the final concentration of 500 μM , and there was no significant difference between the drugs and single and combined treatments. Dapagliflozin had an EC_{50} of 0.17 μM and $77.2 \pm 10.49\%$ of vasorelaxation at a concentration of 500 μM (Figure 12). Although not significant, dapagliflozin exhibited superior vasorelaxation activity compared to ARBs. The EC_{50} of fimasartan was 0.9 μM , the combination treatment was 0.41 μM , and the vasorelaxation rate was $58.1 \pm 24.86\%$ at a concentration of 500 μM when treated alone and $58.7 \pm 22.07\%$ when combined with dapagliflozin (Figure 12A). The EC_{50} of telmisartan was 0.35 μM in the single group and 0.16 μM in the combination group. At a concentration of 500 μM , the vasorelaxation rate was $67.5 \pm 6.92\%$ in the single group and $75.0 \pm 16.12\%$ in the combination treatment (Figure 12B). The EC_{50} of candesartan was 0.49 μM in the single treatment and 0.23 μM in the combination treatment. The vasorelaxation at 500 μM was $64.0 \pm 12.34\%$ in the single treatment and $73.6 \pm 5.43\%$ in the combination treatment, appearing at a higher level (Figure 12C). Although not significant, dapagliflozin exhibited superior vasorelaxation activity compared to ARBs.

Since NO, an endothelial-derived vasodilator that controls the relaxation of the aorta, is produced by eNOS activation, the phosphorylation level of eNOS after treatment with ARB and dapagliflozin was examined in the EA. hy926 cell line (Figure 12D). The activation level of eNOS, as indicated by the ratio of phosphorylated eNOS to eNOS, increased approximately 1.8-fold compared to the control group when dapagliflozin was treated. The co-treatment of dapagliflozin with either fimasartan or candesartan led to a significant increase of 1.6 times

relative to the control group. Meanwhile, the single treatment of ARBs increased than control at 1.4, 1.2, and 1.4 times for fimasartan, telmisartan, and candesartan, respectively. In summary, results confirmed that dapagliflozin and three types of ARBs showed direct vasorelaxation effects. In addition, when combined treatment of fimasartan and candesartan with dapagliflozin showed an increased level of eNOS activation compared to alone.

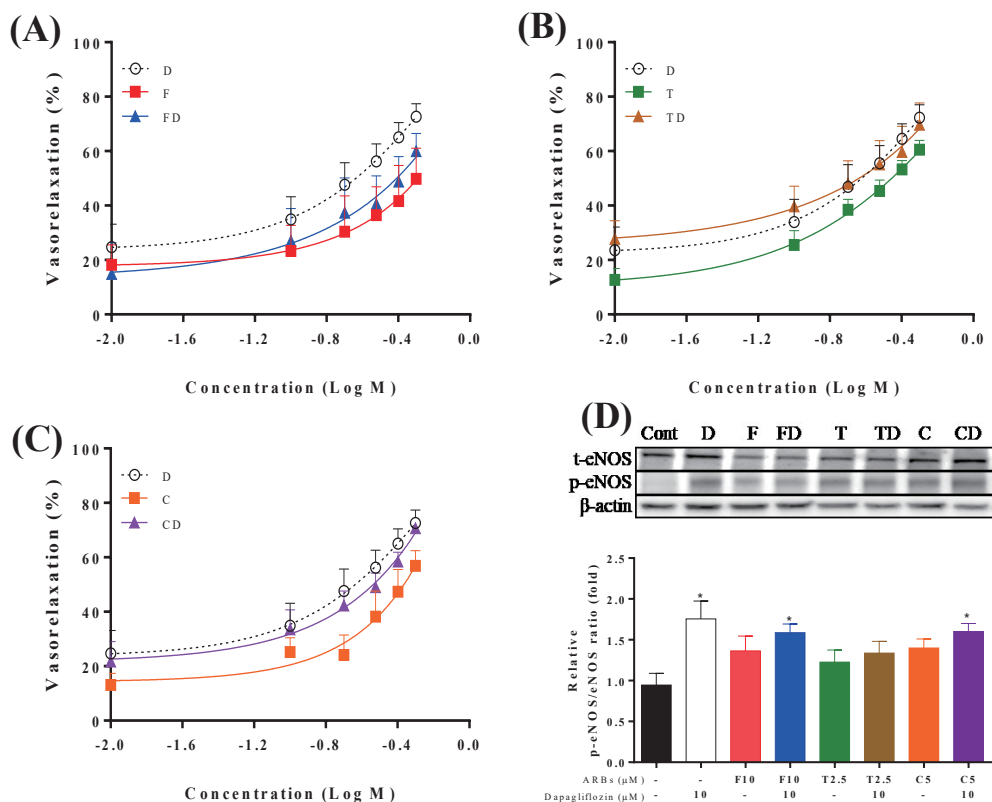


Figure 12. Effects of vasorelaxation and eNOS activation of ARBs and dapagliflozin.

Male Wistar Kyoto rats were euthanized using CO₂ gas, and the thoracic aorta was excised. Then, the aorta was placed in an organ bath with Krebs solution for measuring the contractile and relaxation using a myograph. The responses to drug treatments were calculated based on phenylephrine (PE) induced contracted tension. EA.hy926 cells were treated with drugs for 24 hours and extracted protein. The expression levels of eNOS and p-eNOS were performed by western blotting. To investigate the activation level of eNOS, we normalized the expression level of p-eNOS to the total eNOS protein. The relative ratio was calculated using the control (-/-). (A) vasorelaxation effects of fimasartan and dapagliflozin. (B) vasorelaxation effects of telmisartan and dapagliflozin. (C) vasorelaxation effects of candesartan and dapagliflozin. (D) eNOS activation in ARBs and dapagliflozin-treated EA.hy926 cells. All data are expressed as mean ± standard error mean. *, ** means a significant difference at the p < 0.05 and 0.01 levels compared to the control group. Cont, normal control; D, dapagliflozin; F, fimasartan; FD, fimasartan with dapagliflozin combined treatment; T, telmisartan; TD, telmisartan with dapagliflozin combined treatment; C, candesartan; CD, candesartan with dapagliflozin combined treatment.

1-2.4. Combination with hydrochlorothiazide

During the experimental period, all the dapagliflozin-administrated groups showed increased water intake (Supplementary Figure 1 to 3). Therefore, alterations in fluid volume could be an additional mechanism underlying the synergistic effect of dapagliflozin on blood pressure reduction. Consequently, we selected telmisartan as the representative ARB to compare the results of dapagliflozin and HCTZ, the most frequently used diuretic in combination with ARBs.

The mean SBP during the experimental period in the hydrochlorothiazide-administrated group (TZ) was 202.7 ± 4.11 mmHg, which showed a decrease compared to 220.1 ± 1.41 mmHg in the control group and 220.6 ± 0.95 mmHg in the dapagliflozin group, but not significant (Figure 13A). The mean SBP of the combination of telmisartan with the dapagliflozin (TelD) group was 166.4 ± 4.61 mmHg, and the telmisartan and HCTZ combination group (TelTZ) was 144.7 ± 9.49 mmHg, indicating that TelTZ reduced blood pressure better. On the other hand, TelD showed significantly lower SBP than the control group from Day 1 (3h), and the TelTZ group showed from Day 4, confirming that the TelD group has an earlier reduction. The hourly mean SBP values of the telmisartan alone group (Tel) and the combination groups were significantly lower than the control group at -1 h, 1 h, and 3 h (Figure 13B). The TZ group showed a significant decrease compared to the control group only at -1 h. On the other hand, the mean SBP of the TelTZ group at -1h and 3h was significantly lower than the TelD group, but there was no significant difference at 1h.

The amount of water intake investigated before administration, on the 14th day of administration, and on the seventh day after the end of administration was as follows (Figure 13C). On Day 14, the water intake volume in the dapagliflozin and the TelD groups significantly increased compared to the control group. Increased water intake of the

dapagliflozin-administrated groups was returned to normal value on Re7. On the other hand, the TZ and TeTZ groups did not show significant changes in water intake. In summary, the combination of dapagliflozin and telmisartan resulted in less SBP reduction than HCTZ and telmisartan, but a significant decrease was observed earlier.

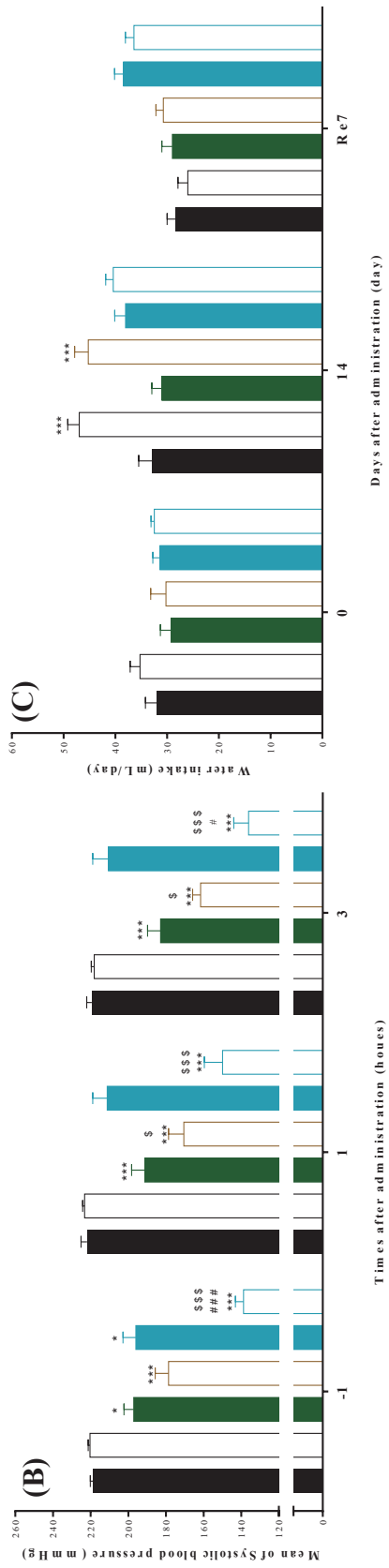
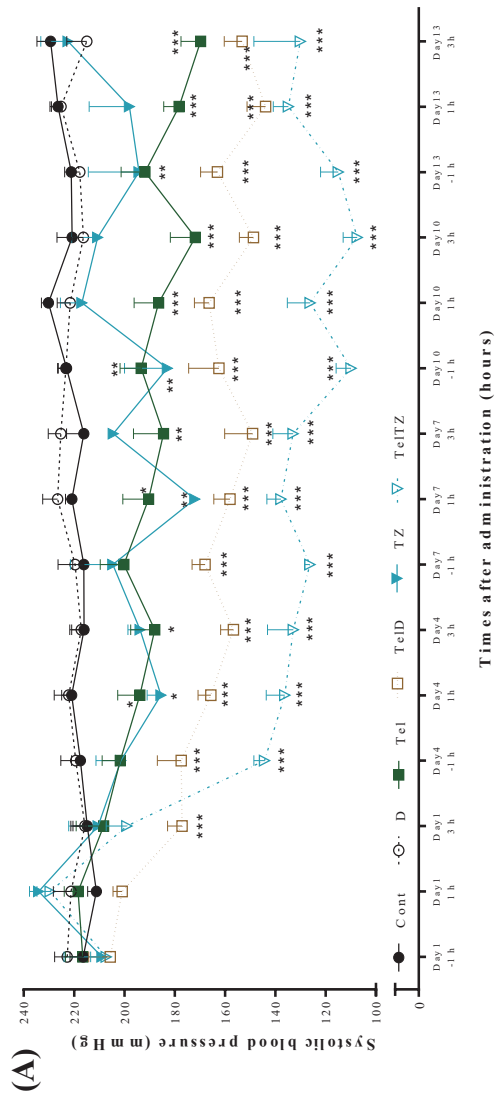


Figure 13. Effects of dapagliflozin, hydrochlorothiazide, and telmisartan on systolic blood pressure and water intake.

All experimental animals received oral drug administration once a day for two weeks. Systolic blood pressure (SBP) was measured one hour before (-1 h), one hour after (1 h), and three hours after (3 h) administration. The water intake was measured before (0), after (14), and seven days after (Re7) drug administration. (A) SBP of SHR was administered individually/combined with telmisartan, dapagliflozin, and HCTZ. (B) The mean SBP at each time point for the entire days of the experimental period. (C) Daily water intake volume of SHR administered individually/combined with telmisartan, dapagliflozin, and HCTZ. All data are expressed as mean \pm standard error mean. *, **, *** means a significant difference at the $p < 0.05$, 0.01 , and 0.001 levels compared to the control group. ^{s, \$\$\$} means a significant difference at the $p < 0.05$ and 0.001 levels exists between the combined and single administration groups. ^{#, ###} means a significant difference between the TeID and TeITZ groups at the $p < 0.05$ and 0.001 levels. Cont, SHR control group; D, dapagliflozin alone group (1 mg/kg); Tel, telmisartan alone (8 mg/kg); TeID, telmisartan (8 mg/kg) and dapagliflozin (1 mg/kg) combination group; TZ, hydrochlorothiazide alone (15 mg/kg); TeITZ, telmisartan (8 mg/kg) and hydrochlorothiazide (15 mg/kg) combination group.

1-3. Discussion

In this study, we investigated the blood pressure-lowering effects of dapagliflozin in combination with fimasartan, telmisartan, and candesartan. Our results demonstrate that dapagliflozin enhances the blood pressure-lowering effect of ARBs, with telmisartan exhibiting particularly notable effects. This enhancement is attributed to several factors, including the interaction with the AT1 and renal pumps, vasorelaxation through eNOS activation, and regulation of body fluid volume.

Hypertension is a severe public health issue worldwide. Pharmacological treatments for hypertension typically include various antihypertensive agents, such as ARBs, CCB, and diuretics [80]. However, using these agents alone may not adequately control blood pressure in some patients, necessitating combination therapy [102, 140]. Our study findings also indicated an insufficient reduction in blood pressure in SHR when administered with low doses used in clinical. Dapagliflozin is a type of SGLT2 inhibitor known to positively affect the cardiovascular system in various clinical trials. Several studies have demonstrated that dapagliflozin administration can effectively reduce blood pressure in patients with type 2 diabetes [141]. In clinical practice, short-term administration of SGLT2 inhibitors (12 weeks or less) has been shown to reduce SBP by 3-5 mmHg, while long-term treatment of more than one year can decrease SBP by 4-6 mmHg [142, 143]. However, dapagliflozin did not show significant blood pressure changes in this study. Some studies have reported that canagliflozin, an SGLT2 inhibitor, can temporarily increase blood pressure during the first two weeks of administration and that administering canagliflozin and empagliflozin for eight weeks increases plasma Ang2 and aldosterone concentrations [144, 145]. In addition, studies have also shown that dapagliflozin does not affect short-term blood pressure fluctuations in type 2 diabetic patients [146]. As such, short-term administration of SGLT2 inhibitors can activate

compensatory blood pressure increase mechanisms such as RAAS for preserving body fluid volume. Therefore, the two-week dosing period in this study may have been insufficient to demonstrate a significant reduction in blood pressure due to dapagliflozin.

Although dapagliflozin could not reduce blood pressure in this study, it was confirmed that the combined administration of fimasartan and telmisartan with dapagliflozin significantly lowered blood pressure and extended the duration of response compared to the same dose of the monotherapy group. Indeed, some clinical studies reported that combination therapy with SGLT2 inhibitors and ACE inhibitors/ARBs reduced SBP and 24 h ambulatory SBP compared with ACEIs/ARBs alone [42, 147]. Additionally, studies showed that dapagliflozin could be tolerated and improve BP control in T2DM patients with inadequately controlled hypertension despite using a therapeutic dose of ACE inhibitor or ARB [142]. One possible mechanism for this is that dapagliflozin reduces Ang2 by down-regulating the renal RAAS component expression [148]. Our results show that dapagliflozin has a similar hydrophobic binding with ARB to AT1. It was confirmed that dapagliflozin could bind to several residues of AT1 that have been reported in the literature to participate in Ang2 binding, specifically Thr88 and Tyr92 [149]. In addition, docking results of fimasartan and telmisartan pre-bounded AT1 and dapagliflozin showed notable interactions with TYR184, known as Ang2's interaction site. On the other hand, when pre-bounded with candesartan, which did not show a synergistic effect with dapagliflozin in blood pressure, dapagliflozin showed a completely different binding form from that of Ang2 and other drugs. It means that TYR184 hydrogen bond with dapagliflozin, seen when fimasartan and telmisartan were pre-bounded, may affect the improvement in blood pressure control by dapagliflozin. Our findings also suggested that drugs exhibit a high binding affinity for sodium/potassium ATPase, aquaporin 2, and MR. This implies that it not only inhibits AT1 but also influences the subsequent mechanisms of aldosterone and Ang2, which are known to increase blood pressure [26, 150]. Notably, the MR

is activated by aldosterone and promotes the reabsorption of sodium ions in the kidneys, thus water reabsorption [24]. The results that dapagliflozin demonstrated a high binding affinity of -7.1 with the MR raises the possibility that it can affect the functions of other RAAS components beyond interfering with AT1.

Indeed, since we observed an increase in water intake by dapagliflozin administration, it was necessary to compare the effects of dapagliflozin with thiazide diuretics, which are most commonly used in combination with ARBs (Supplementary Figure 1 to 3). Several clinical studies have reported that dapagliflozin and thiazide can reduce blood pressure, body weight, and GFR by reducing body fluid volume by 7% and 8% [144]. When telmisartan, which demonstrated the highest increase, was administered with thiazide diuretics, blood pressure was significantly decreased. Meanwhile, the dapagliflozin combination-administered group exhibited a marked decrease in blood pressure at one and three hours, and the HCTZ combination group showed at 23 hours. As a basis for these differences in the duration of action, some studies on the combination of telmisartan and HCTZ reported that more effective 24-hour blood pressure control was possible [104, 105]. On the other hand, an increase in water intake appeared only in the dapagliflozin-treated group. Several studies have reported that HCTZ does not affect water intake even though it increases urine volume, and SGLT2 inhibition includes a compensatory increase in water intake as part of a homeostatic mechanism [151-153]. It may be due to the different diuretic mechanisms of the two drugs; dapagliflozin has an osmotic diuretic effect by blocking glucose reabsorption in the kidneys to reduce body fluid volume. On the other hand, HCTZ increases urine volume by inhibiting the reabsorption of sodium and chloride ions in the kidneys. As a basis for the difference in the effects, several studies have reported that dapagliflozin decreases plasma volume, which is not observed with HCTZ and reduces GFR more than HCTZ [144, 154]. Meanwhile, HCTZ can cause electrolyte imbalances such as hypokalemia and hyponatremia and other side effects

such as hyperuricemia and glucose intolerance [151, 155]. However, dapagliflozin has been reported not to affect electrolytes, and since it is a drug that improves glucose imbalance, one of the most significant risks of thiazide, it can be used as a safer combination drug with ARB. Our results showed no significant differences in the mean SBP among the three ARB-administered groups. However, when combined with dapagliflozin, telmisartan showed the most significant reduction in blood pressure. Specifically, the high-dose group exhibited an earlier decline in blood pressure and a more extended maintenance period than fimasartan and candesartan. These differences can be partly due to pharmacokinetic profile differences. Among the three drugs, the half-life of telmisartan is 24 hours, whereas the half-lives of fimasartan and candesartan are 7-10 hours and 5-9 hours, respectively, shorter than telmisartan. Moreover, several studies of concomitant administration have shown that combining candesartan and thiazide improves candesartan's bioavailability, increasing C_{max} and half-life, while the co-administration of telmisartan and thiazide has not shown significant changes in pharmacokinetic profile [156, 157]. On the other hand, the combination of telmisartan and canagliflozin study showed that the tissue concentration of each drug could increase [158]. As such, pharmacokinetic changes in combination may vary depending on the structure and characteristics of the drug. In other words, our study's different interactions with dapagliflozin may be due to pharmacokinetic characteristics, including excretion route and lipophilicity. The lipophilicity of the three ARBs is significantly higher for telmisartan, with a log P value of 7.1, compared to fimasartan at 5.8 and candesartan at 3.5. Lipophilicity constitutes the essential property in drug action, influencing pharmacokinetic and pharmacodynamics processes and toxicity [159]. Due to this difference in lipophilicity, the excretion route of the three drugs also differ; telmisartan and fimasartan urinary excretion is less than 1% and less than 3%, respectively, whereas candesartan is excreted in urine at 33-59% [160, 161]. Lipophilicity is the fundamental property that is overwhelmingly involved in most antihypertensive agents, so

in most cases, the hydrophobic interaction plays a significant role in drug action [162]. Indeed, in our results, telmisartan showed the highest binding affinity and various hydrophobic interactions. However, further studies are needed to elucidate these differences and their impact on therapeutic interventions. These differences may be affected by individual patient characteristics, administration dose, and duration, so a careful approach is required.

As another mechanism, dapagliflozin improves endothelial function via normalizing eNOS levels in non-diabetic and heart failure animal models; it appeared distinct from its blood glucose reduction [163, 164]. In our results, dapagliflozin demonstrated superior vasorelaxation activity compared to ARBs. In addition, when fimasartan and candesartan were combined with dapagliflozin, they showed increased eNOS activation compared to alone. This finding suggests that the blood pressure-lowering enhancement effect brought about by dapagliflozin might be partially attributed to its direct vasorelaxation properties.

In summary, dapagliflozin enhanced the blood pressure-regulating efficacy of ARBs, especially telmisartan, leading to beneficial outcomes such as reduced blood pressure, extended blood pressure maintenance, and shortened duration of action. These outcomes are anticipated to be associated with mechanisms including vasorelaxation, Ang2 receptor modulation, and diuretic activity. However, it's noted that this study has certain limitations. While dapagliflozin is an anti-diabetic drug, our study used non-diabetic, hypertensive animal models. Additionally, more evidence should be given regarding changes in urine volume and the associated mechanisms. In a subsequent part of our study, we plan to investigate more specific mechanisms using aged SHR models with coexisting hyperglycemia to address this.

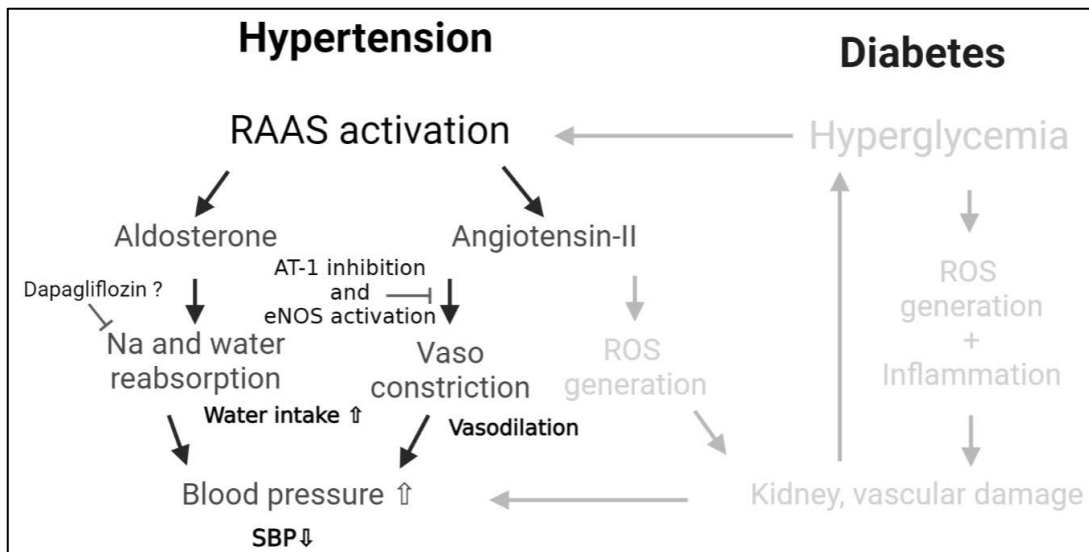


Figure 14. The anti-hypertensive effects of dapagliflozin and ARBs.

Part 2. Vascular Protection of ARB and Dapagliflozin

2-1. Materials and methods

2-1.1. Materials and experimental animals

The ARBs, including fimasartan, telmisartan, and candesartan cilexetil, were provided by Dr. Yong-Ha Ji. The SGLT2 inhibitor dapagliflozin was obtained as Forxiga™ tablets containing 10 mg of the active ingredient.

SHRs were purchased from Charles River and housed at the Jeju National University animal facility for at least seven days before use in the experiments. Animals were fasted for four hours before drug administration, and water was provided *ad libitum*. The animals were housed under controlled conditions with a temperature of $22 \pm 5^\circ\text{C}$, a humidity of $50 \pm 10\%$, and a 12-hour light/dark cycle. All animal experiments were performed under the guidelines of the ‘Institutional Animal Care and Use Committee at Jeju National University’ (protocol number: 2018-0019).

2-1.2. Experiment

Male SHR rats, 60-65 weeks of age and weighing between 380-420 g, were used in this study with four to five animals per group. The experimental groups consisted of a control group, a dapagliflozin single administration group, low and high doses of ARB single administration groups, and low and high doses of ARB and dapagliflozin combination groups (Figure 6). All doses were calculated using body surface area conversion factors from FDA, which provides an equivalent dose relative to clinical applications; dapagliflozin 1 mg/kg, fimasartan 3 and 12 mg/kg, telmisartan 2 and 8 mg/kg, and candesartan 0.8 and 3.2 mg/kg. The animals were administered with drugs for one week and euthanized with CO₂ gas, and aortas were collected.

2-1.3. Measuring vasorelaxation

The thoracic aorta was prepared into 3-5 mm sections, suspended to metal rings, and mounted

to isometric force-displacement transducers. Aortas were placed on the organ bath filled with 37°C Krebs buffer, which was adjusted to pH 7.4 while supplying 95% O₂ and 5% CO₂ gas (Figure 7). The tension of the aorta was adjusted to 1.0 g and stabilized for two hours with solution changes every 20 minutes. After stabilization, the aortas were pre-contracted with 1 μM PE. When the contractile response was stabilized, relaxation was evaluated by cumulative addition of acetylcholine (Ach, 10⁻¹⁰ to 10⁻⁵ M). The changes in vascular tone in response to Ach treatment were recorded using a physiograph recorder and quantified using the Chart7 program. The levels of vasorelaxation responses by treatment were calculated based on PE-induced contracted tension.

2-1.4. Cell culture

(1) Raw-Blue™ cells: Mouse macrophage reporter cell line, Raw-Blue™ (InvivoGen, CA, US), was cultured in DMEM supplemented with 10% FBS, 100 U/mL P/S, and 100 μg/mL Normocin (InvivoGen). Cells were seeded into a 96-well culture plate and treated with drugs and lipopolysaccharide (LPS, Sigma, MO, US).

(2) Raw264.7 cells: The mouse macrophage cell line, Raw264.7, was cultured in DMEM supplemented with 10% FBS and 100 U/mL P/S. Cells were seeded into a 90 mm plate and treated with LPS. After 24 hours, the cell culture supernatant was collected by centrifugation at 3,000 rpm for 10 minutes and used as an LPS-treated conditioned medium (L/CM).

(3) EA. hy926 cells: EA. hy926 cells were seeded into a 96-well, 6-well plate, or 90 mm plate and treated with L/CM and drugs. The cells were collected 1 hour and 24 hours after treatment. All drug doses were selected based on their non-toxic doses, as confirmed by the MTT assay and aligned with the reported maximum serum concentration (Supplementary Figure 9).

2-1.5. Nitrite measurement

After the treatment described in 2-1.4(1), nitrite levels were measured using the Griess assay. The cell culture supernatant was mixed with an equal volume of Griess reagent (sigma) and incubated for 15 minutes at room temperature. The absorbance was measured at 540 nm. All results were quantified by drawing a standard curve with sodium nitrite and expressed as a percentage of the negative control group treated with LPS.

2-1.6. Reporter gene assay

After the treatment described in 2-1.4 (1), Secreted embryonic alkaline phosphatase (SEAP) levels were measured to evaluate the level of NF- κ B activation. Briefly, the cell culture medium was incubated with QUANTI-Blue™ (InvivoGen) reagent for 1 hour at 37°C, and the absorbance was measured at 620 nm. The inhibition of NF- κ B activation was expressed as a percentage relative to the LPS-treated control group.

2-1.7. ROS generation

The permeable fluorescent dye, 2',7'-dichlorodihydrofluorescein diacetate (H₂DCF-DA), was used to measure intracellular ROS production. H₂DCF-DA reacts quickly with ROS, forming the fluorescent product 2,7-dichlorofluorescein (DCF), and the intracellular fluorescence intensity of DCF is proportional to the amount of ROS the cell generates. After treatment, according to the instructions in section 2-1.4 (3), the cells were incubated with 20 μ M H₂DCF-DA (Invitrogen, MA, US) for 30 minutes. After washing with PBS, the intracellular fluorescence intensity of DCF (excitation 492-495 nm, emission 517-527 nm) was measured using a plate reader (SynergyHTX, Agilent, CA, US). The results were expressed as a percentage of the L/CM treatment group.

2-1.8. Protein Analysis

(1) Protein Preparation: The aortic tissues from experimental animals were disrupted using RIPA buffer with Tissue Lyser-II (Qiagen, Germany). The homogenate was centrifuged at 13,000 rpm, 4°C for 15 minutes, and the supernatant was collected. The cells were treated according to 2-1.4, washed with PBS, and then solubilized in RIPA buffer for 30 minutes. The solution was centrifuged at 13,000 rpm for 15 minutes at 4°C, and the resulting supernatant was collected. To obtain cytoplasm and the nuclear fraction, cells were first solubilized with cytoplasmic extraction buffer for 10 minutes on ice and then centrifuged at 3,000 rpm for ten minutes at 4°C. The resulting supernatant was collected, the residue was solubilized with nuclear extraction buffer for 30 minutes on ice, and the supernatant was collected after centrifugation at 13,000 rpm for 20 minutes.

(2) Western Blotting: The protein contents of lysates were quantified using the Bradford assay, and the same amount of protein was mixed with sample buffer and denatured. 30 µg of protein per well was loaded onto 8-12% SDS-PAGE and electrophoresed at 120-150 V for one hour. The separated proteins were transferred to the PVDF membrane at 100 V for two hours using wet transfer methods. After washing with TBST, the membranes were blocked with 5% blocking grade buffer for 30 minutes to prevent nonspecific binding. The membranes were incubated overnight at 4°C with primary antibodies. The following primary antibodies were used: anti-AMP-activated protein kinase (AMPK), p-AMPK, Microtubule-associated protein one light chain 3 (MAP1LC3B, LC3), and NLRP3 (Cell Signaling); anti-caspase-1, cyclooxygenase-2 (COX-2), ICAM-1, inducible nitric oxide synthase (iNOS), NF-κB, p-NF-κB, nuclear factor erythroid 2-related factor 2 (Nrf2), p47phox, sequestosome-1 (SQSTM1, p62), β-actin, α-Tubulin, and Lamin A (Santa Cruz Biotechnology). After washing, the membranes were incubated for one hour with a secondary antibody conjugated with HRP. The

protein was visualized using electrochemiluminescence and detected using Chemi-Doc molecular imaging system. The expression levels of each protein were obtained using the Evolution Capt software and normalized by housekeeping proteins (β -actin, α -Tubulin, and Lamin A) and further calculated to relative values based on control. The activation level was calculated by the expression ratio of the active form (p-AMPK, cleaved-caspase-1, and LC3-II) to the total protein (AMPK, caspase-1, and LC3-I). The activation level of NF- κ B and Nrf2 was calculated by the expression ratio of the nucleus to the cytosolic level.

(3) Immunocytochemistry: After treatment as described in section 2-1.4 (3), we performed immunocytochemistry to detect the p62 protein in the cells. Briefly, treated cells in a 6-well plate were washed with PBS and fixed with 100% methanol for five minutes. To block the non-specific binding, the cells were incubated with a solution containing 1% BSA and 22.52 mg/mL glycine in PBST (PBS with 0.1% Tween20) for 30 minutes. Then, the cells were incubated overnight at 4°C with the primary antibody (anti-SQSTM1, Santa Cruz Biotechnology). After washing, the cells were incubated for 1 hour with the secondary antibody (Goat anti-Mouse IgG Secondary Antibody-FITC, Invitrogen). Then, the cells were rewashed, and Hoechst was added for 5 minutes during the washing step. To prevent drying, PBS was added, and the cells were stored at 4°C until measurement. Fluorescence images were obtained using a real-time cell imaging system (BioTek-CYTATION5, Agilent, CA, US).

2-1.9. Statistical analysis

All data were presented as mean \pm SEM. Statistical analyses were performed using GraphPad Prism 6 program, conducting one-way and two-way ANOVA and using Tukey's post hoc test for significance verification. A p-value of less than 0.05 was considered significant.

2-2. Results

2-2.1. Endothelium-dependent vasorelaxation

The vascular reactivity of the aorta from aged SHR rats was examined seven days after drug administration to investigate the effect of dapagliflozin and ARB administration on Ach-induced endothelium-dependent vasorelaxation. All drug-treated groups showed a significantly increased vasorelaxation compared to 36.6±9.92% of the control group when treated with 10⁻⁵ M Ach (Figure 15). In particular, the EC₅₀ of the dapagliflozin-administrated group was 0.17 μM, which was significantly lower than that of the control group, which was 82.98 μM. In addition, when treated with 10⁻⁵ M Ach, the relaxation rate was also 72.1±4.62%, 1.9 times increased compared to the control group.

In the case of fimasartan, the relaxation rate of 10⁻⁵ M Ach treatment in the aortas of the FL group was 54.7±13.71%, which was significantly increased compared to the control group, but lower than that of 73.0±6.98% and 72.3±3.27% of the FH and FLD groups (Figure 15A). Meanwhile, the vascular reactivity of the FLD and FHD groups was not significantly different from that of the dapagliflozin group, and the EC₅₀ was 0.80 μM and 0.35 μM, respectively, which were higher than those of the dapagliflozin alone group. Fimasartan and dapagliflozin increased the endothelium-dependent vasorelaxation, and the combined administration increased relaxation more than fimasartan alone but had no synergistic effect.

In the case of telmisartan, the relaxation rates of the TL and TH groups when treated with 10⁻⁵ M Ach were 48.6±3.01% and 50.0±1.07%, respectively, which were significantly increased compared to the control group (Figure 15B). The TLD group showed the highest relaxation rate among the telmisartan groups at 53.8±1.19% when treated with 10⁻⁵ M Ach. On the other hand, the THD group not shown an increase compared to the control group in all concentrations of Ach. The TLD group showed a significantly higher relaxation rate than the

THD group when treated with 10^{-8} and 10^{-7} M Ach. The EC_{50} values of the TL, TH, TLD, and THD groups were also 4.72, 6.90, 2.81, and 21.10 μ M, respectively, with the TLD group showing the lowest levels. It was confirmed that low-dose telmisartan increased endothelium-dependent vasorelaxation, but combined administration of high telmisartan and dapagliflozin reduced the vasorelaxation of the two drugs.

In candesartan groups, the relaxation rate of the aortas of the CH group was significantly increased by $72.5 \pm 8.09\%$ when treated with 10^{-5} M Ach, compared to $55.4 \pm 3.35\%$ of the CL group (Figure 15C). Meanwhile, the CLD group showed $68.8 \pm 7.03\%$ and the CHD group $67.7 \pm 5.63\%$, displaying increased relaxation rates similar to dapagliflozin alone. However, the CLD group showed a significantly increased relaxation response compared to the CL group when treated with 10^{-8} , 10^{-7} , and 10^{-5} M Ach. In addition, the EC_{50} of the CL, CH, CLD, and CHD groups were 2.44, 0.41, 0.41, and 0.34 μ M, respectively, showing a significant decrease in the combination group compared to the single group. In other words, candesartan and dapagliflozin enhance endothelium-dependent vasorelaxation.

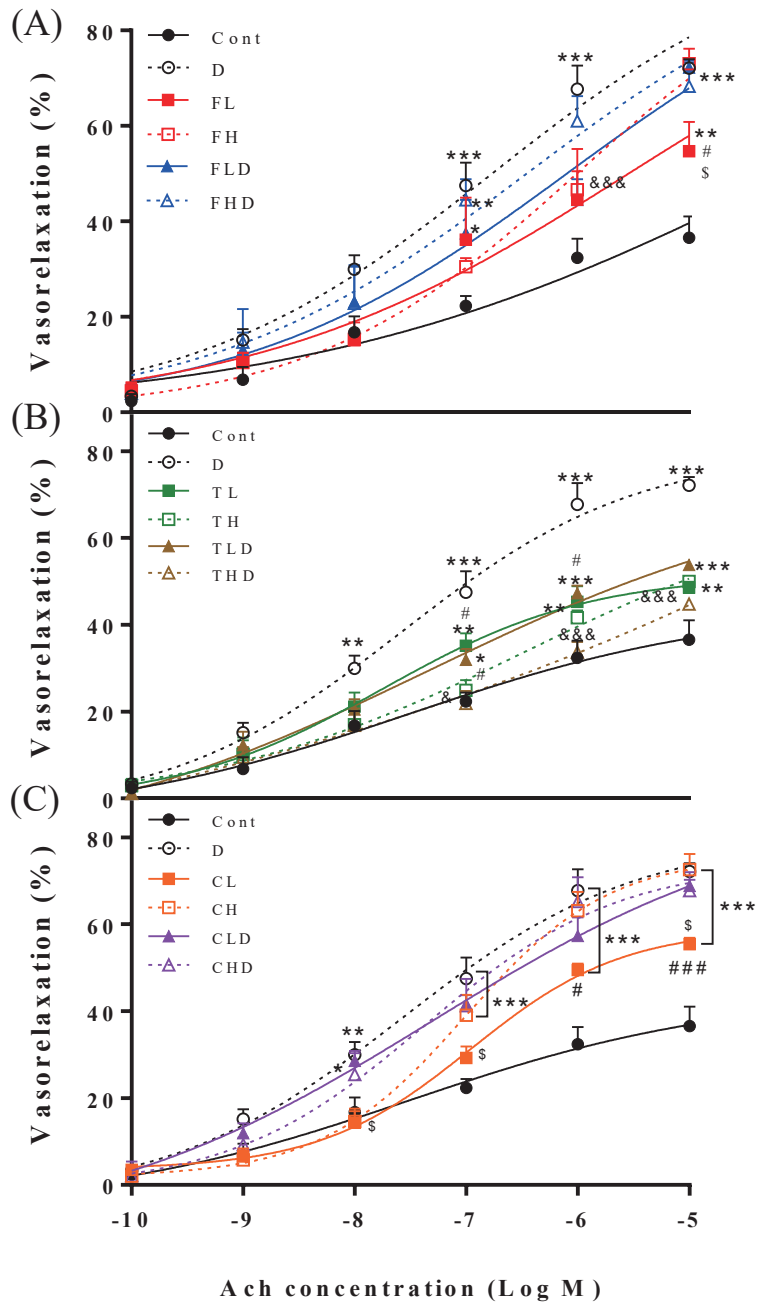


Figure 15. Effects of ARBs and dapagliflozin on acetylcholine-induced vasorelaxation in the aorta of aged SHR.

Male SHRs over 60 weeks of age received oral administration of the drugs for one week, and the aorta was excised after being euthanized using CO₂ gas. Aortas were placed in Krebs's buffer, and the vascular activity was measured

using a myograph. The responses of acetylcholine treatments in the aortas were calculated based on phenylephrine (PE) induced contracted tension. (A) Acetylcholine responsiveness of the aorta when administered with fimasartan and dapagliflozin alone and in combination. (B) Acetylcholine responsiveness of the aorta in administered with telmisartan and dapagliflozin alone and in combination. (C) Acetylcholine responsiveness of the aorta in administered with candesartan and dapagliflozin alone and in combination. All data are expressed as mean \pm standard error mean. *, **, *** means a significant difference at the $p < 0.05$, 0.01 , and 0.001 levels compared to the control group. &.&&& means a significant difference at the $p < 0.05$ and 0.001 levels compared to the dapagliflozin alone group. #, ### means a significant difference between the low and high concentration groups at the $p < 0.05$ and 0.001 levels. § means a significant difference at the $p < 0.05$ level exists between the same dose of the combined group and the single administration group. Cont, SHR control group; D, dapagliflozin alone group (1 mg/kg); FL, low-dose fimasartan alone (3 mg/kg); FH, high-dose fimasartan alone group (12 mg/kg); FLD, low-dose fimasartan (3 mg/kg) and dapagliflozin (1 mg/kg) combination group; FHD, high-dose fimasartan (12 mg/kg) and dapagliflozin (1 mg/kg) combination group; TL, low-dose telmisartan alone (2 mg/kg); TH, high-dose telmisartan alone group (12 mg/kg); TLD, low-dose telmisartan (2 mg/kg) and dapagliflozin (1 mg/kg) combination group; THD, high-dose telmisartan (8 mg/kg) and dapagliflozin (1 mg/kg) combination group; CL, low-dose candesartan alone (0.8 mg/kg); CH, high-dose candesartan alone group (3.2 mg/kg); CLD, low-dose candesartan (0.8 mg/kg) and dapagliflozin (1 mg/kg) combination group; CHD, high-dose candesartan (3.2 mg/kg) and dapagliflozin (1 mg/kg) combination group.

2-2.2. NOX/ROS and Nrf2

We examined molecules linked with oxidative stress to investigate the mechanisms of increased endothelium-dependent vasorelaxation. Dapagliflozin did not significantly affect the Nrf2 expression in both aortic and endothelial cells (Figure 16A and B). However, dapagliflozin significantly decreased aortic p47phox expression compared to the control group by 1.85-fold and significantly inhibited the inflammation-induced ROS generation in endothelial cells (Figure 16C and D).

Fimasartan also did not affect aortic Nrf2 expression, but notably, when combined with dapagliflozin, significantly elevated nuclear translocation of Nrf2 in endothelial cells to 2.11 ± 0.15 compared to L/CM controls (Figure 16A and B). Aortic p47phox expression significantly decreased in all fimasartan-treated groups, particularly in the FHD group, which showed a 1.84-fold decrease compared to the control group (Figure 16C). The inflammation-induced intracellular ROS generation in EA. hy926 cells were also significantly reduced at all concentrations (Figure 16D).

In summary, dapagliflozin and fimasartan exhibited ROS-reducing effects via decreasing NOX expression. Notably, although individual treatments did not affect Nrf2 activation, but when combined, Nrf2 activation in endothelial cells was synergistically increased.

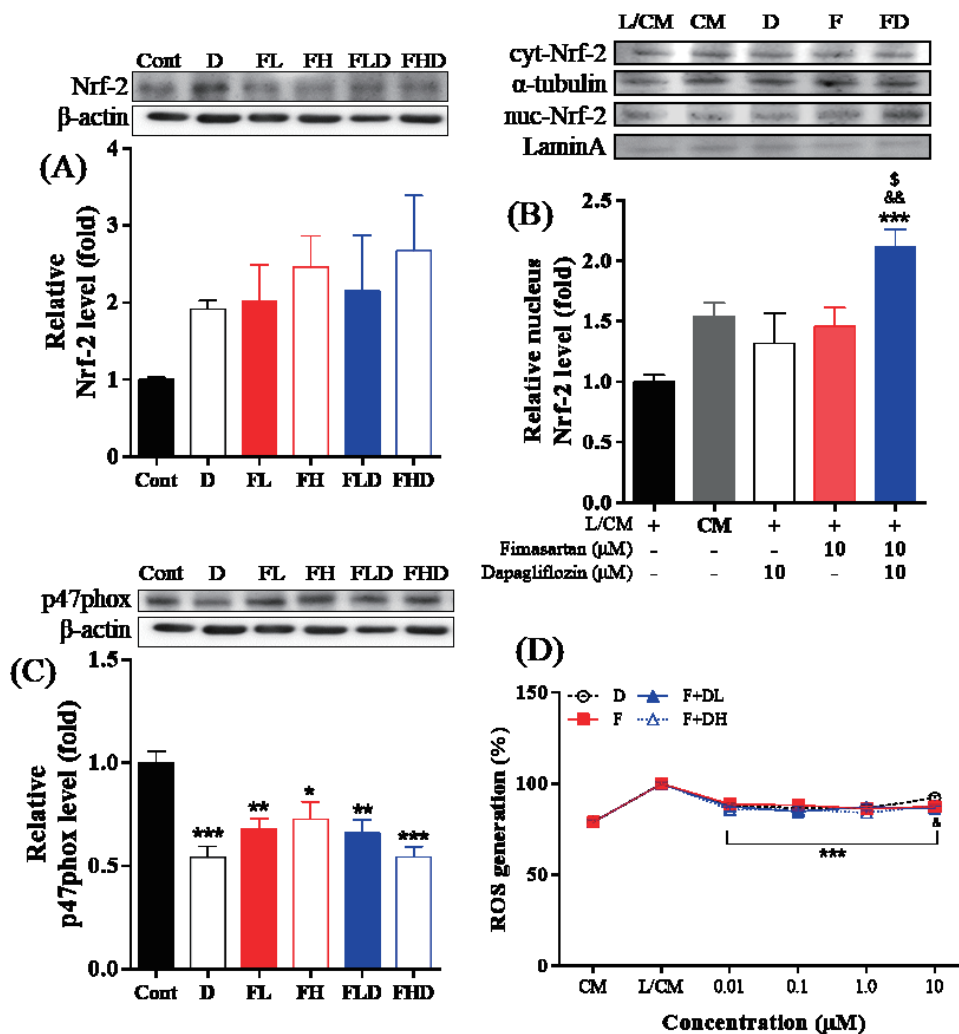


Figure 16. Effects of fimasartan and dapagliflozin on NOX/ROS and Nrf2 in the aorta of aged SHR and L/CM treated EA. hy926 cells.

Male spontaneously hypertensive rats (SHRs) over 60 weeks of age received oral administration of the drugs for one week. After one week of drug administration, the experimental animals were euthanized using CO₂ gas, and aorta proteins were extracted for performing western blotting. EA. hy926 cells were treated with drugs and L/CM for one or 24 hours, and protein was extracted for performing western blotting. Western blot images were visualized using the Chemi-Doc system. The expression levels of Nrf2 and p47phox in the aorta were normalized by β-actin. The expression levels of Nrf2 in the cytosol and the nucleus of EA. hy926 cells were normalized by α-tubulin and Lamin A. The intracellular ROS level was measured by H₂DCFDA assay. The relative ratio and percentage were

calculated based on the control and L/CM group. (A) The expression levels of Nrf2 in the aorta of SHRs administered with fimasartan and dapagliflozin alone and in combination. (B) The activation of Nrf2 in the EA. hy926 cells treated with fimasartan and dapagliflozin alone and in combination. (C) The expression levels of p47phox in the aorta of SHRs administered with fimasartan and dapagliflozin alone and in combination. (D) The intracellular ROS levels in the EA. hy926 cells treated with fimasartan and dapagliflozin alone and in combination. All data are expressed as mean \pm standard error mean. *, **, *** means a significant difference at the $p < 0.05$, 0.01 , and 0.001 levels compared to the control and L/CM group. ^s means a significant difference at the $p < 0.05$ level exists between the same dose of the combined group and the single group. &.&& means a significant difference at the $p < 0.05$ and 0.01 levels compared to the dapagliflozin alone group. Cont, SHR control group; D, dapagliflozin alone group (1 mg/kg); FL, low-dose fimasartan alone (3 mg/kg); FH, high-dose fimasartan alone group (12 mg/kg); FLD, low-dose fimasartan (3 mg/kg) and dapagliflozin (1 mg/kg) combination group; FHD, high-dose fimasartan (12 mg/kg) and dapagliflozin (1 mg/kg) combination group; D, dapagliflozin; F, fimasartan; FD, fimasartan 10 μ M with dapagliflozin 10 μ M combined treatment; F+DL, fimasartan with 0.01 μ M of dapagliflozin; F+DH, fimasartan with 10 μ M of dapagliflozin; L/CM, Raw264.7 cells culture media with LPS; CM, Raw264.7 cells culture media without LPS.

Telmisartan individual groups not shown significant effects on aortic Nrf2 expression, but the THD group significantly increased aortic Nrf2. Additionally, combined treatment significantly increased the nuclear translocation of Nrf2 also in endothelial cells, to 2.40 ± 0.22 , compared to the L/CM control group (Figure 17A and B). This was significantly higher than observed in treatment with dapagliflozin alone ($p < 0.01$). In contrast, aortic p47phox expression decreased only in the telmisartan-alone group; a p47phox level of the THD group showed as 0.97 ± 0.09 , which was significantly higher than the TH group ($p < 0.001$) (Figure 17C). Telmisartan significantly reduced the inflammation-induced increase in ROS across all concentrations in endothelial cells, with the reduction being particularly significant at a concentration of $10 \mu\text{M}$ (Figure 17D).

In summary, telmisartan showed the reduction of ROS by inhibiting NOX, but this effect was attenuated when administered in combination with dapagliflozin. In contrast, Nrf2 expression and activation synergistically increased when combined with dapagliflozin.

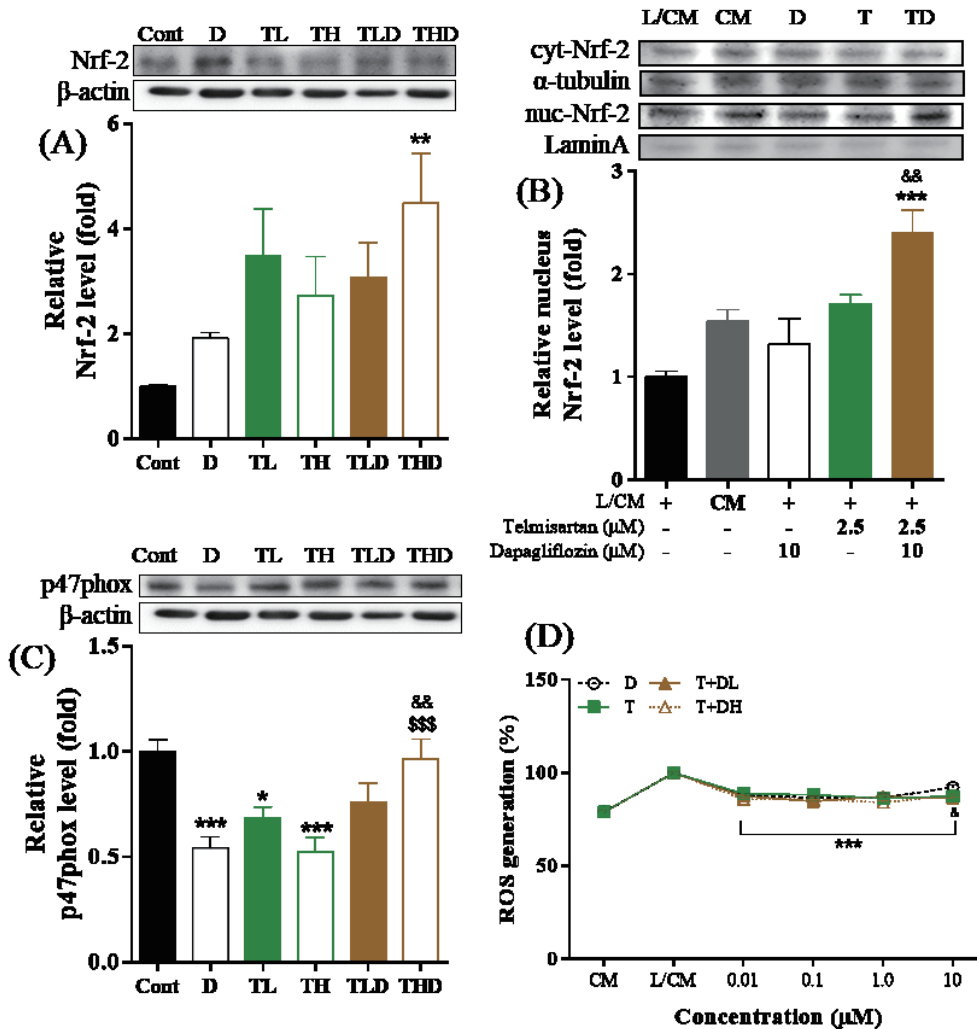


Figure 17. Effects of telmisartan and dapagliflozin on NOX/ROS and Nrf2 in the aorta of aged SHR and L/CM treated EA. hy926 cells.

Experimental progress is the same as described in Figure 16. (A) The expression levels of Nrf2 in the aorta of SHRs administered with telmisartan and dapagliflozin alone and in combination. (B) The activation of Nrf2 in the EA. hy926 cells treated with telmisartan and dapagliflozin alone and in combination. (C) The expression levels of p47phox in the aorta of SHRs administered with telmisartan and dapagliflozin alone and in combination. (D) The intracellular ROS levels in the EA. hy926 cells treated with telmisartan and dapagliflozin alone and in combination. All data are expressed as mean \pm standard error mean. *, **, *** means a significant difference at the $p < 0.05$, 0.01, and 0.001 levels compared to the control group. \$\$\$ means a significant difference at the $p < 0.001$ level exists

between the same dose of the combined group and the single group. & and && means a significant difference at the $p < 0.05$ and 0.01 levels compared to the dapagliflozin alone group. Cont, SHR control group; D, dapagliflozin alone group (1 mg/kg); TL, low-dose telmisartan alone (2 mg/kg); TH, high-dose telmisartan alone group (12 mg/kg); TLD, low-dose telmisartan (2 mg/kg) and dapagliflozin (1 mg/kg) combination group; THD, high-dose telmisartan (8 mg/kg) and dapagliflozin (1 mg/kg) combination group; D, dapagliflozin; T, telmisartan; TD, telmisartan 2.5 μM with dapagliflozin 10 μM combined treatment; T+DL, telmisartan with 0.01 μM of dapagliflozin; T+DH, telmisartan with 10 μM of dapagliflozin; L/CM, Raw264.7 cells culture media with LPS; CM, Raw264.7 cells culture media without LPS.

When administrated alone, candesartan did not affect the aortic Nrf2 (Figure 18A). In EA.hy926 cells, candesartan alone treatment increased change Nrf2 levels to 1.80 ± 0.27 relative to the L/CM control group, but not significant. However, when combined with dapagliflozin, it significantly increased the nuclear translocation of Nrf2 in endothelial cells to 2.08 ± 0.19 , compared to the L/CM control group (Figure 18B). Aortic p47phox showed a significant decrease in all groups treated with candesartan; the CHD group showed a 1.31-fold decline compared to the CLD group (Figure 18C). Interestingly, the CL group exhibited a 1.36-fold reduction in p47phox levels compared to the CH group. In addition, the CHD group showed significantly lower p47phox levels than the dapagliflozin alone group ($p < 0.05$). Inflammation-induced ROS increase in endothelial cells was significantly reduced at all concentrations. Notably, at a concentration of 10 μ M, both the C+DL and C+DH groups showed a significant reduction compared to dapagliflozin treatment alone ($p < 0.05$ and $p < 0.001$) (Figure 18D).

In summary, candesartan exhibited a ROS-reducing function by inhibiting NOX. Additionally, it demonstrated a synergistic interaction with dapagliflozin, enhancing Nrf2 activation.

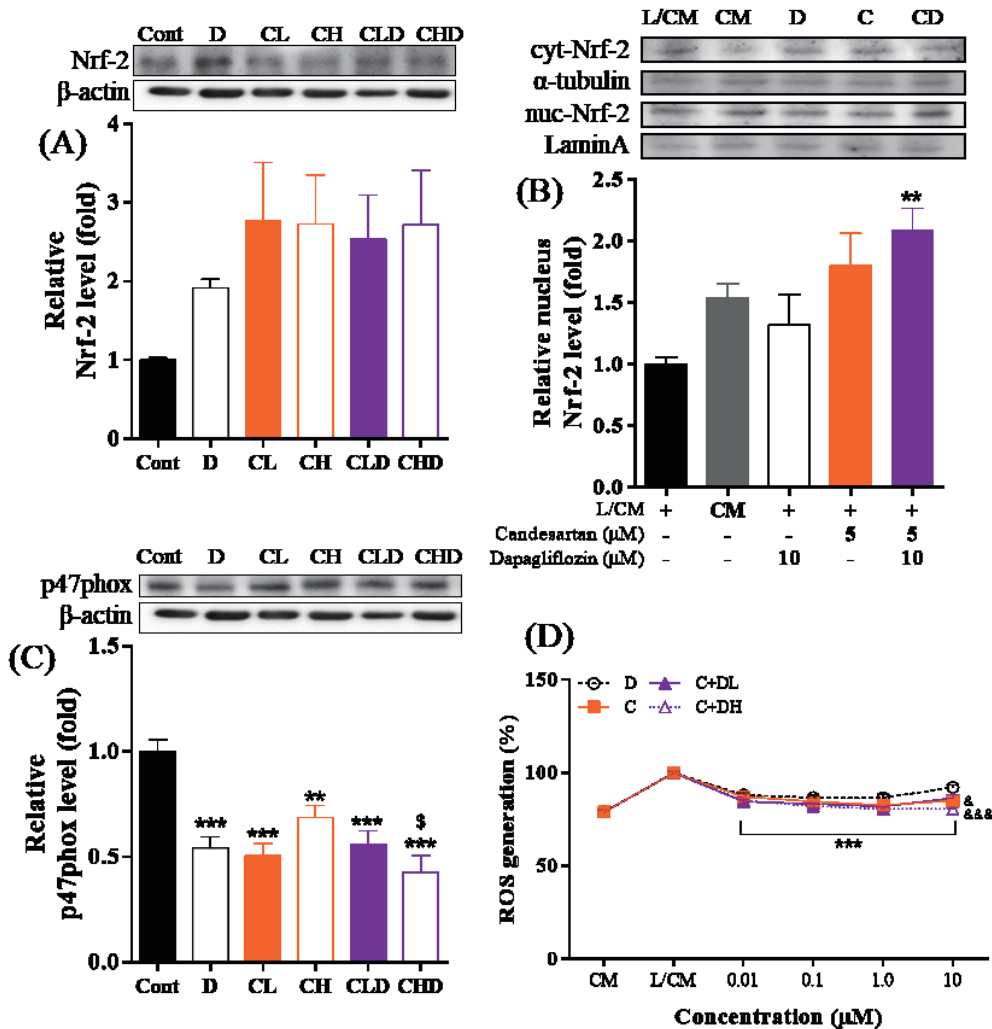


Figure 18. Effects of candesartan and dapagliflozin on NOX/ROS and Nrf2 in the aorta of aged SHR and L/CM treated EA. hy926 cells.

Experimental progress is the same as described in Figure 16. (A) The expression levels of Nrf2 in the aorta of SHRs administered with candesartan and dapagliflozin alone and in combination. (B) The activation of Nrf2 in the EA. hy926 cells treated with candesartan and dapagliflozin alone and in combination. (C) The expression levels of p47phox in the aorta of SHRs administered with candesartan and dapagliflozin alone and in combination. (D) The intracellular ROS levels in the EA. hy926 cells treated with candesartan and dapagliflozin alone and in combination. All data are expressed as mean \pm standard error mean. **,*** means a significant difference at the $p < 0.01$ and 0.001 levels compared to the control group. ^s means a significant difference at the $p < 0.05$ level exists between the same

dose of the combined group and the single group. & && means a significant difference at the $p < 0.05$ and 0.001 levels compared to the dapagliflozin alone group. Cont, SHR control group; D, dapagliflozin alone group (1 mg/kg); CL, low-dose candesartan alone (0.8 mg/kg); CH, high-dose candesartan alone group (3.2 mg/kg); CLD, low-dose candesartan (0.8 mg/kg) and dapagliflozin (1 mg/kg) combination group; CHD, high-dose candesartan (3.2 mg/kg) and dapagliflozin (1 mg/kg) combination group. D, dapagliflozin; C, candesartan; CD, candesartan 5 μM with dapagliflozin 10 μM combined treatment; C+DL, candesartan with 0.01 μM of dapagliflozin; C+DH, candesartan with 10 μM of dapagliflozin; L/CM, Raw264.7 cells culture media with LPS; CM, Raw264.7 cells culture media without LPS.

2-2.3. Regulation of Inflammatory Pathways

Inflammation is closely related to endothelium-dependent vasorelaxation and NOX activation. Therefore, we investigated the effect of dapagliflozin and ARBs on various inflammatory molecules in the aged SHR's aorta and L/CM-exposed EA. hy926 cells.

Dapagliflozin significantly reduced the expression of ICAM-1, NLRP3, caspase-1, and NF- κ B in aortic tissue (Figure 19A, C, and E). In addition, dapagliflozin decreased NLRP3 expression in EA. hy926 cells that were exposed to L/CM, and activation of caspase-1 and NF- κ B were also diminished to 0.68 ± 0.07 and 0.59 ± 0.12 , respectively (Figure 19D and F).

In the fimasartan groups, FH and the dapagliflozin combined groups demonstrated a significantly reduced ICAM-1 compared to the control group (Figure 19A). The ICAM-1 expression in endothelial cells showed a significant decrease only in the combined group ($p < 0.05$) (Figure 19B). Aortic NLRP3 showed a significant reduction only in the FH group, and caspase-1 was significantly decreased in all groups except FLD ($p < 0.01$ and 0.001) (Figure 19C). In endothelial cells, NLRP3 and c-caspase-1 were significantly decreased only in the dapagliflozin combined group (Figure 19D). Aortic NF- κ B expression decreased in all groups, with a more significant decrease in the dapagliflozin combination groups (Figure 19E). The nuclear translocation of NF- κ B in the endothelial cells was decreased to 0.56 ± 0.13 in the fimasartan alone group and 0.57 ± 0.08 in the combination group, but no significant (Figure 19F). In conclusion, fimasartan and dapagliflozin possess inhibitory efficacy against a series of inflammatory molecules leading to NF- κ B/NLRP3/ICAM-1 and confirming a synergistic effect on inhibition of NLRP3/ICAM-1, particularly in endothelial cells.

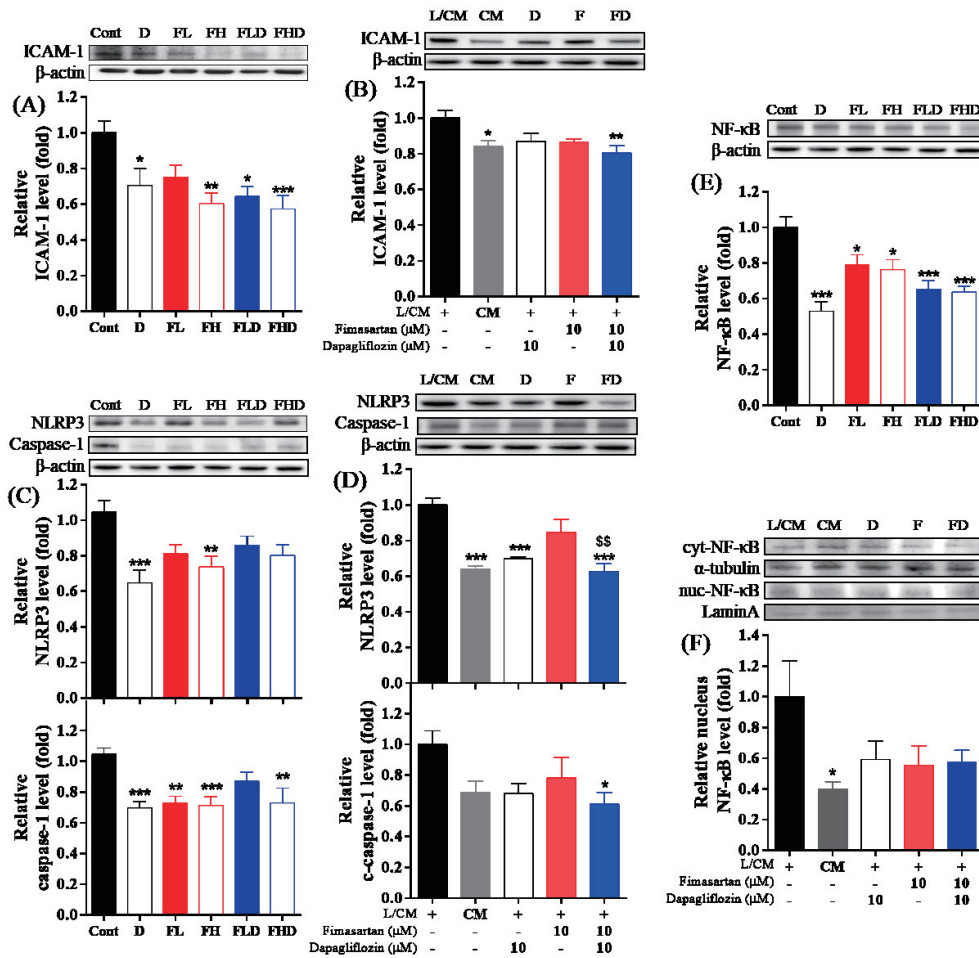


Figure 19. Effects of fimasartan and dapagliflozin on inflammatory molecules in the aorta of aged SHR and L/CM treated EA. hy926 cells.

Experimental progress and groups are the same as described in Figure 16. (A) The expression levels of ICAM-1, (C) NLRP3/caspase-1, and (E) NF-κB in the aorta of SHRs administered with fimasartan and dapagliflozin alone and in combination. (B) The expression levels of ICAM-1 and (D) NLRP3/caspase-1, (F) activation level of NF-κB in the EA. hy926 cells treated with fimasartan and dapagliflozin alone and in combination. All data are expressed as mean ± standard error mean. *, **, *** means a significant difference at the p < 0.05, 0.01, and 0.001 levels compared to the control group. ^{SS} means a significant difference at the p < 0.01 level exists between the same dose of the combined group and the single group.

In the aortas of telmisartan-administrated SHR, ICAM-1 expression was significantly reduced except for the TLD group (Figure 20A); conversely, ICAM-1 expression in endothelial cells did not show significant alterations in all groups (Figure 20B). Aortic NLRP3 did not exhibit significant differences in all groups compared to the control group; furthermore, the THD showed significantly higher levels than the dapagliflozin group ($p < 0.05$) (Figure 20C). The caspase-1 expression significantly decreased in all groups except the THD group. Conversely, endothelial NLRP3 exhibited a significant decrease in all telmisartan-treated groups; however, as observed in the aorta, the combined group showed significantly higher levels than the alone group. c-caspase-1 showed no significant changes in all groups (Figure 20D). Aortic NF- κ B expression also significantly decreased, excluding THD (Figure 20E). The nuclear translocation of NF- κ B in EA. hy926 cells showed no significant difference, but it appeared at a higher level of 0.76 ± 0.10 in the combined group compared to 0.68 ± 0.09 in the single group (Figure 20F). In conclusion, telmisartan decreased the expression of inflammatory molecules leading to NF- κ B/NLRP3/ICAM-1 but showed reduced anti-inflammatory effects when combined with dapagliflozin.

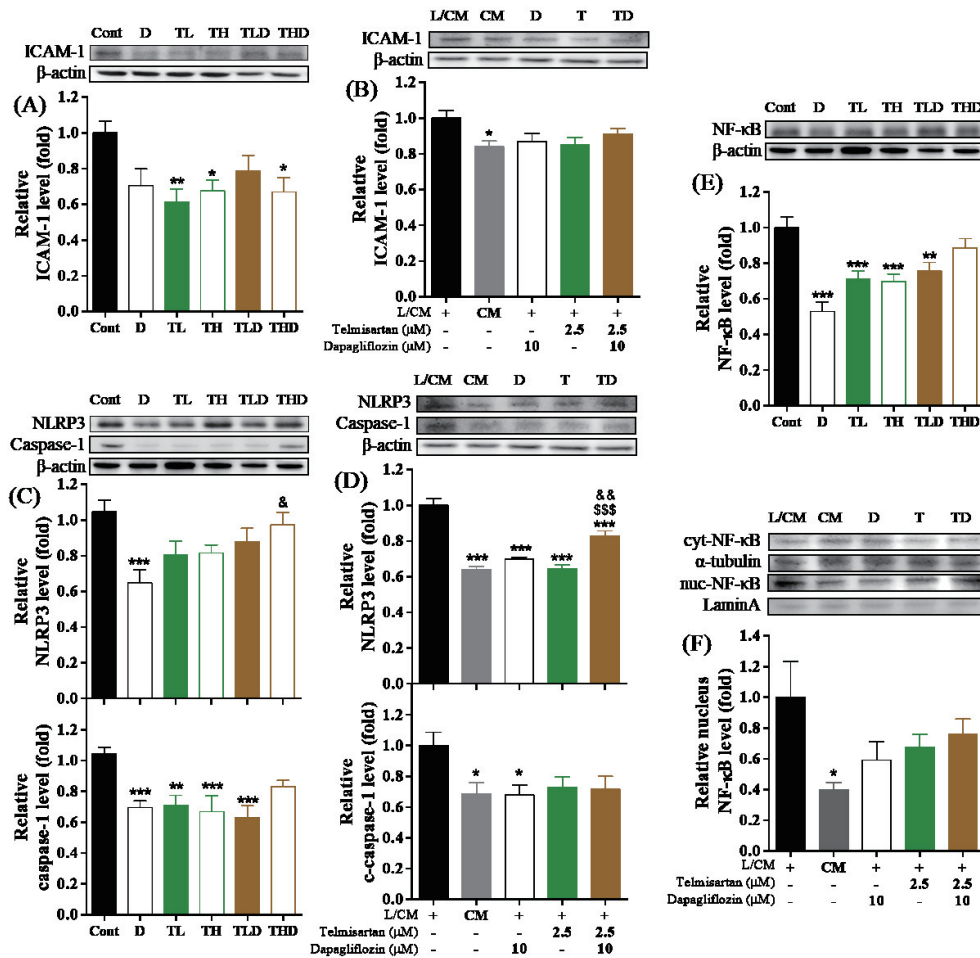


Figure 20. Effects of telmisartan and dapagliflozin on inflammatory molecules in the aorta of aged SHR and L/CM treated EA. hy926 cells.

Experimental progress and groups are the same as described in Figures 16 and 17. (A) The expression levels of ICAM-1, (C) NLRP3/caspase-1, and (E) NF-κB in the aorta of SHRs administered with telmisartan and dapagliflozin alone and in combination. (B) The expression levels of ICAM-1 and (D) NLRP3/caspase-1, (F) activation level of NF-κB in the EA. hy926 cells treated with telmisartan and dapagliflozin alone and in combination. All data are expressed as mean ± standard error mean. *, **, *** means a significant difference at the p < 0.05, 0.01, and 0.001 levels compared to the control group. \$\$\$ means a significant difference at the p < 0.001 level exists between the same dose of the combined group and the single group. &, && means a significant difference at the p < 0.05 and 0.01 levels compared to the dapagliflozin alone group.

In candesartan-administrated SHR, aortic ICAM-1 expression was significantly reduced in low-dose groups of both single and combination (Figure 21A). Conversely, ICAM-1 expression in endothelial cells did not show significant changes by all treatments (Figure 21B). Aortic NLRP3 was significantly decreased in all groups compared to the control group (Figure 21C). On the other hand, caspase-1 expression exhibited a decrease in all groups, particularly the CHD group, which showed a significant decrease compared to the dapagliflozin group ($p < 0.05$). In endothelial cells, NLRP3 showed a significant decrease in all groups, but the expression level in the combination group was 0.83 ± 0.04 , significantly higher than dapagliflozin ($p < 0.05$) (Figure 21D). The c-caspase-1 did not show significant changes across all groups. Aortic NF- κ B expression was significantly reduced in all groups; it was lower in low-dose groups, similar to ICAM-1 (Figure 21E). The nuclear translocation of NF- κ B in EA.hy926 cells were significantly reduced only in the combined treatment group ($p < 0.05$) (Figure 21F).

In summary, candesartan showed anti-inflammatory mechanisms leading to NF- κ B/NLRP3/ICAM-1 exhibiting different patterns depending on doses and cell types. Particularly in the aorta, NLRP3/caspase-1 inhibition was effective at high doses and enhanced by combination with dapagliflozin, while NF- κ B/ICAM-1 was more suppressed at low doses independently of dapagliflozin. On the other hand, endothelial NF- κ B activation was reduced only in the combined group, confirming a synergistic interaction of candesartan and dapagliflozin.

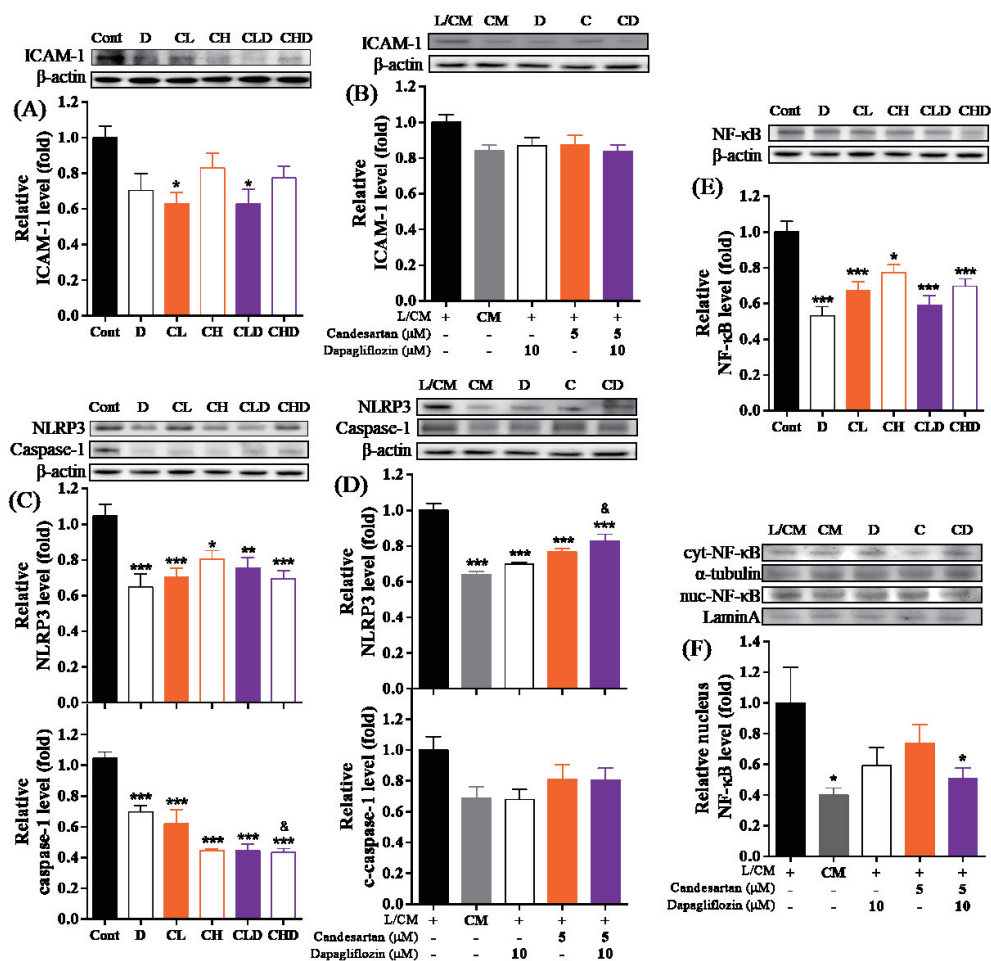


Figure 21. Effects of candesartan and dapagliflozin on inflammatory molecules in the aorta of aged SHR and L/CM treated EA. hy926 cells.

Experimental progress and groups are the same as described in Figures 16 and 18. (A) The expression levels of ICAM-1, (C) NLRP3/caspase-1, and (E) NF-κB in the aorta of SHRs administered with candesartan and dapagliflozin alone and in combination. (B) The expression levels of ICAM-1 and (D) NLRP3/caspase-1, (F) activation level of NF-κB in the EA. hy926 cells treated with candesartan and dapagliflozin alone and in combination. All data are expressed as mean ± standard error mean. *, **, *** means a significant difference at the $p < 0.05$, 0.01, and 0.001 levels compared to the control group. & means a significant difference at the $p < 0.05$ level compared to the dapagliflozin alone group.

When inflammation contributes to vascular dysfunction, it is well-known that the recruitment and activation of macrophages can exacerbate this process. In this, we investigated the effects of dapagliflozin and ARB on the inflammatory pathway of macrophages. Dapagliflozin showed decreased expression of NLRP3 and COX-2 but was insignificant (Figure 22A and B). iNOS expression significantly decreased to 1.46 ± 0.07 compared to the 2.28 ± 0.11 of LPS control (Figure 22C). Although nitrite production was not reduced significantly, it decreased to $80.4 \pm 10.6\%$ (Figure 22D). SEAP production, an indicator of NF- κ B activation, showed a significant reduction to $82.1 \pm 3.10\%$ at a concentration of $10 \mu\text{M}$ ($p < 0.05$) (Figure 22E).

Fimasartan also did not affect NLRP3 expression (Figure 22A), but COX-2 expression was significantly decreased with combined treatment, even significantly lower than dapagliflozin alone (Figure 22B). iNOS expression was decreased in all groups, while nitrite production was only reduced in the combined treatment group with dapagliflozin (Figure 22C and D). Combined treatment with $0.01 \mu\text{M}$ and $10 \mu\text{M}$ of dapagliflozin (F + DL and F + DH) significantly decreased the nitrite to 92.21 ± 5.4 and $76.0 \pm 4.59\%$, respectively, at a concentration of $10 \mu\text{M}$ compared to the LPS control (Figure 22D). 0.01 , $1.0 \mu\text{M}$ of F + DL, and all concentrations of the F + DH group showed significantly lower nitrite levels than the dapagliflozin alone group. SEAP production significantly decreased at 0.01 , 0.1 , and $10 \mu\text{M}$ concentrations in the F + DH group (Figure 22E).

In summary, dapagliflozin suppresses LPS-induced inflammation by inhibiting NF- κ B/iNOS in macrophages. Furthermore, fimasartan showed potent anti-inflammatory effects in the macrophage by inhibiting NF- κ B/iNOS/COX-2 and confirmed synergistic effect with dapagliflozin, particularly in inhibiting NO production.

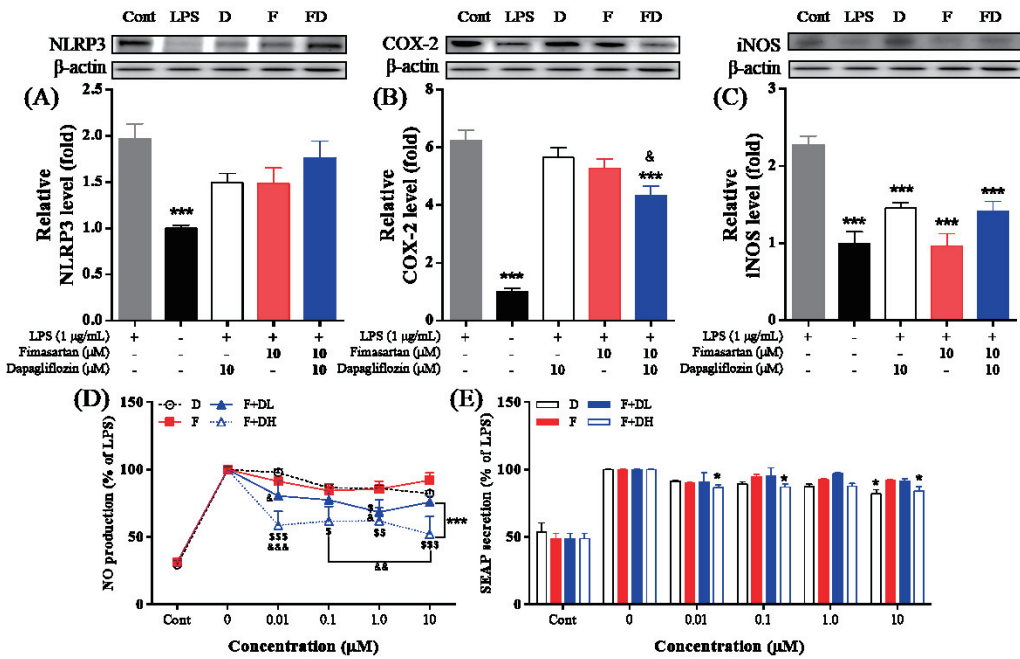


Figure 22. Effects of fimasartan and dapagliflozin on inflammatory molecules in the Raw264.7 cells.

Raw264.7 and Raw-BlueTM cells were treated with drugs and LPS for 24 hours. The Raw264.7 cells were extracted for performing western blotting. Western blot images of proteins in Raw264.7 cells were visualized using the ChemiDoc system. The expression levels were normalized by β -actin. The relative ratio was calculated using the control (-/-). The cultured media from treated Raw-BlueTM cells were used to measure nitrite content using the Griess assay and SEAP content using the QUANTI-BlueTM assay. The relative percentage was calculated using the LPS control (+/-). (A) The expression levels of NLRP3, (B) COX-2, and (C) iNOS in Raw264.7 cells treated with fimasartan and dapagliflozin alone and in combination. (D) The nitrite production and (E) the activation level of NF- κ B in the Raw-BlueTM cells treated with fimasartan and dapagliflozin alone and in combination. All data are expressed as mean \pm standard error mean. *,*** means a significant difference at the $p < 0.05$ and 0.001 levels compared to the control group. &, &&, &&& means a significant difference at the $p < 0.05$, 0.01 , and 0.001 levels compared to the dapagliflozin alone group. ^s, ^{ss}, ^{sss} means a significant difference at the $p < 0.05$, 0.01 , and 0.001 levels exist between the same dose of the combined group and the single group. The experimental groups name and treated concentrations are the same as described in Figure 16.

All telmisartan groups have not significantly affected NLRP3 expression (Figure 23A), but COX-2 expression was significantly decreased with combined treatment (Figure 23B). iNOS expression was decreased in all groups, while nitrite production was only reduced in the combined treatment group with dapagliflozin (Figure 23C and D). Combined treatment with 0.01 μ M and 10 μ M of dapagliflozin (T + DL and T + DH) significantly decreased to 70.22 ± 7.95 and $54.0\pm 11.6\%$, respectively, at a concentration of 10 μ M compared to the LPS control (Figure 23D). T + DH significantly reduced compared to the dapagliflozin alone group at 1.0 μ M. The T + DH group demonstrated significantly lower levels of nitrite at all concentrations than the dapagliflozin and telmisartan alone groups. SEAP production did not significantly change in all groups (Figure 23E).

In summary, telmisartan demonstrated anti-inflammatory effects by inhibiting iNOS/NO and has a synergistic effect with dapagliflozin, particularly in inhibiting COX-2 and nitrite production.

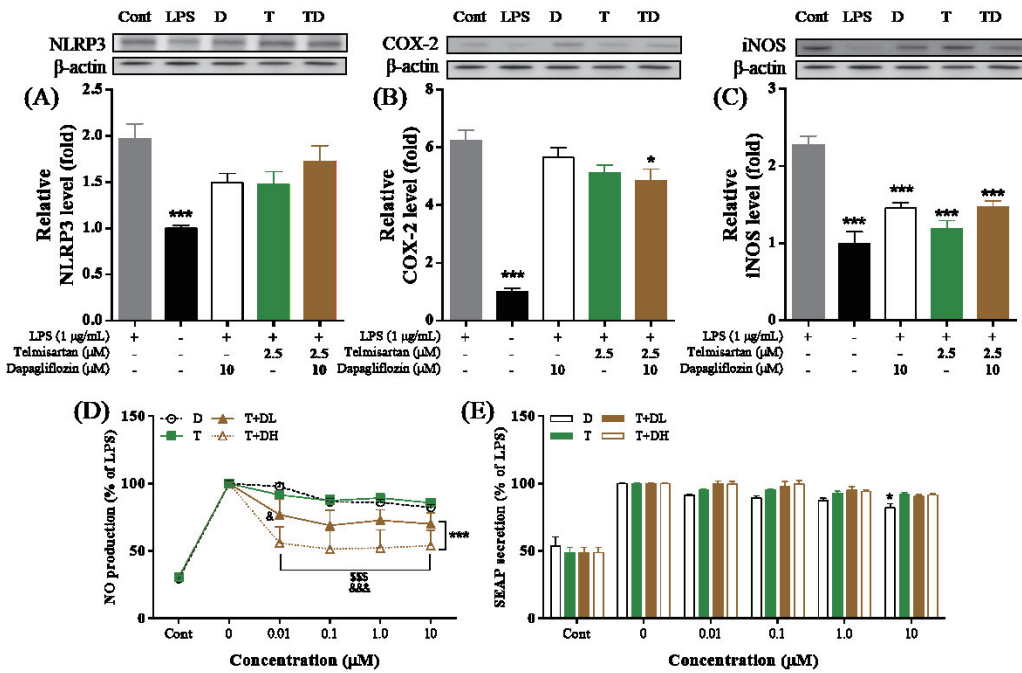


Figure 23. Effects of telmisartan and dapagliflozin on inflammatory molecules in the Raw264.7 cells.

Experimental progress is the same as described in Figure 22. (A) The expression levels of NLRP3, (B) COX-2, and (C) iNOS in Raw264.7 cells treated with telmisartan and dapagliflozin alone and in combination. (D) The nitrite production and (E) the activation level of NF- κ B in the Raw-Blue™ cells treated with telmisartan and dapagliflozin alone and in combination. All data are expressed as mean \pm standard error mean. *, *** means a significant difference at the $p < 0.05$ and 0.001 levels compared to the control group. &, &&& means a significant difference at the $p < 0.05$ and 0.001 levels compared to the dapagliflozin alone group. ^{SSS} means a significant difference at the $p < 0.001$ level exists between the same dose of the combined group and the single group. The experimental group's name and treated concentrations are the same as described in Figure 17.

In macrophages, candesartan showed a significant reduction in NLRP3 and no change in COX-2 expression, unlike the previous two ARBs (Figure 24A and B). iNOS expression decreased in all groups, and nitrite production also decreased in all treatment groups (Figure 24C and D). The single treatment group showed a significant reduction compared to the LPS control at 0.1 and 1.0 μM , by 81.7 ± 4.61 and $65.3\pm 9.68\%$, respectively. When combined with 0.01 and 10 μM dapagliflozin (C + DL and C + DH), the nitrite production significantly decreased to 69.4 ± 9.24 and $55.0\pm 12.4\%$ respectively, at a concentration of 10 μM . There was a significant reduction for the C + DH group compared to the dapagliflozin alone group at concentrations of 0.01 and 1.0 μM . The C + DH group showed significantly lower levels than the dapagliflozin alone group at all concentrations except for 1.0 μM were significantly lower than the candesartan alone group. SEAP production was significantly reduced in the 10 μM combined treatment group (Figure 24E).

In summary, candesartan may exert anti-inflammatory effects by inhibiting NF- κB /NLRP3/iNOS/NO pathways, with particularly potent NLRP3 inhibition observed. Additionally, like the other two ARBs, candesartan exhibited a synergistic effect with dapagliflozin in NO production.

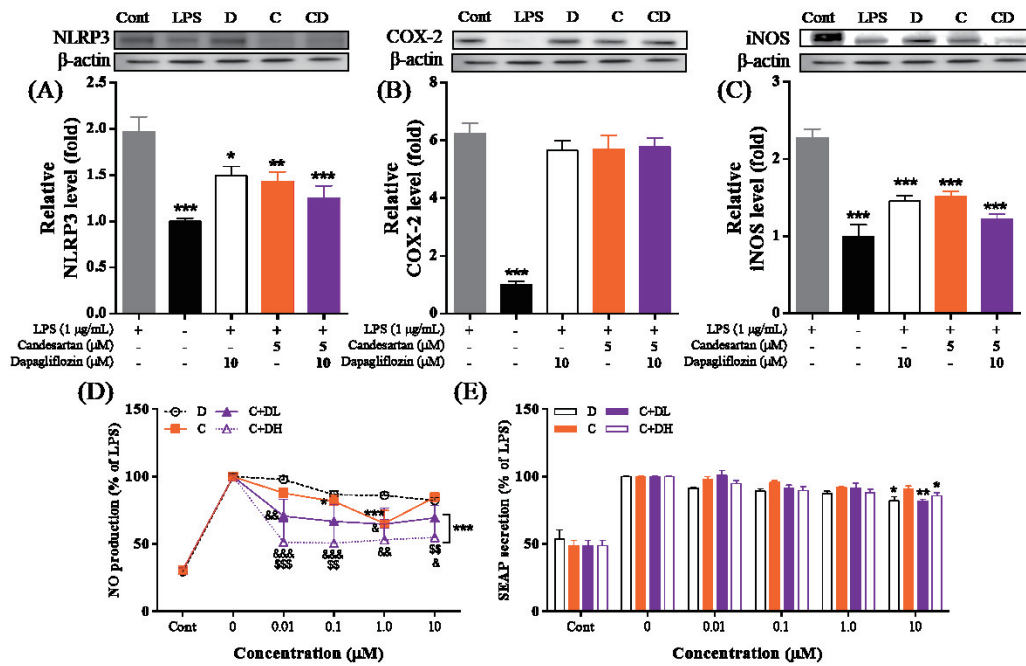


Figure 24. Effects of candesartan and dapagliflozin on inflammatory molecules in the Raw264.7 cells.

Experimental progress is the same as described in Figure 22. (A) The expression levels of NLRP3, (B) COX-2, and (C) iNOS in Raw264.7 cells treated with candesartan and dapagliflozin alone and in combination. (D) The nitrite production and (E) the activation level of NF-κB in the Raw-Blue™ cells treated with candesartan and dapagliflozin alone and in combination. All data are expressed as mean ± standard error mean. *, **, *** means a significant difference at the p < 0.05, 0.01, and 0.001 levels compared to the control group. &, &&, &&& means a significant difference at the p < 0.05, 0.01, and 0.001 levels compared to the dapagliflozin alone group. \$\$, \$\$\$ means a significant difference at the p < 0.01 and 0.001 levels exists between the same dose of the combined group and the single group. The experimental groups name and treated concentrations are the same as described in Figure 18.

2-2.4. Regulation of autophagy

As an additional mechanism, we probed the effects of each drug on autophagy, a cellular recuperative process that counters excessive inflammation and oxidative stress. Dapagliflozin has not shown any significant changes in the expression of autophagy-related molecules in both the aortas and inflammation-exposed endothelial cells of aged SHR (Figure 25).

Although fimasartan didn't show a significant difference compared to controls in the aorta, it exhibited elevated AMPK and LC3 activation levels at lower concentrations under individual and combined administration (Figure 25A). Conversely, the reduction of p62 was most significant in the dapagliflozin combination group, particularly in the FHD group. Fimasartan did not affect AMPK activation in induced endothelial cells but demonstrated a significant increase in LC3 activation in the combined group (Figure 25B). P62 reduced by 0.80 ± 0.05 and 0.81 ± 0.05 in single and combined treatments, respectively, compared to the L/CM control group, though the difference was not statistically significant. Upon examination of the intracellular distribution morphology of p62, a distinct dot-like distribution was evident in both the fimasartan alone and combined groups (Figure 25C).

In summary, while dapagliflozin showed no impact on autophagy activation, fimasartan elevated LC3 activation, reduced p62, and amplified autophagosome formation. These effects were particularly pronounced in the combination treatment with dapagliflozin.

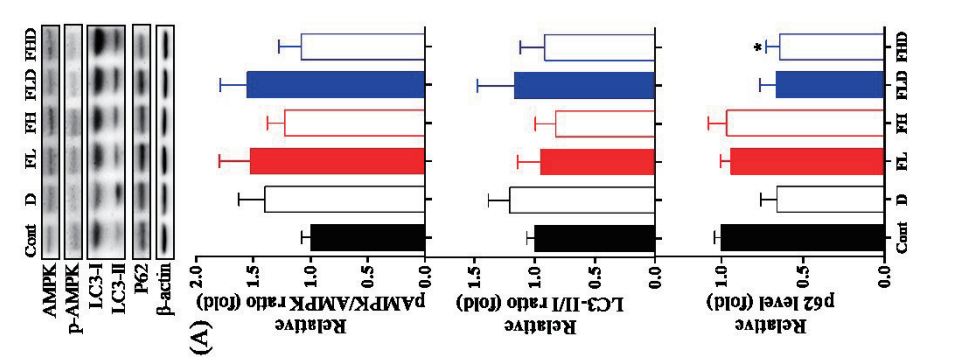
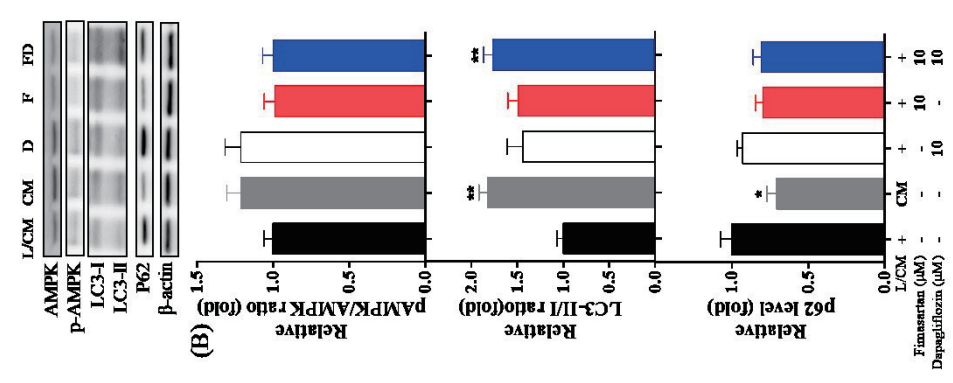
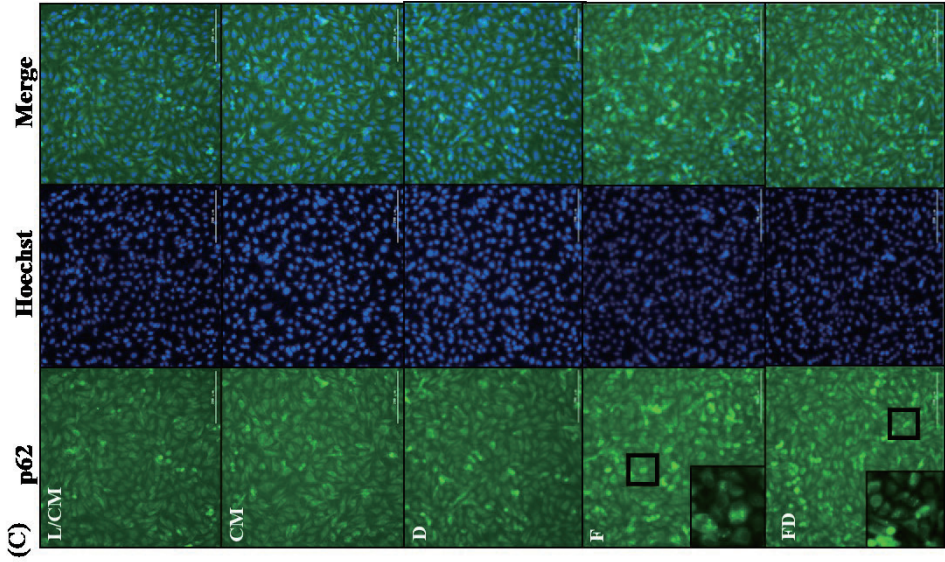
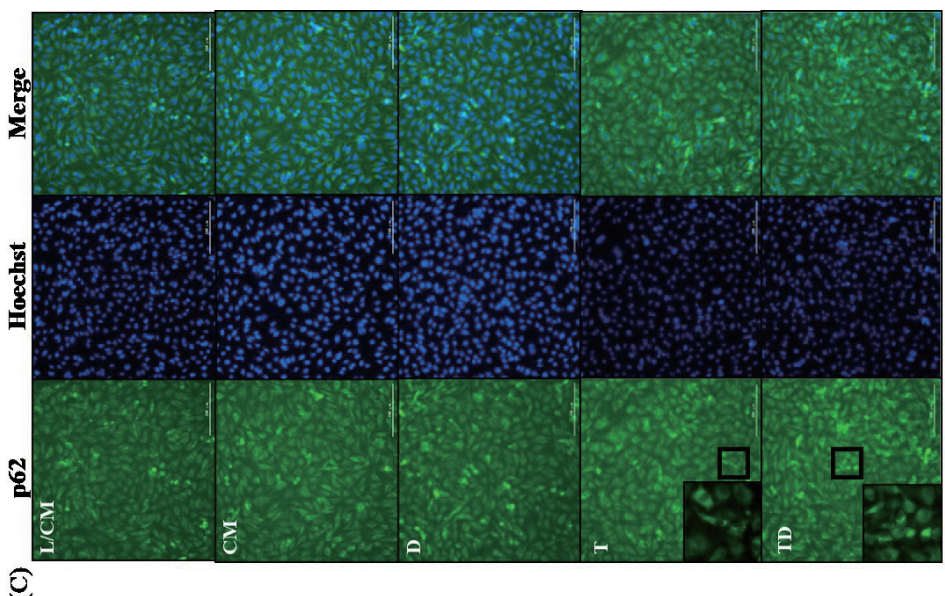


Figure 25. Effects of fimasartan and dapagliflozin on autophagy in aorta of aged SHR and L/CM treated EA. hy926 cells.

Experimental progress and groups are the same as described in Figure 16. EA. hy926 cells were treated with drugs and L/CM for 24 hours, and the p62 protein was detected by immunocytochemistry. Cells were stained to p62-FICT (green) and Hoechst (blue). (A) The activation levels of AMPK and LC3, expression levels of p62 in the aorta of SHRs administered with fimasartan and dapagliflozin alone and in combination. (B) The activation levels of AMPK and LC3, expression levels of p62 in EA. hy926 cells treated with fimasartan and dapagliflozin alone and in combination. (C) Immunocytochemistry images of p62 in EA. hy926 cells treated with fimasartan and dapagliflozin alone and in combination. All data are expressed as mean \pm standard error mean. * ** means a significant difference at the $p < 0.05$ and 0.01 level compared to the control group.

Telmisartan did not induce significant changes in markers of autophagy activation within the aorta (Figure 26A). However, in contrast, in endothelial cells exposed to inflammation significantly increased LC3 activation when combined with dapagliflozin (Figure 26B). In addition, the reduction in p62 shows in both the single treatment and combination groups. Especially, combined treatment showed significantly lower levels than dapagliflozin alone. Examination of the intracellular distribution morphology of p62 confirmed a dot-like distribution in both the single and combination treatment groups (Figure 26C).

In summary, telmisartan enhanced the activation of LC3, reduced p62 levels, and increased autophagosome formation in inflammation-damaged endothelial cells. These effects were particularly pronounced in combination treatment with dapagliflozin.



(C)

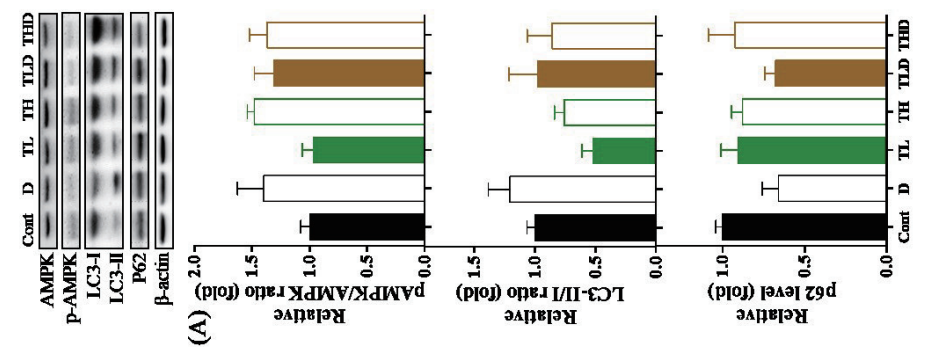
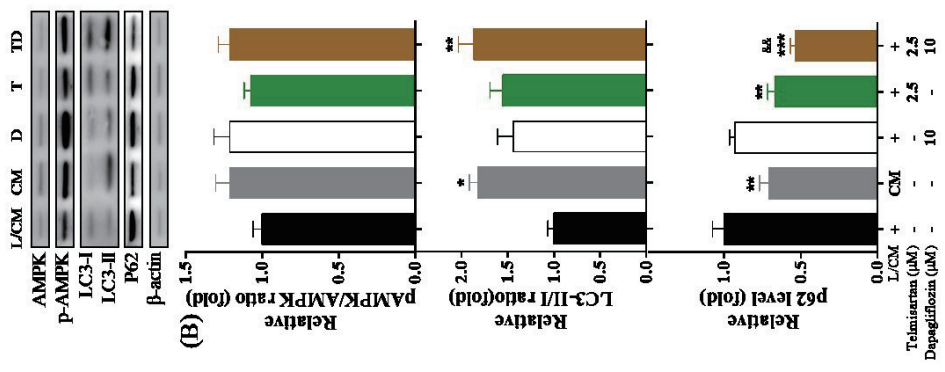


Figure 26. Effects of telmisartan and dapagliflozin on autophagy in aorta of aged SHR and L/CM treated EA. hy926 cells.

Experimental progress and groups are the same as described in Figures 16 and 17. (A) The activation levels of AMPK and LC3, expression levels of p62 in the aorta of SHRs administered with telmisartan and dapagliflozin alone and in combination. (B) The activation levels of AMPK and LC3, expression levels of p62 in EA. hy926 cells treated with telmisartan and dapagliflozin alone and in combination. (C) Immunocytochemistry images of p62 in EA. hy926 cells treated with telmisartan and dapagliflozin alone and in combination. All data are expressed as mean \pm standard error mean. *, **, *** means a significant difference at the $p < 0.05$, 0.01 , and 0.001 levels compared to the control group. & means a significant difference at the $p < 0.01$ level compared to the dapagliflozin alone group.

Candesartan significantly amplified aortic AMPK activation in the CHD group compared to the control group ($p < 0.05$) (Figure 27A). While LC3 activation didn't exhibit a significant difference, p62 expression also decreased in the CHD group. Contrarily, candesartan showed no appreciable impact on AMPK activation in endothelial cells but demonstrated increased LC3 activation and decreased p62 expression in both the single and dapagliflozin combined treatment (Figure 27B). In addition, the subcellular distribution morphology of p62 confirmed a distinct dot-like pattern in both the single and combined groups (Figure 27C).

In conclusion, candesartan influences AMPK and p62 in the aorta and LC3 and p62 in endothelial cells. Especially within the aorta, the combination treatment with dapagliflozin exhibited a synergistic effect.

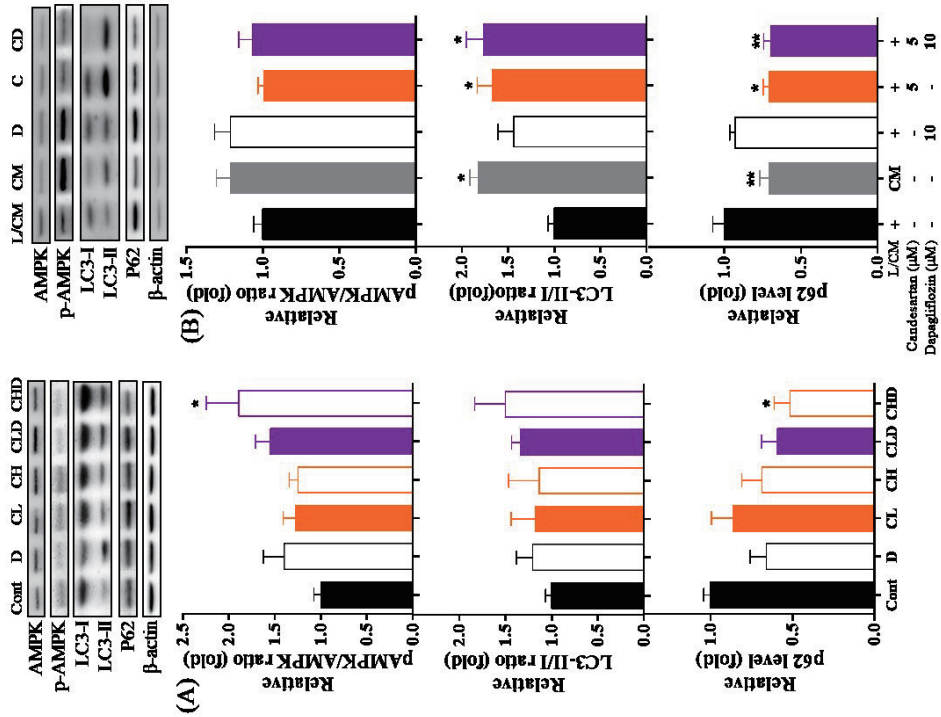
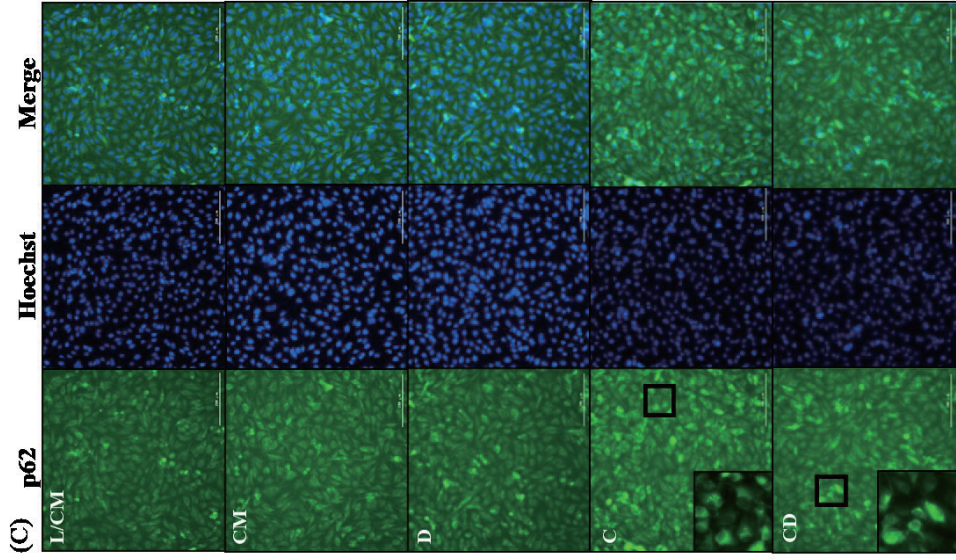


Figure 27. Effects of candesartan and dapagliflozin on autophagy in aorta of aged SHR and L/CM treated EA. hy926 cells.

Experimental progress and groups are the same as described in Figures 16 and 18. (A) The activation levels of AMPK and LC3, expression levels of p62 in the aorta of SHRs administered with candesartan and dapagliflozin alone and in combination. (B) The activation levels of AMPK and LC3, expression levels of p62 in EA. hy926 cells treated with candesartan and dapagliflozin alone and in combination. (C) Immunocytochemistry images of p62 in EA. hy926 cells treated with candesartan and dapagliflozin alone and in combination. All data are expressed as mean \pm standard error mean. *,** means a significant difference at the $p < 0.05$ and 0.01 levels compared to the control group.

2-3. Discussion

In this result, dapagliflozin enhanced Ach response in the aorta of aged SHR and improved vasorelaxant effects of ARBs when combined. Telmisartan and dapagliflozin combination significantly enhanced Nrf2 expression and activation in aortic and endothelial cells. Co-administration of candesartan and dapagliflozin reduced NOX expression and ROS production. NF- κ B levels were decreased by dapagliflozin in the aorta, macrophages, and endothelial cells when combined with candesartan. Fimasartan and candesartan combined with dapagliflozin showed the most significant decrease in NF- κ B, while telmisartan exhibited an increase. ICAM-1 levels were lowest in the fimasartan and dapagliflozin combination group in the aorta and endothelial cells. The expression of NLRP3 was least at the aorta of the dapagliflozin group, endothelial cells of the telmisartan and fimasartan combined group, and the macrophages of the candesartan combined group, respectively. Caspase-1 was significantly reduced in the aorta of candesartan alone and combination groups and in endothelial cells of fimasartan and dapagliflozin co-treatment. Autophagy activity, indicated by LC3 activation and p62 reduction, increased significantly in the aorta with the candesartan and dapagliflozin combination and in endothelial cells with telmisartan and dapagliflozin co-treatment.

In diabetes and hypertension conditions, the blood vessels are exposed to continuous and excessive stresses, leading to endothelial dysfunction and complications [45]. In diabetes, hyperglycemia is associated with inflammatory mediators, including the production of AGEs, activation of protein kinase C (PKC), overactivity of the hexosamine pathway, and increased flux through the polyol pathway [165]. Endothelial dysfunction can lead to many vascular complications, including retinopathy, nephropathy, and neuropathy, and increases the risk of atherosclerosis [34, 166, 167]. Similarly, in hypertension, elevated blood pressure causes mechanical stress on the blood vessel walls leading to endothelial injury [168]. It also leads to

vascular remodeling, including hypertrophy and hyperplasia of the vascular smooth muscle cells, which can further elevate blood pressure [169]. It is well known that damage to the endothelium caused by various stresses in hypertension and diabetes leads to disorders in the contraction and relaxation of blood vessels [170, 171]. For this reason, we investigated the effects of ARB and dapagliflozin on Ach-induced vasorelaxation in aged SHR accompanied by hyperglycemia. In the hypertensive state, it has been reported that the vasodilatory response is reduced due to the reduced production of vasodilators, such as NO, and increased constrictive substances, such as endothelin-1 [172]. As well as it has been confirmed that hypertensive patients have a reduced vasorelaxation response to bradykinin and Ach, the potent vasodilators [173, 174]. Our results showed that all four drugs increased the endothelium-dependent relaxation and enhanced it when fimasartan and candesartan were combined with dapagliflozin. On the other hand, the group receiving high-concentration telmisartan and dapagliflozin did not show a significantly increased response compared to the control group. Indeed, several studies have shown that the administration of dapagliflozin improves vascular endothelial function in type 2 diabetic patients and endothelial function in non-diabetic heart failure model rats [163, 175]. Fimasartan and candesartan have also been reported could effectively prevent vascular aging caused by Ang2 and improves peripheral vascular function in hypertensive patients [176, 177]. Meanwhile, some studies have reported that telmisartan improves endothelial function in hypertensive patients only when administered with amlodipine and has no effect when administered alone [178]. Conversely, considering the reports that demonstrate the effects of telmisartan on improved vascular function in various animal models, we have to recognize that the vascular improvement effects of telmisartan can vary depending on the animal model and administered dose [179]. Although this study has a limitation as short-term administration, it is noteworthy that these results are the first to identify the increase of ARB's Ach response following co-administration with

dapagliflozin.

Excessive oxidative stress plays a significant role in the development and progression of various cardiovascular diseases, and antioxidants have been reported to reduce atherosclerotic plaques and improve vascular function decline [58, 66]. In addition, because Ang2 activates NOX, it is known that ARB can effectively suppress the increase in oxidative stress caused by RAAS [25, 180]. Indeed, various studies have shown that candesartan and telmisartan reduce NOX activity [181, 182]. In addition, as one of the mechanisms underlying the cardiovascular benefits of dapagliflozin, its antioxidant properties have been widely studied. It has been reported that dapagliflozin down-regulates oxidative stress and DNA damage biomarkers, including NOX, and up-regulates antioxidants in H9C2 cells [183]. Our results also showed that all four drugs have ROS-reducing effects functionality by inhibiting NOX.

This study's distinctive finding is a synergistic increase of Nrf2 expression and activation when ARBs, particularly telmisartan, combine with dapagliflozin. Nrf2, a representative regulator of the endogenous antioxidant system, is a transcription factor that regulates the expression of a wide range of genes involved in the clearance of ROS and maintenance of cellular redox balance [184]. Indeed, several studies have shown that Nrf2 activation increases the expression of antioxidant enzymes such as HO-1 and catalase, which can clear ROS and reduce oxidative stress [185, 186]. In addition, activation of Nrf2 can protect endothelial cells from oxidative stress and reduce endothelial dysfunction [187, 188]. Various studies have indicated that dapagliflozin, fimasartan, and telmisartan activate the Nrf2/HO-1 pathway [182, 189, 190]. Yet, the explicit mechanism underpinning Nrf2 activation in dapagliflozin combination therapy remains elusive; only one report suggests a synergistic effect with the combination of dapagliflozin [191]. Hence, our findings provide valuable insights, but further investigation is needed into the interaction mechanism between ARBs and dapagliflozin on Nrf2 activation.

Meanwhile, acute or chronic oxidative stress through NOX and the mitochondrial electron transport chain can induce Inflammation [69]. In addition, NOX promotes the release of adhesion molecules and pro-inflammatory mediators by activating NF- κ B signaling through ROS generation, eNOS decoupling, and antioxidant scavenging [192, 193]. Nrf2 activation also reduces the expression of pro-inflammatory cytokines and can inhibit activation of the NF- κ B/AP-1 pathway [186]. In other words, the decrease in ROS seen in our results can partly influence inflammation.

Inflammation is an essential mechanism of endothelial dysfunction, which plays a crucial role in the development of cardiovascular disease. In our results, ARBs and dapagliflozin exhibited inhibitory efficacy against inflammatory molecules leading to NF- κ B/NLRP3/ICAM-1 in the aorta of aged SHR and endothelial cells. Furthermore, we have also demonstrated potent anti-inflammatory effects by inhibiting NF- κ B/iNOS/COX-2 in macrophages. Fimasartan and candesartan showed an even more significant reduction in the combination therapy with dapagliflozin. One peculiarity of our cell experiment was that endothelial cells were treated with an LPS-stimulated macrophage culture medium to simulate a state of low-grade inflammation. These macrophages secrete classic cytokines that, in various diseases, vascular endothelial cells are usually exposed [194, 195]. It investigated the response to L/CM, not by Ang2, suggesting that the inflammation-reducing effect of ARB and dapagliflozin may partly act in a form independent of Ang2 inhibition.

Indeed, ARBs and dapagliflozin have individually shown potential for improving vascular function and exerting anti-inflammatory effects in various studies [196-199]. Like us, dapagliflozin is reported to reduce acetic acid-induced colitis by inhibiting the NF- κ B/AMPK/NLRP3 axis and inhibiting NF- κ B in endothelial cells and macrophages [186, 187]. Mainly, dapagliflozin attenuates the ICAM-1 and NF- κ B expression, improving endothelial

function [200]. Various papers also reported that telmisartan reduced pro-inflammatory cytokines and oxidative stress in the heart, kidney, and other tissues [201, 202]. In addition, telmisartan inhibits NF- κ B phosphorylation in a PPAR γ -independent manner under high glucose conditions [203]. In addition, compared to olmesartan, telmisartan reduces the expression of VCAM-1, IKK β , and inhibits the phosphorylation of NF- κ B p65-Ser (536) [203]. Fimasartan also downregulates the NF- κ B and MAPK pathways and has been reported to prevent inflammation-related cell death [198, 204-206]. Similar to our results on ICAM-1, fimasartan reduced the levels of inflammatory cytokines, including ICAM, in Apolipoprotein E knockout mice. In diabetic patients, candesartan lowered circulating ICAM-1 level and VCAM-1 compared to enalapril [204, 207]. On the other hand, candesartan and telmisartan are known to suppress p38MAPK in various tissues [208, 209], but our results did not show significant changes (Supplementary Figure 10); it may be attributable to an insufficient experimental duration or dosage. Activation of inflammatory pathways contributes to vascular dysfunction and further development of atherosclerosis [15, 18, 210]. Although it was not confirmed whether atheromatous lesions were present in the blood vessels of the experimental animals used in this study, the molecular reduction indicates that the combined administration of ARB and dapagliflozin could contribute to the prevention of atherosclerosis.

ICAM and VCAM promote the adhesion of leukocytes and monocytes to the endothelial surface, resulting in endothelial dysfunction and vascular damage [60]. The endothelium and macrophages have diverse and interdependent effects compared to other immune cells. For example, endothelial cell dysfunction caused by an increase in LDL leads to increased expression of macrophages, and macrophages directly transfer from endothelial to mesenchymal cells, increasing cell metastasis [211, 212]. In our results, ARBs and dapagliflozin also inhibited inflammatory molecules such as COX-2, iNOS, and NO in macrophages. In particular, a significant level of NO reduction was shown in the combined

treatment at concentrations that did not show NO reduction alone. Similar to our results, it has been reported that dapagliflozin reduces the increased iNOS after myocardial ischemia-reperfusion injury and induces the differentiation of M1 macrophages into M2 cells, thereby having a direct anti-inflammatory effect in macrophages [213, 214]. Fimasartan also reduces iNOS and NO in LPS-stimulated Raw264.7 cells, and it has been reported that it acts by inhibiting the transcriptional and DNA binding activities of NF- κ B and AP-1 [206]. Telmisartan showed a superior reduction of COX-2 in neuroblasts compared to candesartan and losartan, and fimasartan is also known to reduce COX-2 expression by hemolysate in astrocytes [215, 216]. In other words, it has been confirmed that ARBs and dapagliflozin reduce adhesion molecules, thereby suppressing the recruitment of macrophages and enhancing vascular reactivity by inhibiting the inflammatory response of macrophages, specifically the overproduction of NO.

Interestingly, in our results, only candesartan and dapagliflozin reduced NLRP3 expression in both blood vessels and macrophages. In particular, it confirmed that the NLRP3 inhibitory activity of the two drugs might have a partial synergistic effect. NLRP3 is upregulated in the vasculature of hypertensive animals, leading to endothelial dysfunction, vascular inflammation, and oxidative stress [62, 217]. Various studies have shown that one of the cardioprotective mechanisms of dapagliflozin is the inhibition of myocardial NLRP3 activation, and inhibition of the AMPK/NLRP3 pathway has been shown to reduce inflammation [218-220]. In addition, candesartan also inhibits NF- κ B in macrophages and significantly inhibits NLRP3 inflammasome and pyroptosis through the reduction of activation of the MAPK pathway [221]. Some research has demonstrated that telmisartan can inhibit NLRP3 in neurovascular units and neural stem cells [222, 223]. Additionally, only one piece of evidence suggests that low-dose fimasartan can ameliorate NLRP3 inflammasome-mediated neuroinflammation and cerebral damage following an intracerebral hemorrhage

[224]. Our results showed that telmisartan and fimasartan reduced NLRP3, specifically in the aorta and endothelial cells, suggesting that their effects may exhibit a degree of tissue specificity. NLRP3 inflammasome is known to be negatively regulated by autophagy; In our results regarding autophagy, ARBs, especially candesartan and dapagliflozin, elevated LC3 activation, reduced p62, and amplified autophagosome formation in EA. hy926 cells and combined administration with dapagliflozin confirmed a synergistic effect. These findings suggest that the underlying mechanism behind the enhancement of vascular function by candesartan and dapagliflozin may involve the inhibition of NLRP3, which is initiated through the activation of autophagy.

Autophagy, which has recently attracted attention in various diseases, is a process that degrades and recycles unnecessary proteins in cells and plays an essential role in the metabolic activity of cells [75, 225]. In addition, autophagy breaks down damaged organelles inside cells under various stress situations, allowing cells to survive. Activation of autophagy has multiple advantages, such as inhibition of apoptosis in pulmonary arterial hypertension and inhibition of ischemia/reperfusion-induced vascular endothelial apoptosis [72, 73].

It has been reported that ARBs, especially fimasartan, have anti-proliferative activity through the activation of autophagy in cancer cells. On the other hand, telmisartan has been reported that Peroxisome proliferator-activated receptor gamma, coactivator 1 alpha (Ppargc1 α) inhibits aging indicators through increased autophagy [226]. Conversely, telmisartan has also been reported that attenuate kidney apoptosis and autophagy-related protein expression levels in an intermittent hypoxia mouse model [227]. These disparities imply that optimal levels of autophagy may vary according to tissue type and the stress level to which cells are subjected. Indeed, according to various reports, Ang2 induces vascular smooth muscle cell hypertrophy by an autophagy-dependent mechanism, and losartan reduces it [228]. At the same time, some

studies reported that autophagy activation attenuates Ang2-induced cardiac dysfunction [229]. From a therapeutic perspective, the fact that autophagy can exhibit diverse responses based on the level of inflammation and cell types can complicate drug selection [230]. However, in our study, which focused on low-grade inflammatory conditions, it's apparent that autophagy was reduced, and both ARB and dapagliflozin were observed to enhance it in endothelial cells. This finding can be proposed as one mechanism of vasoprotective effects through which these two drugs work synergistically.

In another study, candesartan was reported to enhance AMPK-induced autophagy flux [231]. In addition, dapagliflozin has been reported to boost autophagy through the AMPK/mTOR pathway in hepatic steatosis and renal injury [232, 233]. AMPK not only activates autophagy but also improves insulin sensitivity by enhancing the activity of insulin receptors, cellular energy metabolism and promoting glucose uptake [231, 234]. Our study showed that the co-administration of candesartan and dapagliflozin enhanced AMPK activation in the aorta. However, no significant difference in AMPK activation was observed when these drugs were administered individually. This suggests a synergistic effect between candesartan and dapagliflozin in stimulating AMPK activity in the aorta. AMPK also reported additional benefits, including inflammation reduction through NF- κ B and STAT3 inhibition and antioxidative efficacy via Nrf2 activation and glutathione biosynthesis [235-237]. Indeed, when combined with dapagliflozin, candesartan significantly decreased NF- κ B/NLRP3/caspase-1 in the aorta and contributed substantially to the reduction of NOX. This means this combination therapy can have further benefits related to AMPK activation.

In summary, fimasartan increased vasorelaxation by inhibiting inflammation and ROS, also enhancing autophagy; its effects synergized in specific pathways when combined with dapagliflozin. Telmisartan shows less increased vasorelaxation than others, and its anti-

inflammatory effects were reduced when combined with dapagliflozin. Candesartan demonstrated higher efficacy than the other two drugs in enhancing Ach-response and anti-inflammatory effects, also lowering NLRP3 and promoting autophagy. Notably, it also exhibited a synergistic interaction with dapagliflozin in these regards. Interestingly, while the combination of telmisartan and dapagliflozin demonstrated the most significant synergistic effect in lowering blood pressure, this combination did not notably enhance vascular function. In contrast, candesartan, which had a minor interaction with blood pressure control, showed the most substantial complementary effect on vasoprotection. Therefore, exploring additional mechanisms for these two drugs' blood pressure regulation effects is crucial; in Part 3 of this study, we will examine the influence on SGLT2 and renal function.

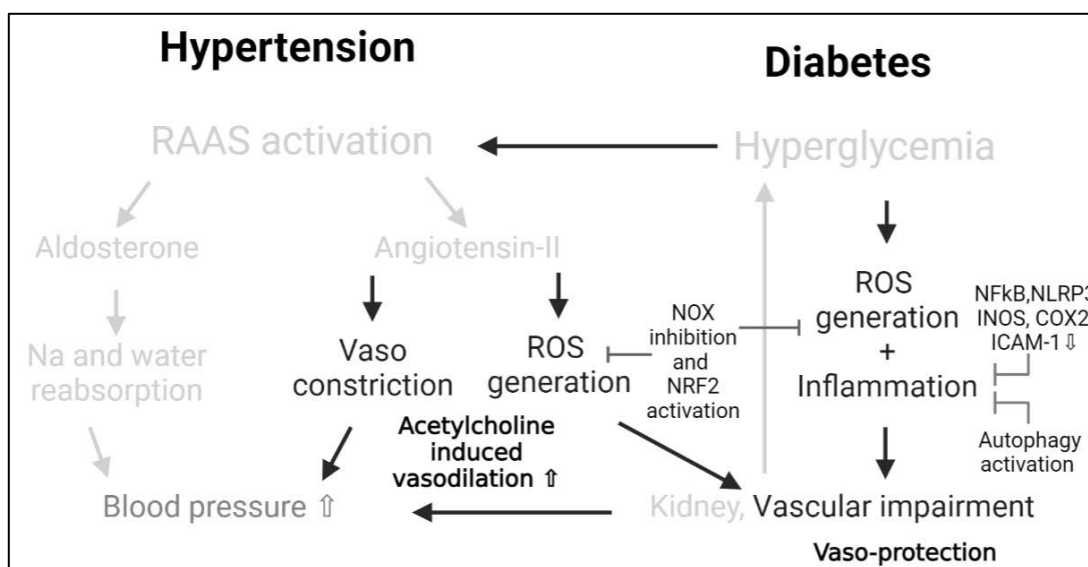


Figure 28. The vasoprotective effects of dapagliflozin and ARBs.

**Part 3. Enhancement of Dapagliflozin by ARB:
Hyperglycemia, SGLT2, and NHE-1**

3-1. Materials and methods

3-1.1. Materials and experimental animals

The ARBs, including fimasartan, telmisartan, and candesartan cilexetil, were provided by Dr. Yong-Ha Ji. The SGLT2 inhibitor dapagliflozin was obtained as Forxiga™ tablets containing 10 mg of the active ingredient.

SHRs were purchased from Charles River and housed at the Jeju National University animal facility for at least seven days before use in the experiments. Animals were fasted for four hours before drug administration, and water was provided *ad libitum*. The animals were housed under controlled conditions with a temperature of $22 \pm 5^\circ\text{C}$, a humidity of $50 \pm 10\%$, and a 12-hour light/dark cycle. All animal experiments were performed under the guidelines of the ‘Institutional Animal Care and Use Committee at Jeju National University’ (protocol number: 2018-0019).

3-1.2. Experiment

Male SHR rats, 60-65 weeks of age and weighing between 380-420 g, were used in this study with four to five animals per group. The experimental groups consisted of a control group, a dapagliflozin single administration group, low and high doses of ARB single administration groups, and low and high doses of ARB and dapagliflozin combination groups (Figure 29). All doses were calculated using body surface area conversion factors from FDA, which provides an equivalent dose relative to clinical applications; dapagliflozin 1 mg/kg, fimasartan 3 and 12 mg/kg, telmisartan 2 and 8 mg/kg, and candesartan 0.8 and 3.2 mg/kg. The animals were housed in a metabolic cage and were acclimatized to the cage two days before the initiation of drug administration. The animals were administered drugs for one week and euthanized with CO₂ gas; serum and organs were collected. During experimental periods, urine

output, water intake, food intake, and body weight were recorded daily. Urine was collected and stored at -20°C for subsequent analysis.

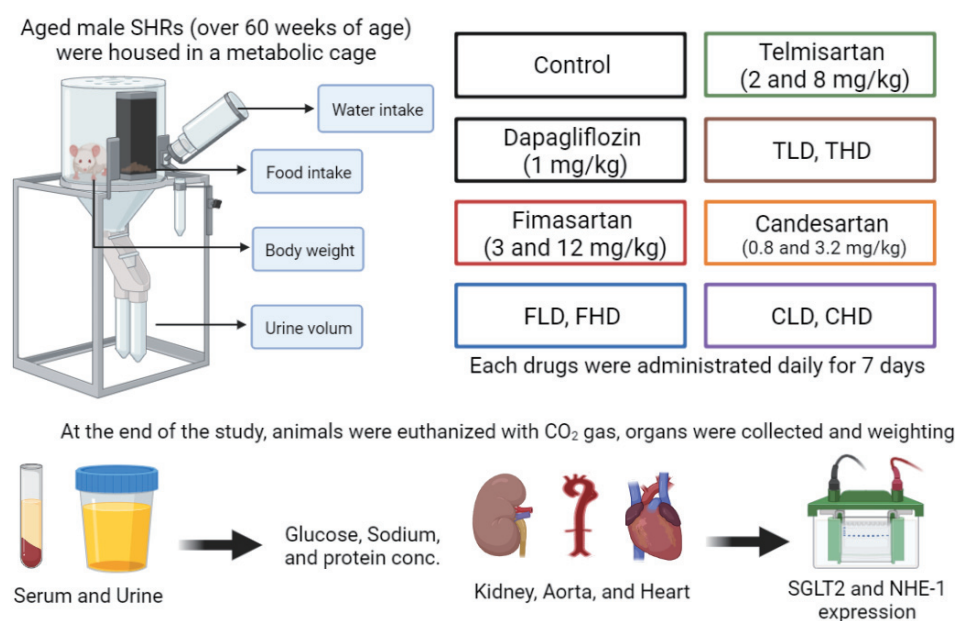


Figure 29. A schematic diagram of the experimental group and the experimental schedule

3-1.3. Urine and blood analysis

All urine samples were centrifuged at 3,000 rpm for five minutes to remove debris. Protein concentration in urine was measured using the Bradford assay, and glucose concentration was measured by colorimetry methods using the Glucose-PAP SL reagent (ELITechGroup, France). Sodium concentration was measured using an electrical conductivity meter (CSF-1000 salinometer, CAS, Korea). Serum glucose and sodium concentrations were determined using the same methods as for urine.

3-1.4. Organ weight

Organs, including liver, lung, brain, kidney, heart, and spleen, were collected and weighed. The organ index was calculated by dividing each organ's weight by the animal's body weight (mg organ/g body weight).

3-1.5. ACHN cells

ACHN cells, human renal epithelial cells derived from a renal adenocarcinoma, were obtained from Professor Chang-Hwan Ahn. The cells were cultured in RPMI-1640 medium (Gibco) supplemented with 10% FBS and 100 U/mL P/S at 37°C in a humidified atmosphere of 5% CO₂. Cells were harvested after 24 hours of drug treatment.

3-1.6. Protein analysis

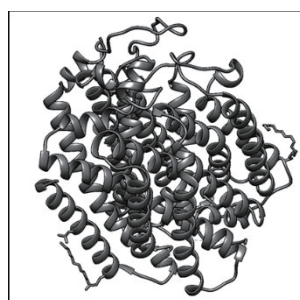
(1) Protein preparation: The Kidney, heart, and aortic tissues from experimental animals were disrupted using RIPA buffer with Tissue Lyser II. The homogenate was centrifuged at 13,000 rpm, 4°C for 15 minutes, and the supernatant was collected. ACHN cells were washed with PBS and then lysed with RIPA buffer for 30 minutes on ice. The supernatant was collected after centrifugation at 13,000 rpm, 4°C for 15 minutes.

(2) Western blotting: The protein contents of lysates were quantified using the Bradford assay, and the same amount of protein was mixed with sample buffer and denatured. 20 µg of protein per well was loaded onto 8-12% SDS-PAGE and electrophoresed at 120-150 V for one hour. The separated proteins were transferred to PVDF membranes at 100 V for two hours using wet transfer methods. After washing with TBST, the membranes were blocked with 5% blocking grade buffer for 30 minutes to prevent nonspecific binding. The membranes were incubated overnight at 4°C with primary antibodies. The following primary antibodies were used; anti-SGLT2 (Cell Signaling) and NHE-1 and β-actin (Santacruz Biotechnology). After washing,

the membranes were incubated for one hour with a secondary antibody conjugated with HRP. The protein was visualized using electrochemiluminescence and detected using Chemi-Doc molecular imaging system. The expression levels of each protein were obtained using the Evolution Capt software and normalized by β -actin and further calculated to relative values based on control.

3-1.7. Molecular docking

The structure of the SGLT2 protein was downloaded in .pdb format from the Protein Data Bank (Figure 30) [238]. The structures of compounds were downloaded in .sdf format from PubChem (Figure 9).



SGLT2
(PDBID: 7VSI)

Figure 30. Structure of SGLT2 obtained from Protein Data Bank.

3-1.8. Statistical analysis

All data were presented as mean \pm SEM. Statistical analyses were performed using GraphPad Prism 6 program, conducting one-way and two-way ANOVA and using Tukey's post hoc test for significance verification. A p-value of less than 0.05 was considered significant.

3-2. Results

3-2.1. SGLT2

To examine the effects of ARBs on the target of dapagliflozin, we measured glucose/sodium and SGLT2 protein expression in aged SHRs with both hyperglycemia and hypertension. Administration of fimasartan led to reductions of 3.58 and 6.32 mg/day in the FL and FH groups, respectively; notably, urinary glucose in the FH group was significantly lower than in the FL group (Figure 31A). On the other hand, glucose excretion in all dapagliflozin-administrated animals showed significantly higher urinary glucose than in the control group. The glucose excretion of the dapagliflozin group was 0.47 ± 0.01 g/day, a 37-fold increase over the control group (12.65 ± 0.06 mg/day). Excreted glucose of FLD and FHD groups was 0.49 ± 0.00 and 0.76 ± 0.01 g/day, respectively, higher than in the fimasartan alone group, with FHD showing a significant increase compared to both the dapagliflozin monotherapy and FLD groups. Blood glucose levels of the dapagliflozin group exhibited a significant decrease compared to the control group (254.0 ± 7.13 mg/dL vs. 200.2 ± 1.81 mg/dL) (Figure 31B). However, in single and combination groups, fimasartan did not significantly decrease blood glucose levels. Daily urine volume was 1.7-fold higher in the dapagliflozin group (34.5 ± 2.06 mL/day) compared to the control group (Figure 31C). The FLD and FHD groups also increased to 31.7 ± 3.38 and 33.7 ± 4.91 mL/day, respectively, although urine output in the FLD group was significantly lower than in the dapagliflozin group.

Sodium excretion was significantly increased by dapagliflozin, but the FLD group presented significantly lower values compared to the dapagliflozin group (Figure 31D). The FHD group had higher levels than the FLD group, but there was no significant difference from the control group. Blood sodium concentrations did not show significant changes in all fimasartan groups but were 1.13-fold lower in the dapagliflozin group (122.3 ± 3.65 mM vs. 138.6 ± 3.60 mM in

the control group). SGLT2 expression in the kidney showed a significant decrease in the dapagliflozin-treated group compared to the control group (Figure 31E). In conclusion, fimasartan reduced the dapagliflozin-induced urinary excretion of glucose and sodium, partially attributed to its interfering with the downregulation of SGLT2 by dapagliflozin.

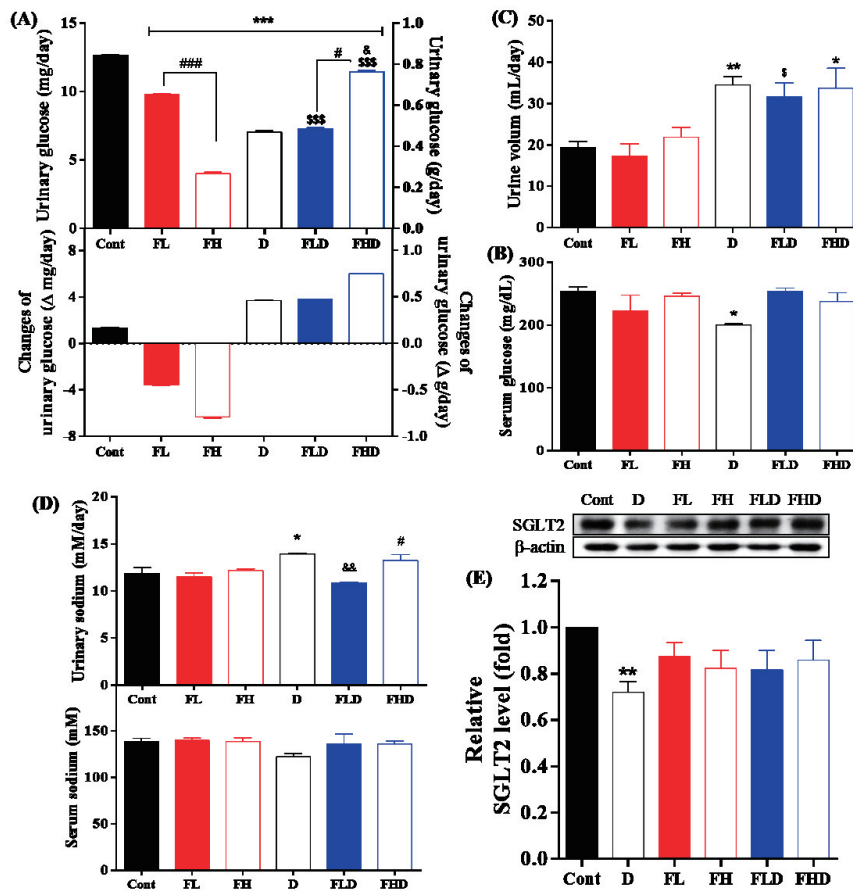


Figure 31. Effects of fimasartan and dapagliflozin on glucose/sodium and SGLT2 in aged SHR.

Male SHRs over 60 weeks were placed in metabolic cages of age and received oral administration of the drugs for one week. Urinary and serum glucose concentrations were measured one week after drug administration. The urinary glucose contents were calculated based on each animal's basal urinary glucose contents and daily urine volume. Urinary and serum sodium concentrations were also measured one week after drug administration. After administration, the experimental animals were euthanized using CO₂ gas, and kidney proteins were extracted for performing western blotting. Western blot images were visualized using the ChemiDoc system. The expression levels of SGLT2 were normalized by β-actin, and the relative ratio was calculated based on the control group. (A) The urinary glucose, (B) serum glucose, (C) daily urine output, (D) urinary and serum sodium, and (E) renal SGLT2 expression levels of SHRs administered with fimasartan and dapagliflozin alone and in combination. All data are expressed as mean ± standard error mean. *, **, *** means a significant difference at the p < 0.05, 0.01, and 0.001

levels compared to the control group. #, ### means a significant difference between the low and high concentration groups at the $p < 0.05$ and 0.001 levels. ^s, ^{sss} means a significant difference at the $p < 0.05$ and 0.001 levels exists between the same dose of the combined group and single administration group. &, && means a significant difference at the $p < 0.05$ and 0.01 levels compared to the dapagliflozin alone group. Cont, SHR control group; D, dapagliflozin alone group (1 mg/kg); FL, low-dose fimasartan alone (3 mg/kg); FH, high-dose fimasartan alone group (12 mg/kg); FLD, low-dose fimasartan (3 mg/kg) and dapagliflozin (1 mg/kg) combination group; FHD, high-dose fimasartan (12 mg/kg) and dapagliflozin (1 mg/kg) combination group.

Telmisartan administration decreased glucose excretion by 1.93 and 5.86 mg/day in the TL and TH groups (Figure 32A). The glucose excretion in the TLD and THE groups increased significantly compared to the control group. Glucose excretion in each group was 0.94 ± 0.01 g/day for TLD and 0.93 ± 0.01 g/day for THD, and both significantly increased compared to dapagliflozin ($p < 0.001$). Blood glucose levels significantly declined in all telmisartan-treated groups compared to the control group (Figure 32B).

Urine volume was 39.0 ± 6.56 and 40.7 ± 5.78 mL/day for TLD and THD, respectively, significantly increased compared to the control and dapagliflozin alone groups (Figure 32C).

Sodium excretion did not show a significant change in the telmisartan alone group, and the TLD group showed significantly higher than the TL group (13.0 ± 0.24 mM/day vs. 10.4 ± 0.49 mM/day in the TL group) (Figure 32D). The THD group displayed 16.7 ± 0.67 mM/day, considerably higher than the control group, the dapagliflozin alone group, and the TH group. In addition, blood sodium concentrations were significantly reduced in all groups receiving dapagliflozin compared to both the control group and the group receiving telmisartan alone (Figure 32D). Renal SGLT2 expression was significantly reduced in all dapagliflozin-treated and TH groups compared to the control group (Figure 32E).

In summary, telmisartan lowers blood glucose, partly due to reduced SGLT2 expression; it also amplifies the urinary excretion of glucose and sodium induced by dapagliflozin.

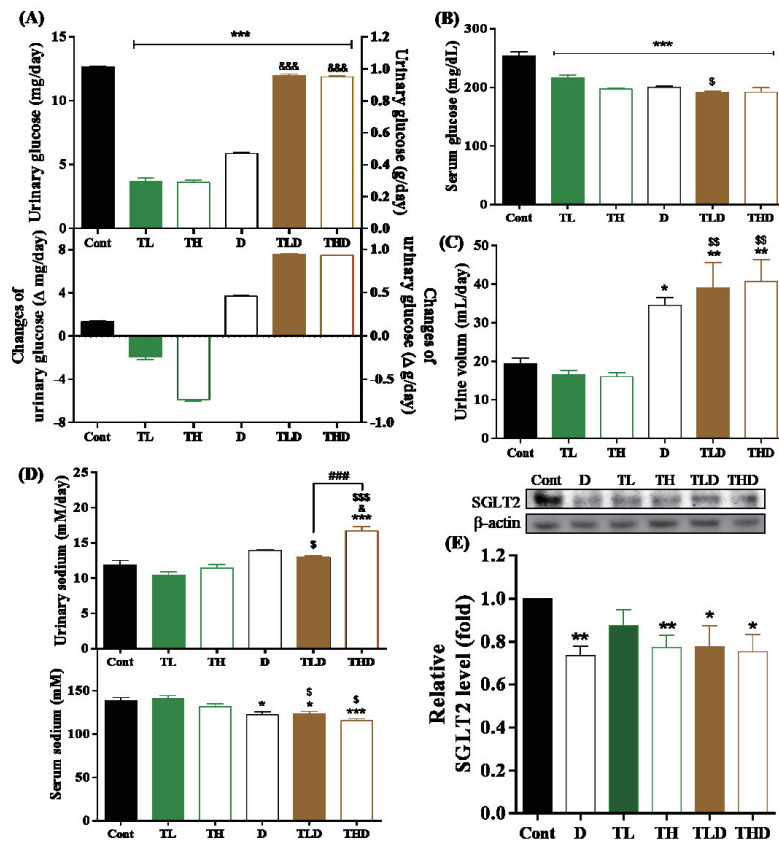


Figure 32. Effects of telmisartan and dapagliflozin on glucose/sodium and SGLT2 in aged SHR.

Experimental progress is the same as described in Figure 31. (A) The urinary glucose, (B) serum glucose, (C) daily urine output, (D) urinary and serum sodium, and (E) renal SGLT2 expression levels of SHRs administered with telmisartan and dapagliflozin alone and in combination. All data are expressed as mean \pm standard error mean. *, **, *** means a significant difference at the $p < 0.05$, 0.01 , and 0.001 levels compared to the control group. ### means a significant difference between the low and high concentration groups at the $p < 0.001$ level. \$, \$\$, \$\$\$ means a significant difference at the $p < 0.05$, 0.01 , and 0.001 levels exist between the same dose of the combined group and single administration group. &, &&& means a significant difference at the $p < 0.05$ and 0.001 levels compared to the dapagliflozin alone group. Cont, SHR control group; D, dapagliflozin alone group (1 mg/kg); TL, low-dose telmisartan alone (2 mg/kg); TH, high-dose telmisartan alone group (12 mg/kg); TLD, low-dose telmisartan (2 mg/kg) and dapagliflozin (1 mg/kg) combination group; THD, high-dose telmisartan (8 mg/kg) and dapagliflozin (1 mg/kg) combination group.

Candesartan administration alone significantly reduced glucose excretion in the CH group more than in the CL group (Figure 33A). However, glucose excretion in the CLD and CHD groups significantly increased compared to the control and individual treatment groups. Neither the CLD nor CHD group exhibited a significant level difference compared to the dapagliflozin group. Blood glucose levels did not significantly change across all groups compared to the control group (Figure 33B).

Urinary volume was 37.3 ± 5.70 and 35.3 ± 4.37 mL/day for the CLD and CHD groups, an increase compared to the control and single administration groups but not significantly different from the dapagliflozin group (Figure 33C). Sodium excretion significantly decreased in the CHD group compared with the control and CH groups, while blood sodium concentration showed no significant level differences (Figure 33D). Renal SGLT2 expression levels did not change significantly in all candesartan-administered groups, with the CLD group significantly increasing compared to the dapagliflozin alone group (Figure 33E).

In conclusion, candesartan does not significantly affect dapagliflozin-induced glucose and sodium excretion but interferes with SGLT2 expression.

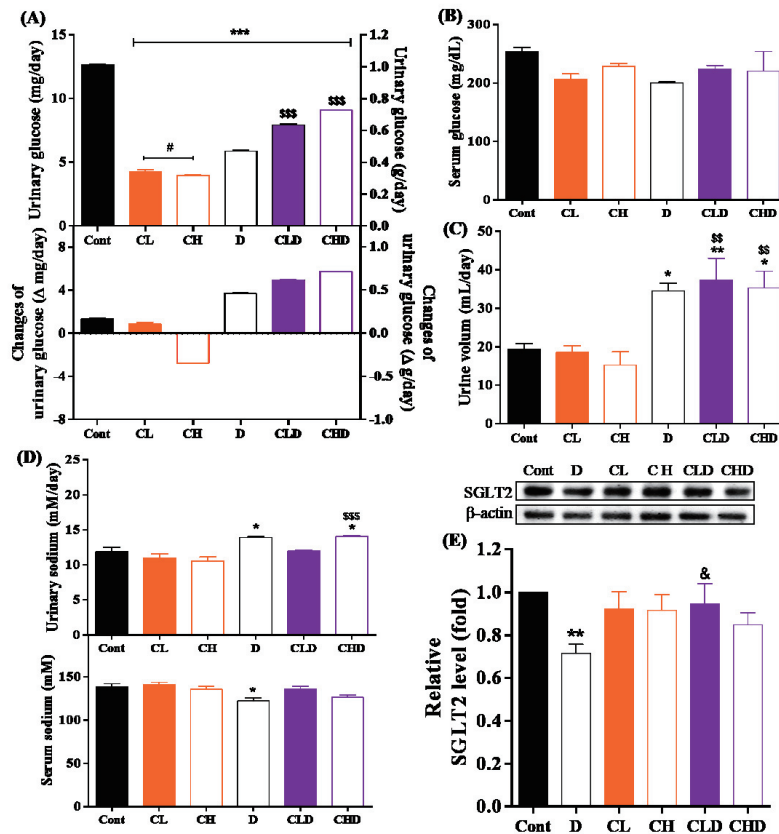


Figure 33. Effects of candesartan and dapagliflozin on glucose/sodium and SGLT2 in aged SHR.

Experimental progress is the same as described in Figure 31. (A) The urinary glucose, (B) serum glucose, (C) daily urine output, (D) urinary and serum sodium, and (E) renal SGLT2 expression levels of SHRs administered with candesartan and dapagliflozin alone and in combination. All data are expressed as mean \pm standard error mean. *, **, *** means a significant difference at the $p < 0.05$, 0.01 , and 0.001 levels compared to the control group. # means a significant difference between the low and high concentration groups at the $p < 0.05$ level. \$\$\$, \$\$\$ means a significant difference at the $p < 0.01$ and 0.001 levels exists between the same dose of the combined group and single administration group. & means a significant difference at the $p < 0.05$ level compared to the dapagliflozin alone group. Cont, SHR control group; D, dapagliflozin alone group (1 mg/kg); CL, low-dose candesartan alone (0.8 mg/kg); CH, high-dose candesartan alone group (3.2 mg/kg); CLD, low-dose candesartan (0.8 mg/kg) and dapagliflozin (1 mg/kg) combination group; CHD, high-dose candesartan (3.2 mg/kg) and dapagliflozin (1 mg/kg) combination group.

The docking studies investigating the interactions of three types of ARBs and dapagliflozin with the SGLT2 protein revealed that these drugs' binding affinities and interaction patterns varied (Table 5 and Supplementary Figure 13-16). This high affinity may be attributed to the various van der Waals interactions telmisartan forms with the SGLT2 protein and a conventional hydrogen bond with PHE 504 amino acid. Furthermore, telmisartan displayed a pi-pi-stacked binding with TYR 455, similar to the interaction between dapagliflozin and SGLT2. In contrast, fimasartan and candesartan exhibited lower binding affinities than telmisartan, at -7.3 and -8.5 kcal/mol, respectively. Both fimasartan and candesartan showed binding with ASP 454 of SGLT2.

When dapagliflozin was already bound to the SGLT2 structure, an increased binding affinity was observed upon subsequent binding of fimasartan and telmisartan. Telmisartan formed new hydrogen bonds with GLU503 and GLY507, replacing the previous bond with PHE504. Its hydrogen bond with SER362 was maintained for candesartan, yet its binding affinity diminished to -8.4 kcal/mol. Fimasartan and telmisartan binding affinity to SGLT2 increased when dapagliflozin was pre-bound. All three ARBs demonstrated significant alterations in their binding form under these conditions.

Table 5. Binding affinity and interactions of sodium-glucose cotransporter 2 with ARBs and dapagliflozin.

SGLT2	Binding affinity (kcal/mol)	Hydrogen bond	Hydrophobic interaction
Dapagliflozin	-8.1	GLN451, SER508	PHE152, SER156, TRP440, VAL443, ALA446, ALA447, GLN448, LEU452, TYR455, PHE504
Fimasartan	-7.3	ASP273	THR87, ALA90, SER91, CYS255, ARG336, VAL343, ALA344, CYS345, VAL359, GLY360, SER362, GLY450, PHE453, ASP454, SER510
Telmisartan	-9	PHE504	SER156, TRP440, VAL443, VAL444, ALA447, GLN451, LEU452, TYR455, GLU503, SER505, GYS507, SER508
Candesartan	-8.5	THR87, SER362	ALA90, SER91, PHE254, CYS255, ARG257, LEU274, ARG336, VAL359, GLY360, GLY450, ASP454, SER510
SGLT2+Dapa	Binding affinity (kcal/mol)	Hydrogen bond	Hydrophobic interaction
Fimasartan	-7.8	-	THR87, ALA90, SER91, CYS255, ASP273, LEU274, ARG336, VAL359, SER362, GLY450, GLN451, ASP454, SER508, GLY509, SER510, CYS511
Telmisartan	-9.6	GLU503, GLY507	THR87, ASP273, LEU274, GLN451, ASP454, TYR455, ALA458, ARG499, PHE504, SER508, CYS522, VAL524, HIS525, TYR526
Candesartan	-8.4	SER362	THR87, ALA90, SER91, PHE254, CYS255, ARG257, LEU274, ARG336, VAL359, GLY360, GLY450, ASP454, SER510

3-2.2. NHE-1

We investigated the effects of ARBs on NHE-1, another well-known target molecule of dapagliflozin. All groups treated with fimasartan, not only dapagliflozin, showed a significant decrease in renal NHE-1 expression compared to the control group (Figure 34A). The measurements of urinary protein levels demonstrated a significant reduction in all fimasartan-treated groups compared to the controls (Figure 34B). Furthermore, the FLD and FHD groups significantly reduced proteinuria compared to the same concentration-only groups ($p < 0.01$ and $p < 0.05$). However, dapagliflozin alone failed to reduce urinary protein.

In summary, dapagliflozin reduced renal NHE-1 but did not decrease urinary protein. On the other hand, fimasartan synergized with dapagliflozin to reduce urinary protein and lower aortic and cardiac NHE-1.

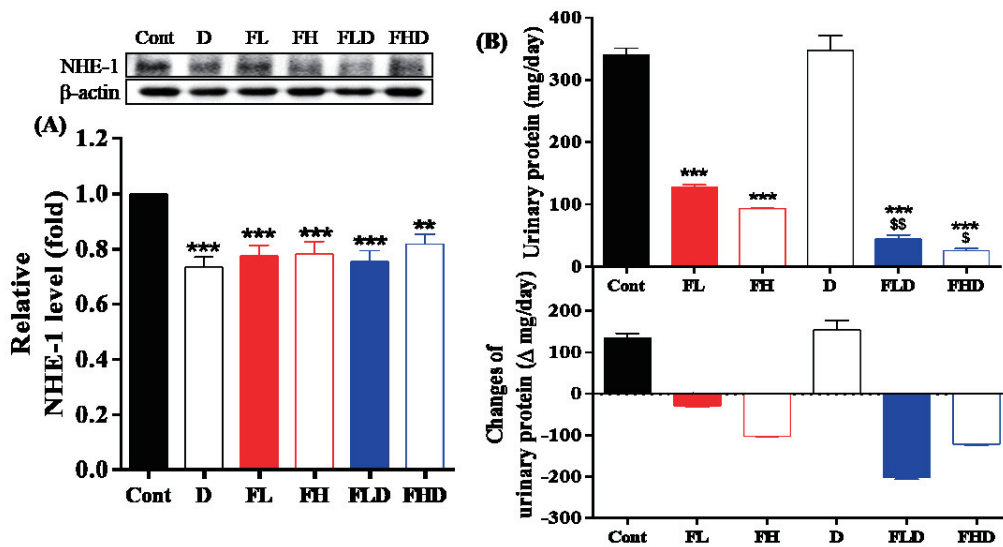


Figure 34. Effects of fimasartan and dapagliflozin on renal NHE-1 expression and proteinuria in aged SHR.

Experimental progress and groups are the same as described in Figure 31. (A) The renal NHE-1 expression levels and (B) urinary protein excretion of SHRs administered with fimasartan and dapagliflozin alone and in combination. All data are expressed as mean \pm standard error mean. **, *** means a significant difference at the $p < 0.01$ and 0.001 levels compared to the control group. $^{\$}$, $^{\$}$ means a significant difference at the $p < 0.05$ and 0.01 levels exist between the same dose of the combined group and single administration group.

Telmisartan administration resulted in a significant reduction in renal NHE-1 levels (Figure 35A). However, when co-administered with dapagliflozin, the levels in the TLD group were 0.97 ± 0.10 and in the THD group were 1.09 ± 0.08 , which were significantly higher than in the groups treated with telmisartan alone or dapagliflozin alone.

The urinary protein concentration was significantly decreased in all groups treated with telmisartan compared to the control group (Figure 35B). The urinary protein content of the TLD and THD groups was higher than that of the telmisartan alone group ($p < 0.001$). Still, there was no difference from the single group due to calculating the baseline value, which is thought to be due to individual differences.

In conclusion, telmisartan decreased renal NHE-1 expression and urinary protein, but these effects were attenuated when co-administered with dapagliflozin.

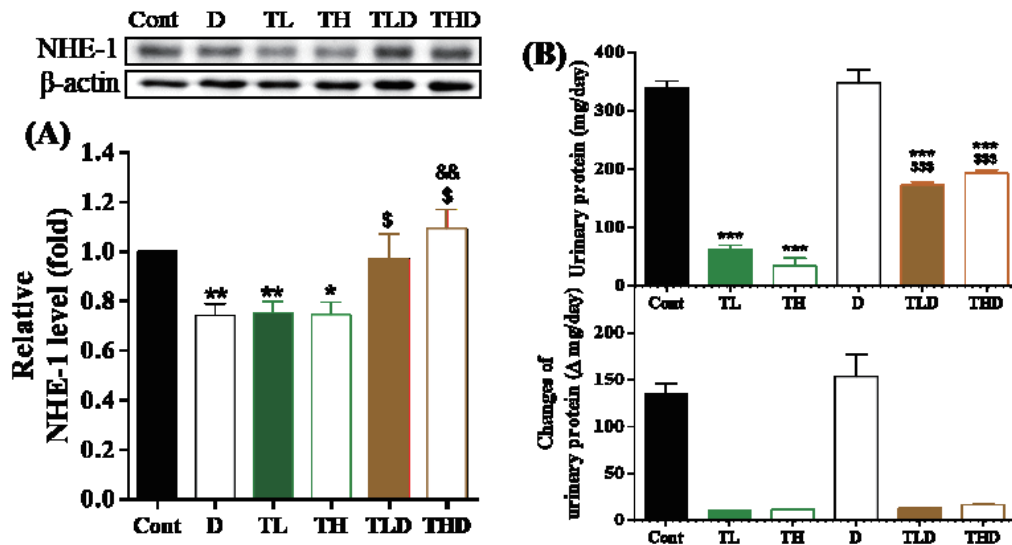


Figure 35. Effects of telmisartan and dapagliflozin on renal NHE-1 expression and proteinuria in aged SHR.

Experimental progress and groups are the same as described in Figures 31 and 32. (A) The renal NHE-1 expression levels and (B) urinary protein excretion of SHRs administered with telmisartan and dapagliflozin alone and in combination. All data are expressed as mean \pm standard error mean. *, **, *** means a significant difference at the $p < 0.05$, 0.01 , and 0.001 levels compared to the control group. \$, \$\$\$ means a significant difference at the $p < 0.05$ and 0.001 levels exists between the same dose of the combined group and single administration group. && means a significant difference at the $p < 0.01$ level compared to the dapagliflozin alone group.

Candesartan reduced the renal NHE-1 expression in both single and combination administration groups (Figure 36A). However, the CLD group didn't show significant changes compared to the control group. The difference in urinary protein excretion levels was 5.7 ± 4.90 and 100.6 ± 9.23 mg/day in the CL and CH groups, respectively, with a higher decrease in the high-concentration group (Figure 36B). In the combined administration groups with dapagliflozin, the CLD group showed 101.6 ± 9.23 mg/day and the CHD group 186.6 ± 7.95 mg/day. The CLD and CHD groups were significantly lower than the control and single administration groups.

In summary, candesartan reduced renal NHE-1 expression and urinary protein and showed a synergistic effect with dapagliflozin in reducing urinary protein. Aortic and cardiac NHE-1 expression also decreased synergistically in the combination therapy group.

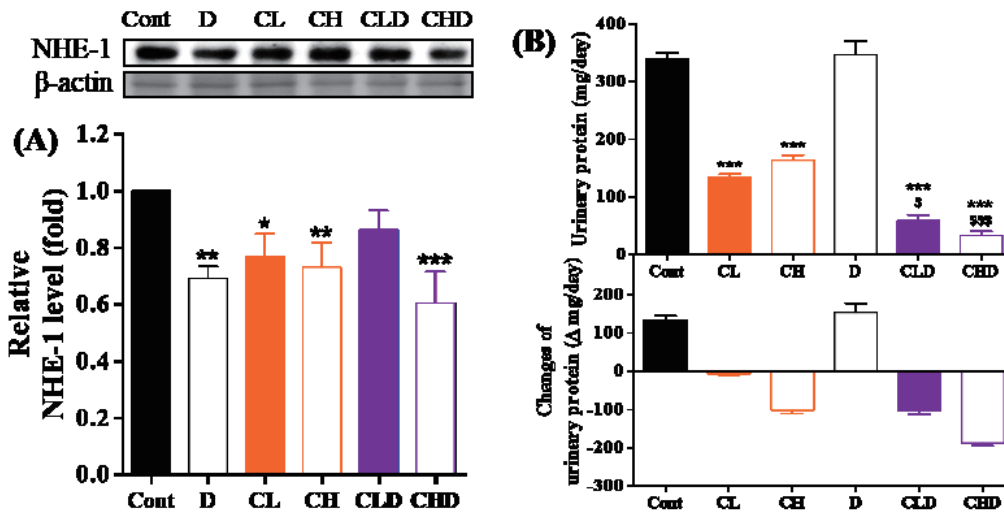


Figure 36. Effects of candesartan and dapagliflozin on renal NHE-1 expression and proteinuria in aged SHR.

Experimental progress and groups are the same as described in Figures 31 and 33. (A) The renal NHE-1 expression levels and (B) urinary protein excretion of SHRs administered with candesartan and dapagliflozin alone and in combination. All data are expressed as mean \pm standard error mean. *, **, *** means a significant difference at the $p < 0.05$, 0.01, and 0.001 levels compared to the control group. ^{s, sss} means a significant difference at the $p < 0.05$ and 0.001 levels exists between the same dose of the combined group and single administration group.

3-3. Discussion

In aged SHR, dapagliflozin increased urine output and water intake. Co-administration of dapagliflozin with fimasartan or candesartan further increased water intake, while urine volume was most increased in the telmisartan combination group. Dapagliflozin elevated urinary glucose and sodium levels while decreasing blood glucose and sodium. When combined, urinary glucose levels were increased, but blood glucose levels did not differ significantly from the ARB alone group. Renal SGLT2 expression was reduced by dapagliflozin, and although candesartan and fimasartan showed a decrease trend, it was not significant. Telmisartan, both alone and in combination with dapagliflozin, exhibited the highest affinity with SGLT2 and decreased its expression. Urine protein levels were significantly decreased in all ARB groups, and combining dapagliflozin with fimasartan or candesartan further reduced urinary protein. However, telmisartan alone had the lowest urinary protein levels among the ARBs, and when combined with dapagliflozin, the levels increased compared to the telmisartan-only group. NHE-1 expression, a marker of renal fibrosis, decreased with dapagliflozin and ARBs. Candesartan showed a further decrease when combined with dapagliflozin, while telmisartan increased. In summary, fimasartan and candesartan showed renoprotective effects when combined with dapagliflozin, while the combination of telmisartan and dapagliflozin exhibited a potent blood glucose-lowering effect but lacked a renoprotective effect.

Inhibition of SGLT2 by dapagliflozin increases urinary glucose concentration as a mechanism for blood glucose lowering. Our results also show an increase in urinary glucose excretion and a decrease in blood glucose by dapagliflozin. On the other hand, in the ARB-alone group, urinary glucose excretion decreased, which is thought to be a phenomenon caused by a decrease in blood pressure. Indeed, the reduction in glucose excretion in the high-dose group,

which showed higher blood pressure lowering in all three types of ARBs, was greater than that in the low-dose group. Indeed, several clinical studies have reported that an increase in blood glucose can be used to predict a rapid reduction in blood pressure [239, 240]. Perhaps for this reason, although fimasartan and candesartan increased glucose excretion in the combined administration group, there was no change in blood glucose. Of course, ARBs and ACE inhibitors are famous for reducing the risk of type 2 diabetes [241]. However, the well-known common side effects of antihypertensive drugs, such as beta-blockers and thiazide diuretics, are abnormal glucose and lipid metabolism, which suggests that the drugs' properties and the reduction in blood pressure may affect blood glucose [240, 242, 243]. Moreover, the duration of drug administration in our current study was brief, lasting only one week. Based on various evidence, short-term administration of antihypertensive drugs may elicit compensatory glucose retention to counteract the reduction in blood pressure. Some reports also suggest intensive blood pressure management could elevate the risk of fasting blood glucose disorder [244]. Hence, it is necessary to conduct further experiments to determine how these observed phenomena change for long-term administration. The critical result is that the combination of fimasartan and dapagliflozin demonstrated a synergistic effect on blood pressure reduction and exhibited vasoprotective effects without inducing significant changes in blood glucose. Thus, it could be proposed as a therapeutic option for hypertensive patients who do not have diabetes.

On the other hand, telmisartan showed a significant decrease in blood glucose in the combined group with dapagliflozin and the single group, which showed a decrease in urinary glucose excretion. Telmisartan has been reported to have potential benefits for various diseases and diabetes, one of which is the well-known effect of improving insulin sensitivity and reducing blood sugar through the activation of PPAR γ [245, 246]. In addition, it has been reported that telmisartan is reported to have a PPAR γ -agonistic effect while avoiding the safety concerns found with thiazolidinediones and has an additional mechanism of increasing insulin secretion

through ion channel stimulation independently of AT1 and PPAR γ [247, 248]. The blood glucose reduction effect shown in all telmisartan groups appears to be attributable to this. In addition, in some studies, telmisartan has been reported to reduce SGLT2 expression in the kidneys of diabetic rats [249]. Indeed, in our result, dapagliflozin, telmisartan alone, and combined treatment groups showed a significant decrease of SGLT2 in kidneys and ACHN cells (Supplementary Figure 17). This contrasts the fact that two other ARBs reversed the decrease in SGLT2 expression caused by dapagliflozin when combined. On the other hand, PPAR γ agonists can increase SGLT2 expression in renal proximal tubular cells and pancreatic alpha cells [250, 251]. This means, telmisartan inhibits not only PPAR γ but also SGLT2 independently; it is thought that it may have an additional advantage in controlling blood glucose.

Given that SGLT2 is a sodium-glucose cotransporter, the increased glucose excretion associated with SGLT2 inhibition accompanies sodium excretion. Zeng et al., reported that low-dose empagliflozin significantly reduced blood pressure via sodium excretion in non-diabetic, high-salt diet-fed rats [252]. Hence, it was inferred that the blood pressure-lowering synergistic effect of ARB and dapagliflozin resulted from increased sodium excretion. Indeed, the telmisartan and dapagliflozin combination group showed increased sodium excretion and decreased blood sodium concentration. In contrast, the combined use of fimasartan and candesartan did not decrease blood sodium concentration and, in particular, reduced sodium excretion by dapagliflozin at low concentrations. Assuming the differences among ARBs are due to differences in binding with SGLT2, a molecular docking study was conducted. The results showed that telmisartan not only has the highest binding affinity for SGLT2 among the ARBs but also binds to SER156, TRP440, VAL 443, ALA447, LEU452, TYR455, PHE 504, and SER508, which are the dapagliflozin binding sites; suggesting that telmisartan could provide additional inhibition of SGLT2. Unlike dapagliflozin and telmisartan, candesartan and

fimasartan were shown to bind commonly to ALA90, SER91, CYS255, ARG336, VAL359, GLY360, GLY450, ASP454, and SER510. On the other hand, when dapagliflozin was pre-bound, the three ARBs exhibited significantly different patterns from the essential binding, making it difficult to ascertain the impact of specific binding changes. Especially when dapagliflozin was pre-bound, telmisartan formed new hydrogen bonds with the GLY507 and GLU503 residues of SGLT2. These molecular interaction changes might contribute to the altered SGLT2 function, particularly when dapagliflozin and telmisartan are co-administered. Future research should investigate the impact of these hydrogen bonds between pre-bound dapagliflozin and telmisartan on SGLT2 function.

In summary, results showed that fimasartan and candesartan inhibited the dapagliflozin-induced decrease in SGLT2 expression and the subsequent reduction in blood glucose and sodium. Although no specific reasoning has been given for this occurrence, it's possible that there were compensatory changes in blood glucose due to the short-term administration. Moreover, the distinctive ways these two drugs bind to SGLT2 and dapagliflozin should also be considered. Conversely, telmisartan not only decreased blood sugar alone, but when combined, it also demonstrated a synergistic effect on sodium excretion. This effect is partially due to the efficacy similar to dapagliflozin in inhibiting SGLT2 and reducing its expression. Considering that telmisartan was the drug that showed the most effective blood pressure reduction in part 1, the primary mechanism of synergy between these two drugs for blood pressure reduction may be the excretion of sodium and glucose. However, when choosing the drug for combination therapy, selecting drugs with a common mechanism of action is typically avoided. Therefore, these results should be considered when deciding on combining these two drugs in clinical practice.

As previously mentioned, a significant complication of diabetes is DKD, and its management

involves controlling blood glucose and blood pressure using RAAS inhibitors [41]. Therefore, we investigated the effects of the ARBs on the expression of NHE-1, a well-known target molecule of dapagliflozin, and urinary protein, a representative indicator of glomerular damage. NHE-1 is the most widely distributed NHEs within the kidney, including plasma membrane expression in all nephron segments, except for dense plaques and interstitial cells in the distal nephron [253]. Interestingly, while it's widely recognized that excessive NHE-1 can adversely affect the heart and blood vessels, studies on renal effects are somewhat limited [254, 255]. The role of renal NHE-1 varies depending on the disease modality. Reports suggest that NHE-1 inhibitors improve renal blood flow, whereas loss of NHE-1 function exacerbates apoptosis [256, 257]. This might be partial because NHE-1 activation is responsible for the initial defense against apoptosis through preserving cell volume. Indeed, proximal tubular cells exposed to staurosporine-induced apoptotic stress initially show increased NHE-1 activity [258]. However, in general, NHE-1 is implicated in the pathogenesis of type 1 diabetes [259] and is known to be significantly increased in models of glomerulosclerosis and fibrosis [260, 261]. There's evidence that NHE-1 inhibitors reduce aldosterone-induced glomerulosclerosis [262]. Therefore, some reports suggested that NHE-1 can be used to predict renal fibrosis [263]. GFR and urinary protein, markers of glomerular damage, and ion channels primarily involved in renal fibrosis often precede GFR damage and may not be suitable markers of fibrosis [263, 264]. Hence, in this study, we interpreted changes in NHE-1 expression as an index of renal fibrosis. Our results show that dapagliflozin significantly reduced renal NHE-1 expression levels; however, there was no significant effect on the urinary protein. Several studies have reported that dapagliflozin may improve eGFR but not proteinuria [265, 266]. Conversely, in animal models of nephropathy with proteinuria, dapagliflozin improved proteinuria at levels similar to commonly used ACE inhibitors, and glomerular lesions improved [267]. There are reports that dapagliflozin shows a more remarkable improvement in eGFR in a high sodium

intake state, suggesting that the decrease in plasma sodium in the previous SGLT2 study might have influenced these results [268].

On the other hand, fimasartan and candesartan reduced both renal NHE-1 expression and urinary protein and kidney weight (Supplementary Figure 12F). Fimasartan has been shown to reduce methotrexate-induced renal toxicity significantly, and according to the K-MetS study, it resulted in a better albumin-to-creatinine ratio reduction in patients with metabolic syndrome [269, 270]. Candesartan has also been shown to reduce proteinuria in patients with diabetic nephropathy [271, 272]. ARBs are primarily used to reduce the risk of CKD by controlling hemodynamic abnormalities [273]. Moreover, Ang2 has been reported to increase NHE-1 activity, and losartan has been demonstrated to decrease NHE-1 activity [274, 275]. Hence, the reduction in urinary protein and the decrease in NHE-1 as an index of fibrosis by the ARBs fimasartan and candesartan are confirmed as inherent effects of these drugs.

Furthermore, our results showed a synergistic effect of fimasartan and candesartan with dapagliflozin in reducing proteinuria. According to some studies, the combination treatment of a RAAS inhibitor and SGLT2 inhibitors in albuminuria CKD patients without diabetes is expected to significantly increase renal failure-free survival [276]. In a study involving 1,757 patients, combination therapy of an SGLT2 inhibitor and ACE inhibitors/ARBs in type 2 diabetes was more effective and better tolerated than monotherapy [42]. It showed better blood pressure control, improved renal outcomes, and reduced long-term renal function. Therefore, combining fimasartan and candesartan with dapagliflozin is expected to offer potential benefits in protecting vascular and renal function.

Meanwhile, when fimasartan and candesartan combined with dapagliflozin, demonstrated a significant decrease in NHE-1 expression in both the aorta and the heart (Supplementary Figure 18 and 19). NHE-1 is implicated in IgE-mediated macrophage protease expression,

extracellular acidification, apoptosis, lesional smooth muscle cell loss, endothelial cell adhesion molecule expression, and inflammatory cell infiltration in an Ang2-induced abdominal aortic aneurysm model [277]. Moreover, Ang2 has been reported to increase the expression of NHE-1 in the cardiovascular system and directly impair vascular function [134, 210]. In atherosclerotic lesions, NHE-1 is reported to promote atherogenesis via acidification of the lesion [254]. The inhibition of NHE-1 has been associated with potential protective effects, such as reducing endothelial cell and monocyte adhesion, decreasing ICAM expression under high glucose conditions, and alleviating Ach-dependent vascular relaxation disorders in diabetic models [278, 279]. Therefore, dapagliflozin's central cardiovascular protective mechanism is considered to be its inhibitory effect on NHE-1 across various tissues [124, 280]. Indeed, dapagliflozin has been reported to reduce myocardial hypertrophy through NHE-1 inhibition and decrease mortality in patients with chronic heart failure when administered with valsartan [281, 282]. In other words, the partial synergistic effects on vascular function protection and inflammation reduction, mainly when dapagliflozin is combined, may be attributed to the decrease in NHE-1. In contrast, telmisartan decreased renal NHE-1 expression and urinary protein, but these effects were attenuated when co-administered with dapagliflozin. A possible mechanism for this is an increase of sodium and water transporters in diabetic kidneys as a compensatory mechanism for preserving excessive loss [283, 284]. This means the combined administration of high concentrations of telmisartan and dapagliflozin can not only inhibit SGLT2 activity but also decrease its expression, and the excretion of excess glucose and sodium and the increase in urine volume may have increased the expression of NHE-1. Considering that the imbalance of various ion channels is involved in the aforementioned renal fibrosis, and an increase in NHE-1 can use to indicator of fibrosis, this hypothesis gains more clarity [263]. Indeed, the combination of fimasartan and candesartan, which did not affect SGLT2, reduced NHE-1 expression.

Another possibility for this is the known side effect of SGLT2 inhibitors, diabetic ketoacidosis (DKA), which is thought to be due to the decrease in blood glucose caused by SGLT2 inhibition, the decrease in insulin, and increased glucagon levels [285]. Concurrently, some research indicates that ARBs can modulate the activation or inhibition of renal uric acid transporter (URAT1)-mediated uric acid uptake differentially, depending on its concentration [286, 287]. For instance, it has been documented that combining telmisartan with HCTZ can lead to diminished urate excretion and increased serum urate concentrations [140]. Moreover, numerous evidences suggest that DKA induces metabolic acidosis, which could, in turn, influence the activity of NHE-1, and elevated uric acid can affect NHE-1 [130, 288, 289]. This potential mechanism could contribute to the onset of renal disease in hypertension and diabetes. Hence, the observed decline in renoprotective efficacy and the upregulation of NHE-1 in the dapagliflozin-telmisartan combination group could stem from the interaction of the side effects of both drugs. Nevertheless, a more comprehensive investigation is warranted to elucidate the direct relationship between DKA, serum urate, and NHE-1 activity or expression. Also, NHE-1, known to regulate intracellular pH by exchanging extracellular sodium with intracellular hydrogen ions, operates in a sodium concentration-dependent manner [129]. Consequently, a reduction in sodium due to SGLT2 inhibition could compromise the functionality of NHE-1. Although no direct interaction between SGLT2 and NHE-1 is currently known, the obliteration of the sodium gradient via Na-K-ATPase disruption could hinder NHE's function, culminating in renal tubular nephropathy and sodium deficiency [135, 290]. It has also been reported that this phenomenon can elevate the expression and activity of NHE3 in the intestine [290]. Thus, the concurrent inhibition of SGLT2 by high concentrations of telmisartan and dapagliflozin could induce alterations in the body's sodium balance. This change could subsequently indirectly impact the expression and activity of NHE-1 in the kidney.

In summary, fimasartan and candesartan demonstrated significant renoprotective efficacy, with

some synergistic effects when used with dapagliflozin. This outcome stems from the combination of the inherent renoprotective effects of ARBs and the well-documented benefits of dapagliflozin. Conversely, while telmisartan exhibited exceptional renal protection when combined with dapagliflozin, it increased kidney weight, urinary protein, and NHE-1 expression compared to the groups receiving individual treatments. This outcome is partially attributed to the electrolyte imbalance caused by the mutual inhibition of SGLT2 by the two drugs, which likely affected renal ion channels.

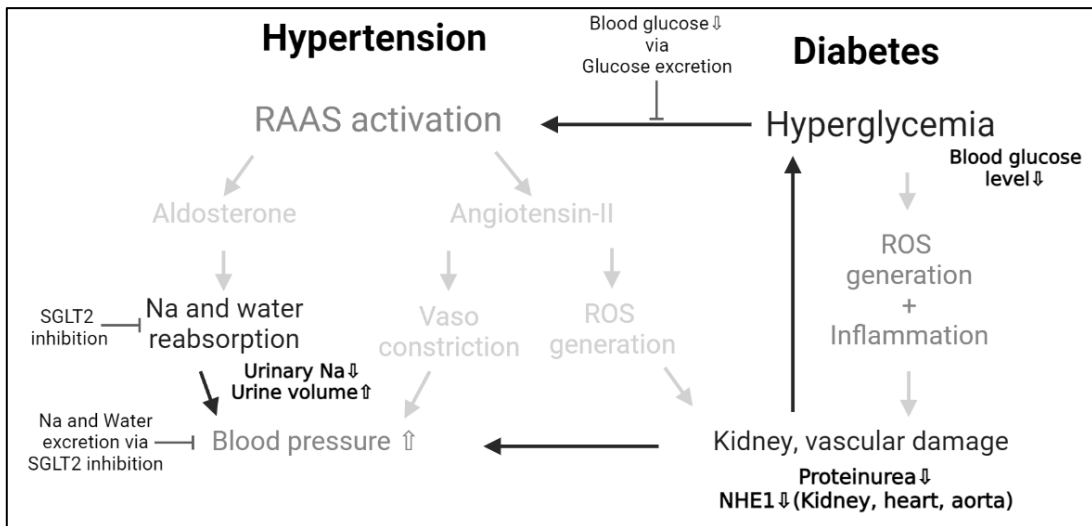


Figure 37. The glucose/sodium regulation and renoprotective effects of dapagliflozin and ARBs.

CONCLUSION

In summary, dapagliflozin demonstrated significant vasorelaxation and eNOS activation, though it exhibited limited blood pressure reduction and binding affinity to AT1. While the blood pressure-lowering capacities of the three ARBs investigated were comparable, telmisartan displayed a notable synergistic effect when combined with dapagliflozin and had the highest binding affinity for AT1. Fimasartan shows less than others, but vasorelaxation was increased in all ARBs when combined with dapagliflozin. Telmisartan demonstrated minor eNOS activation than other ARBs, and when fimasartan and candesartan upon co-treatment with dapagliflozin, eNOS activation was increased. These findings suggest that the enhancement in blood pressure control observed in the combination is likely due to vasorelaxation effects and eNOS activation by dapagliflozin. By introducing an additional vasorelaxation mechanism, the combination of these two medications may be beneficial in controlling blood pressure in patients exhibiting a poor response to RAAS inhibition.

Dapagliflozin enhanced the Ach-induced vasorelaxation in the aorta of aged SHR. While combination therapy with dapagliflozin improved results over the control group and displayed a decreased EC_{50} than monotherapy. Regarding the interactions of inflammatory molecules, fimasartan inhibited the pathway that led to ICAM-1/iNOS/COX-2, whereas candesartan and dapagliflozin, particularly when combined, reduced the pathway leading to NF- κ B/NLRP3/caspase-1. In conclusion, combining fimasartan and candesartan with dapagliflozin can benefit patients with impaired vascular function and inflammation. Specifically, fimasartan demonstrated inhibition of inflammatory responses in macrophages, therefore, may prove beneficial in mitigating various complications associated with inflammation. Expression and activation of Nrf2 were most significantly enhanced when treated with telmisartan and dapagliflozin combination in both aortic and endothelial cells.

Conversely, NOX expression and ROS production most significantly decreased when candesartan and dapagliflozin were co-administered. Therefore, the combination of dapagliflozin and ARBs have a synergistic effect on the inhibition of ROS, and it can offer benefits in preventing various complications associated with oxidative stress. The autophagy activity, leading to activation of LC3 and reduction of p62, showed the most significant increase in the aorta of the candesartan and dapagliflozin combination group and endothelial cells of the telmisartan and dapagliflozin co-treatment group. Therefore, the combination therapy of dapagliflozin with candesartan or fimasartan would be appropriate for patients with vascular dysfunction and inflammation. Moreover, combination therapy of dapagliflozin with either candesartan or telmisartan is more suitable for patients with excessive oxidative stress and autophagy impairment. In summary, the combination of ARB, specially candesartan and dapagliflozin, is projected to provide significant benefits as an alternative treatment for vascular dysfunction that can occur in both hypertension and diabetes.

Dapagliflozin increased urine output and water intake, and conversely, no significant effect was observed in the ARB alone group; however, when combined with dapagliflozin, water intake and urine volume were increased. In the context of SGLT2 inhibition, dapagliflozin elevated urinary glucose and sodium levels while decreasing blood glucose and sodium. Conversely, the ARB-only group tended to decrease both urinary and blood glucose levels; however, when dapagliflozin was co-administered with an ARB, urinary glucose levels were increased beyond those of the dapagliflozin monotherapy group. Nevertheless, blood glucose levels did not differ significantly from the ARB alone group. This suggests that an additional blood glucose control mechanism, other than urinary glucose excretion, may be operative. All ARBs were not markedly affecting urinary and blood sodium levels, but notably, when telmisartan was combined with dapagliflozin, sodium contents were increased in urine sodium and decreased in blood. Telmisartan also showed SGLT2 reduction both as a single and in the

combination group and offered the highest binding affinity with SGLT2. Thus, in patients with high levels of hyperglycemia and hypertension, the combination of telmisartan and dapagliflozin may synergistically affect blood glucose control through glucose excretion and blood pressure control by reducing sodium and fluid. However, drugs with accordant mechanisms are generally not recommended for combination due to potential risks and side effects. Therefore, further studies are warranted investigating the risks of combining these two drugs.

Urinary protein, a key indicator of kidney damage, was not reduced by dapagliflozin but was significantly decreased in all ARB groups. Notably, combining dapagliflozin with either fimasartan or candesartan resulted in a considerably lower urinary protein level than each monotherapy group. In contrast, telmisartan alone demonstrated the lowest urinary protein levels among ARBs, but when combined with dapagliflozin, these levels increased relative to the telmisartan-alone group. The expression of NHE-1, another established target protein of dapagliflozin and an indicator of renal fibrosis, decreased with both dapagliflozin and ARBs. When combined with dapagliflozin, candesartan exhibited an additional decrease compared to the monotherapy group, while telmisartan displayed an increase. In summary, fimasartan and candesartan showed renoprotective effects when combined with dapagliflozin. A combination of telmisartan and dapagliflozin demonstrates a potent blood glucose-lowering effect but cannot exhibit a renal protective effect. Therefore, since the combined use of telmisartan and dapagliflozin cannot reduce the renal impairment factors relative to the monotherapy group of each drug, it is suggested that their usage be limited in patients at risk of renal failure. On the other hand, fimasartan and candesartan showed additional reductions in kidney damage factors when combined with dapagliflozin, highlighting their potential as a new therapeutic combination targeting kidney disease.

These observed interactions and the variable mechanisms among ARBs offer invaluable insights for drug selection in combination therapy. However, the current results are derived from a murine model, emphasizing the need for further clinical studies in humans to corroborate their safety and efficacy. Additionally, as our study only investigated acute responses through short-term administration, future research should explore the response changes upon long-term administration.

In conclusion, while telmisartan exhibited potent blood pressure and blood sugar reduction, its overlapping inhibition of SGLT2 with dapagliflozin suggests carefully considering its usage as a concomitant drug. Candesartan demonstrated superior vascular and renal protection when combined with dapagliflozin, yet its synergy for blood pressure reduction was somewhat less potent than the other two ARBs. Conversely, the combination of fimasartan and dapagliflozin exhibited synergistic effects in blood pressure reduction, vascular protection, and renal protection, thereby suggesting its potential as a new combination drug to deliver multifaceted benefits to patients with hypertension, diabetes, and resultant vascular dysfunction and renal failure.

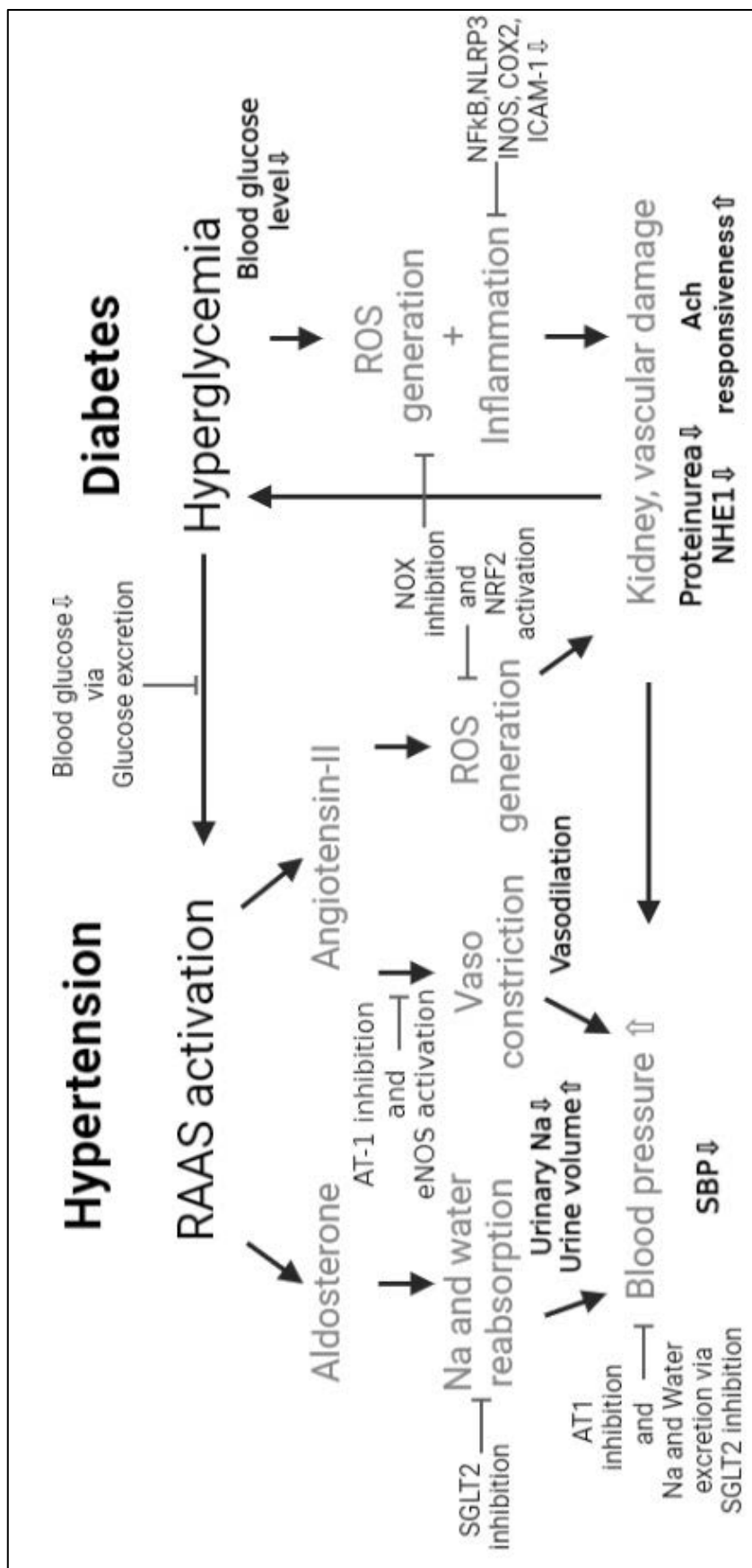
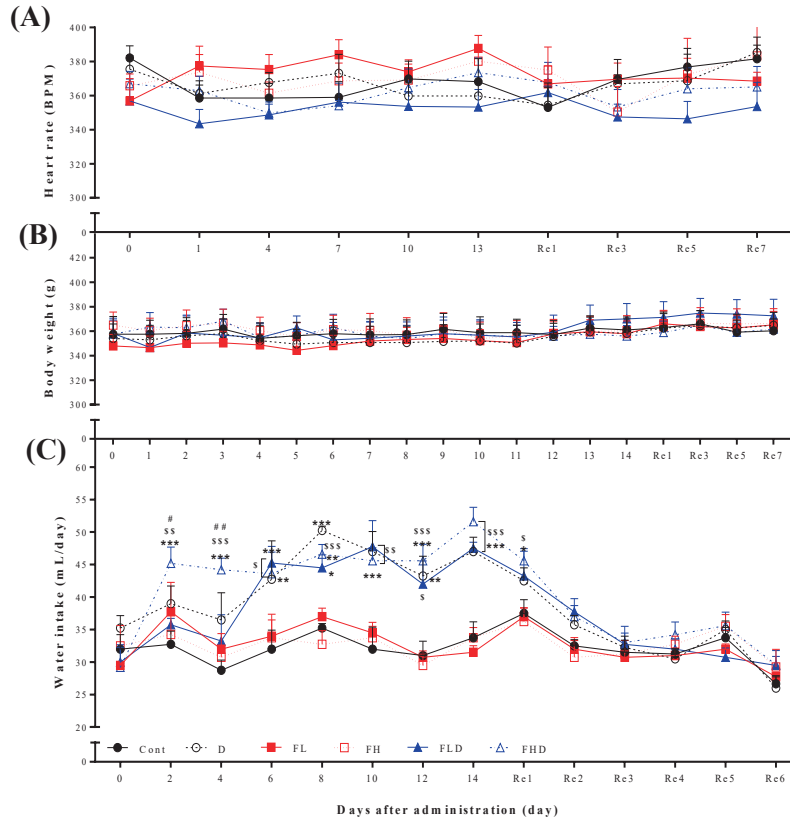


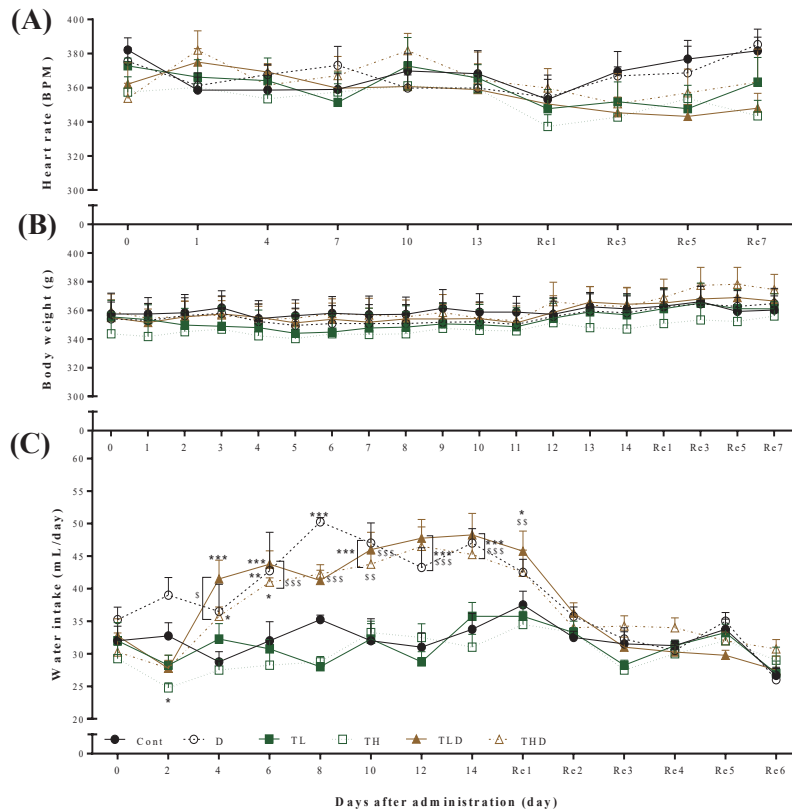
Figure 38. The effects of ARBs and dapagliflozin on blood pressure control, vascular and renal function

SUPPLEMENTARY DATA



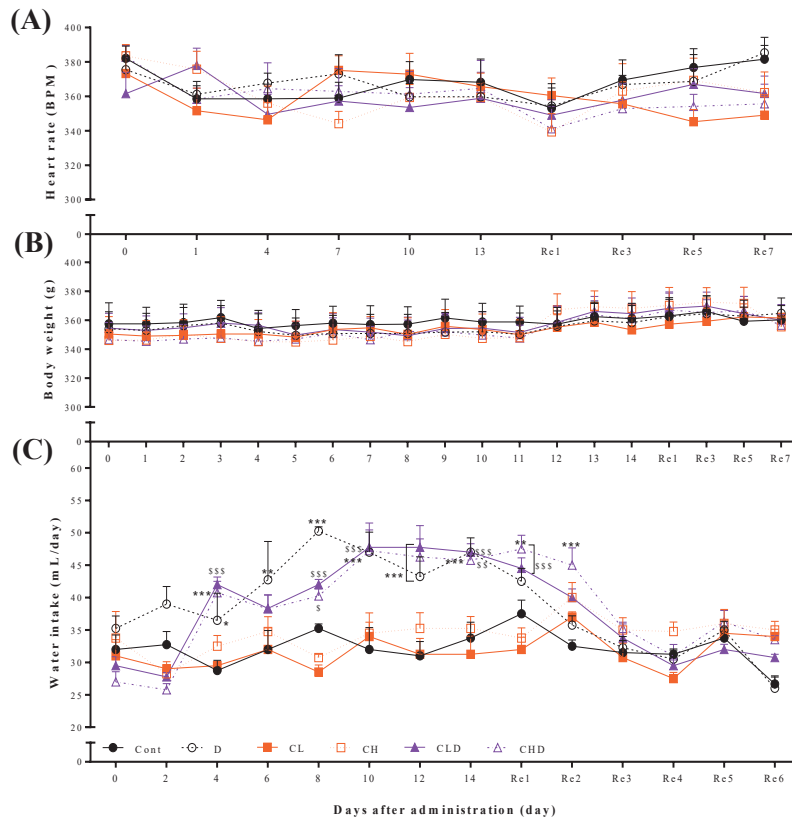
Supplementary Figure 1. Effects of fimasartan and dapagliflozin on heart rate, body weight, and water intake in SHR.

All experimental animals were orally administered the drugs once a day for two weeks. Heart rate (A) was measured one hour after drug administration every three days. Body weight (B) was measured daily during the test period, and water intake (C) was measured every two days. Changes in heart rate, body weight, and water intake were followed for an additional seven days after the end of drug administration (Re1-7). All data are expressed as mean \pm standard error mean. *, **, *** means a significant difference at the $p < 0.05$, 0.01 , and 0.001 levels compared to the control group. ^s, ^{ss}, ^{sss} means a significant difference at the $p < 0.05$, 0.01 , and 0.001 level exists between the same dose of the combined group and the single administration group. [#], ^{##} means a significant difference between the low and high concentration groups at the $p < 0.05$ and 0.01 levels.



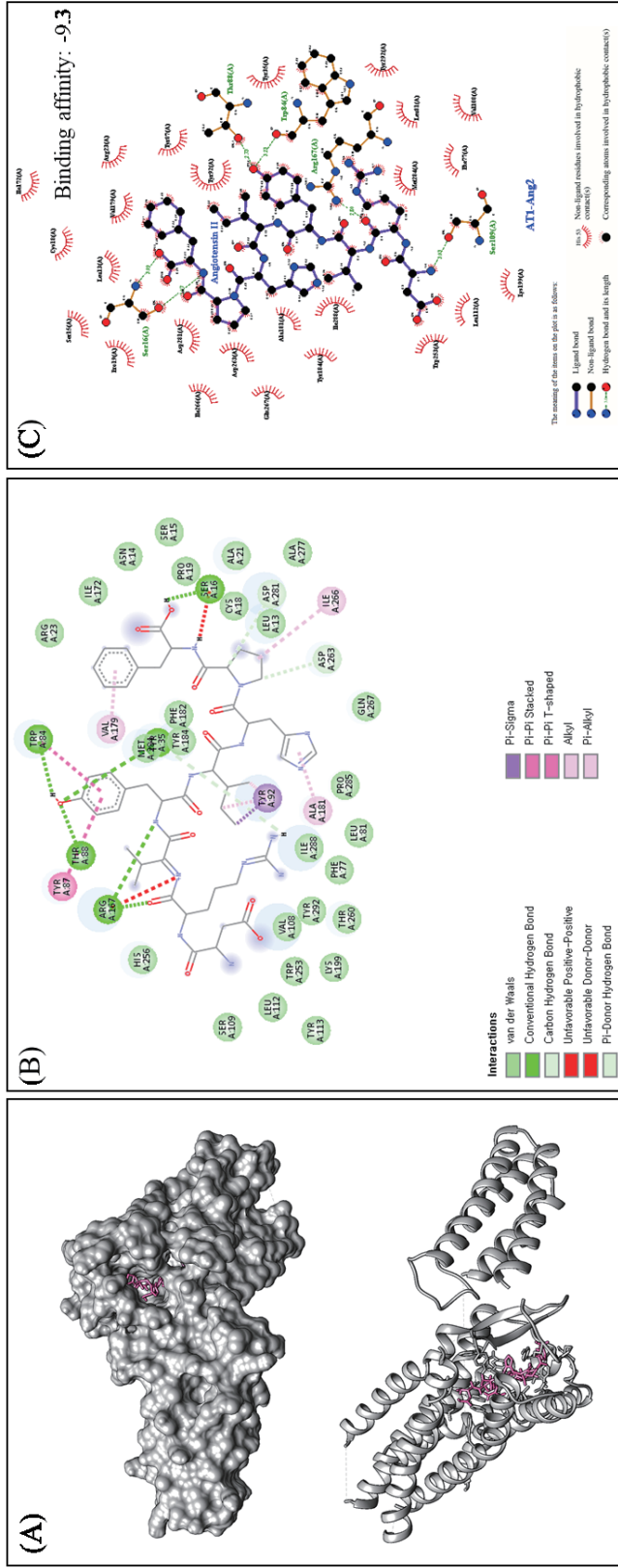
Supplementary Figure 2. Effects of telmisartan and dapagliflozin on heart rate, body weight, and water intake in SHR.

All experimental animals were orally administered the drugs once a day for two weeks. Heart rate (A) was measured one hour after drug administration every three days. Body weight (B) was measured daily during the test period, and water intake (C) was measured every two days. Changes in heart rate, body weight, and water intake were followed for an additional seven days after the end of drug administration (Re1-7). All data are expressed as mean \pm standard error mean. *, **, *** means a significant difference at the $p < 0.05$, 0.01 , and 0.001 levels compared to the control group. \$, \$\$, \$\$\$ means a significant difference at the $p < 0.05$, 0.01 , and 0.001 level exists between the same dose of the combined group and the single administration group.



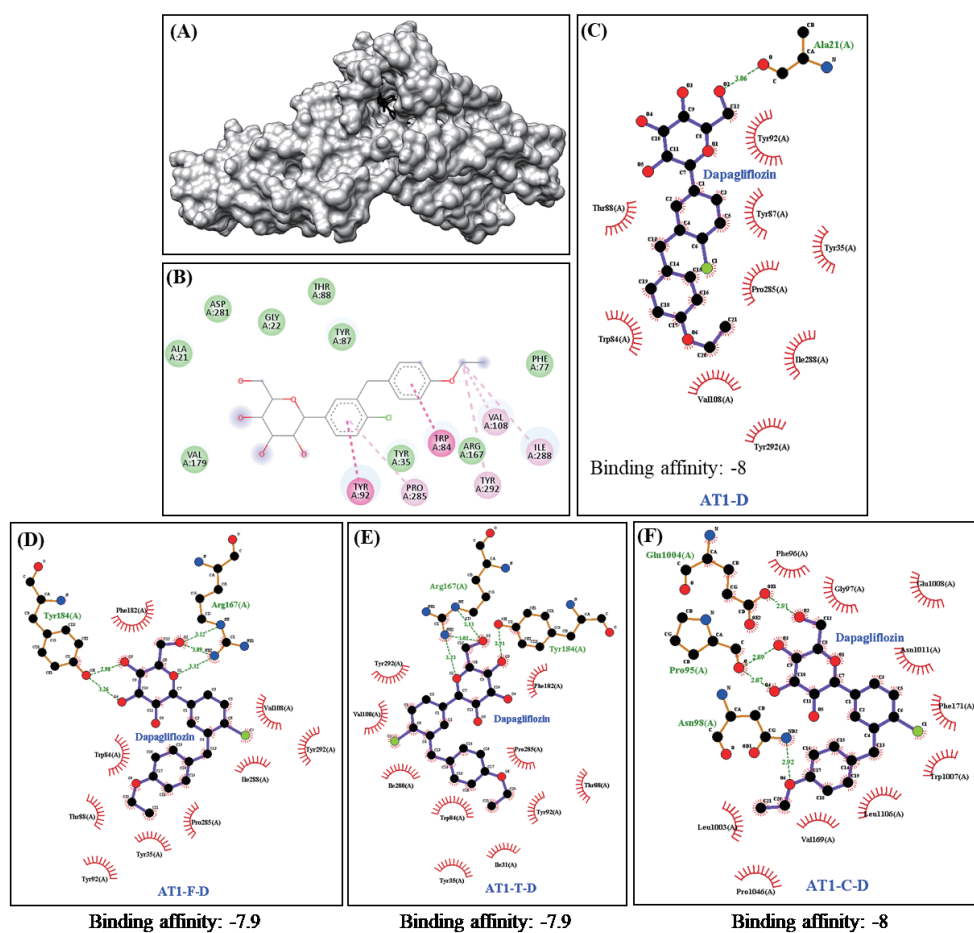
Supplementary Figure 3. Effects of candesartan and dapagliflozin on heart rate, body weight, and water intake in SHR.

All experimental animals were orally administered the drugs once a day for two weeks. Heart rate (A) was measured one hour after drug administration every three days. Body weight (B) was measured daily during the test period, and water intake (C) was measured every two days. Changes in heart rate, body weight, and water intake were followed for an additional seven days after the end of drug administration (Re1-7). All data are expressed as mean \pm standard error mean. *, **, *** means a significant difference at the $p < 0.05$, 0.01 , and 0.001 levels compared to the control group. \$, \$\$, \$\$\$ means a significant difference at the $p < 0.05$, 0.01 , and 0.001 level exists between the same dose of the combined group and single administration group.



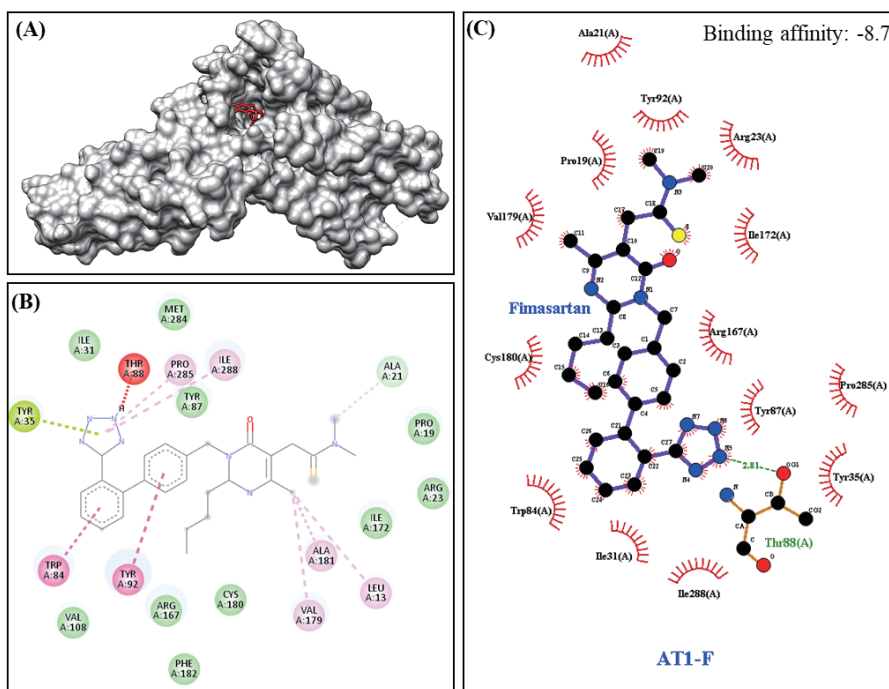
Supplementary Figure 4. The binding interaction of angiotensin receptor type1 and angiotensin-II

Figures presented a comprehensive visualization of molecular docking study: (A) shows the docking simulation, (B) details the ligand's binding form and site within the target protein, and (C) highlights the hydrogen and hydrophobic bonds contributing to the stability of the complex.



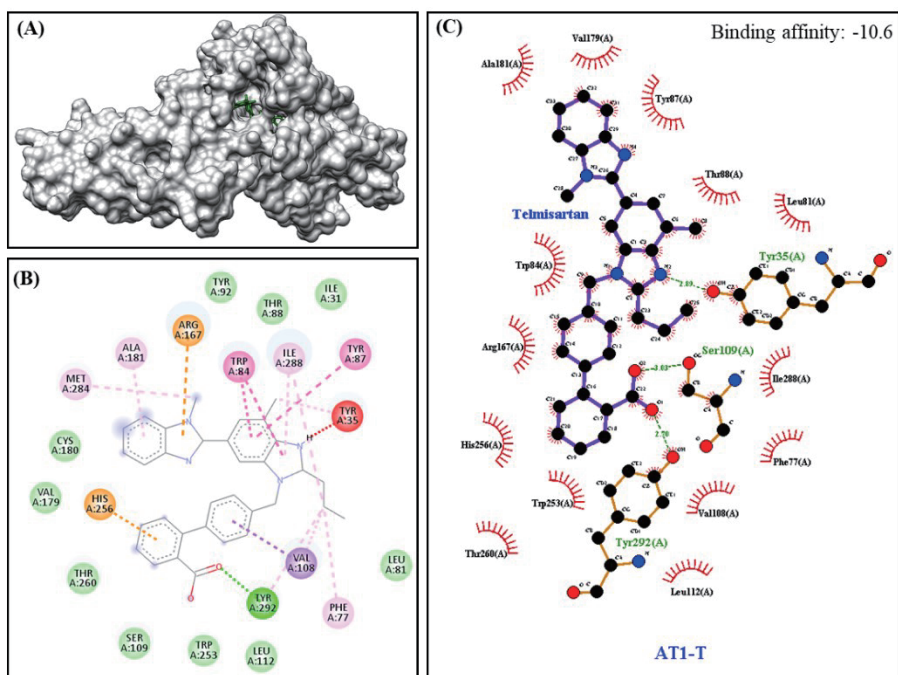
Supplementary Figure 5. The binding interaction of angiotensin receptor type1 and dapagliflozin.

Figures presented a comprehensive visualization of molecular docking study: (A) shows the docking simulation, (B) details the ligand's binding form and site within the target protein, and (C) highlights the hydrogen and hydrophobic bonds contributing to the stability of the complex. (D) shows the hydrogen and hydrophobic bonds of dapagliflozin to AT1 bound to fimasartan. (E) shows the hydrogen and hydrophobic bonds of dapagliflozin to AT1 bound to telmisartan. (F) shows the hydrogen and hydrophobic bonds of dapagliflozin to AT1 bound to candesartan.



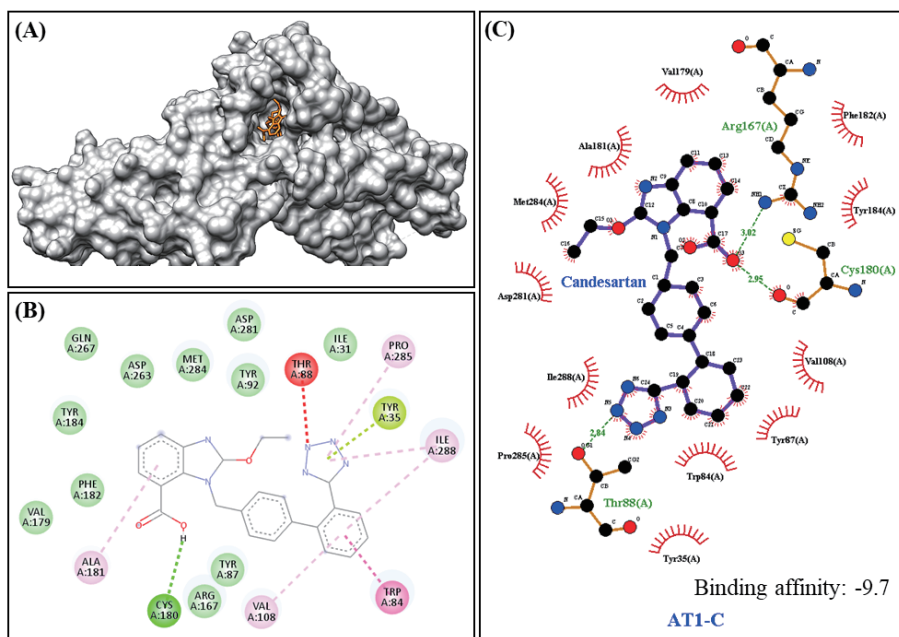
Supplementary Figure 6. The binding interaction of angiotensin receptor type1 and fimasartan

Figures presented a comprehensive visualization of molecular docking study: (A) shows the docking simulation, (B) details the ligand's binding form and site within the target protein, and (C) highlights the hydrogen and hydrophobic bonds contributing to the stability of the complex.



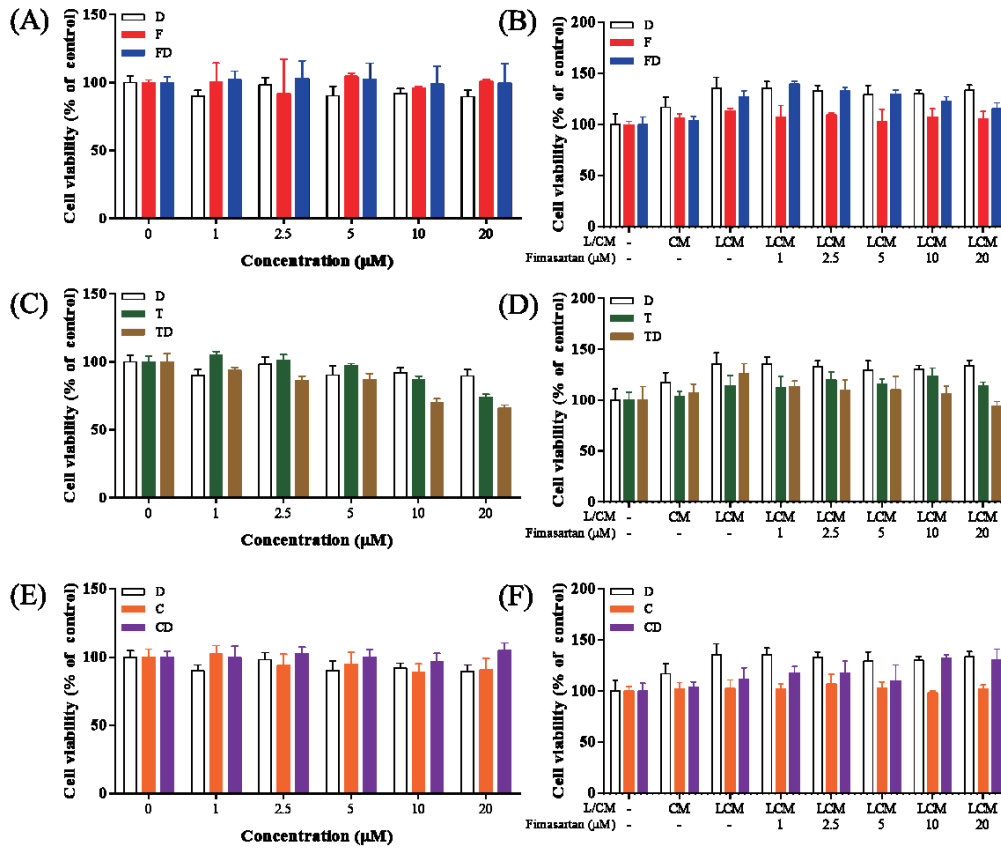
Supplementary Figure 7. The binding interaction of angiotensin receptor type1 and telmisartan

Figures presented a comprehensive visualization of molecular docking study: (A) shows the docking simulation, (B) details the ligand's binding form and site within the target protein, and (C) highlights the hydrogen and hydrophobic bonds contributing to the stability of the complex.



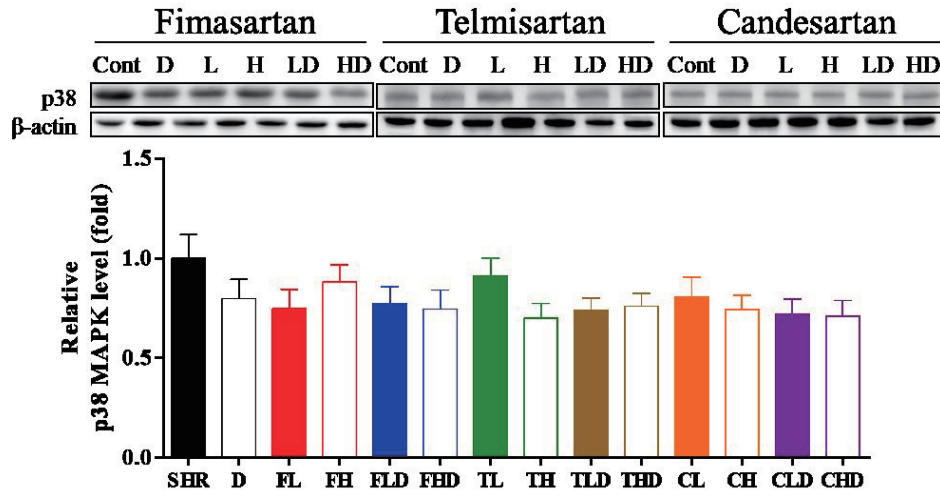
Supplementary Figure 8. The binding interaction of angiotensin receptor type1 and candesartan

Figures presented a comprehensive visualization of molecular docking study: (A) shows the docking simulation, (B) details the ligand's binding form and site within the target protein, and (C) highlights the hydrogen and hydrophobic bonds contributing to the stability of the complex.



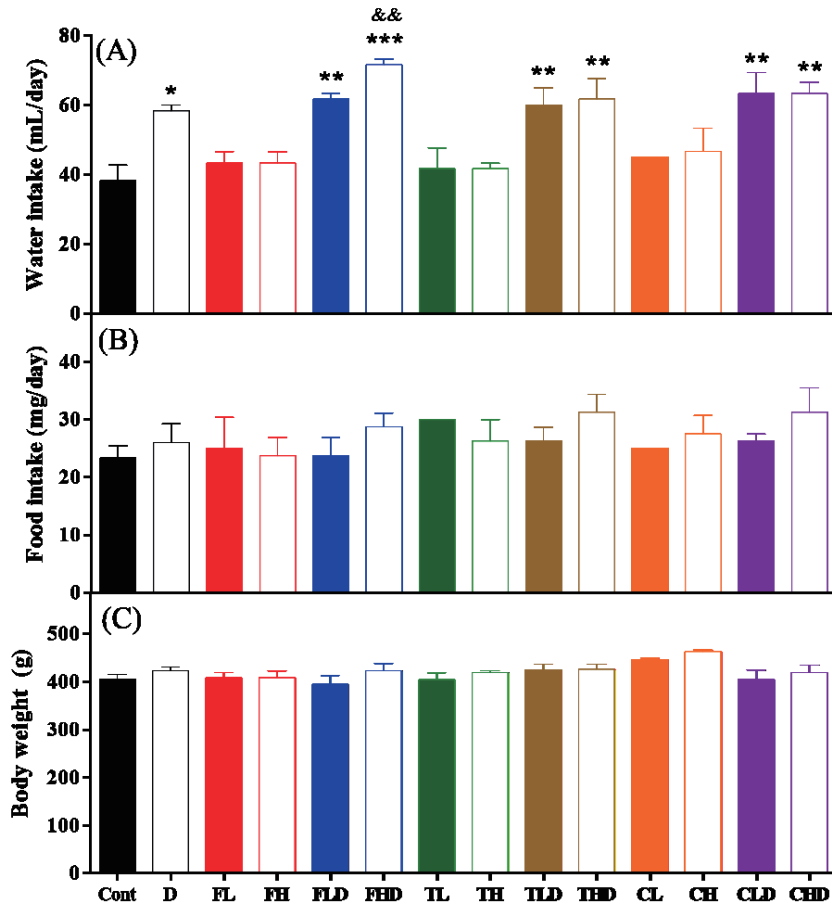
Supplementary Figure 9. Cell viability of ARBs and dapagliflozin treated EA. hy926 cells.

The cell viability of EA. hy926 cells were detected by MTT assay. The fimasartan (A and B), telmisartan (C and D), candesartan (E and F), and dapagliflozin were treated to EA. hy926 cells for 24 hours with or without L/CM. All values were calculated and expressed in percentages relative to the control. D, dapagliflozin; F, fimasartan; T, telmisartan; C, candesartan.



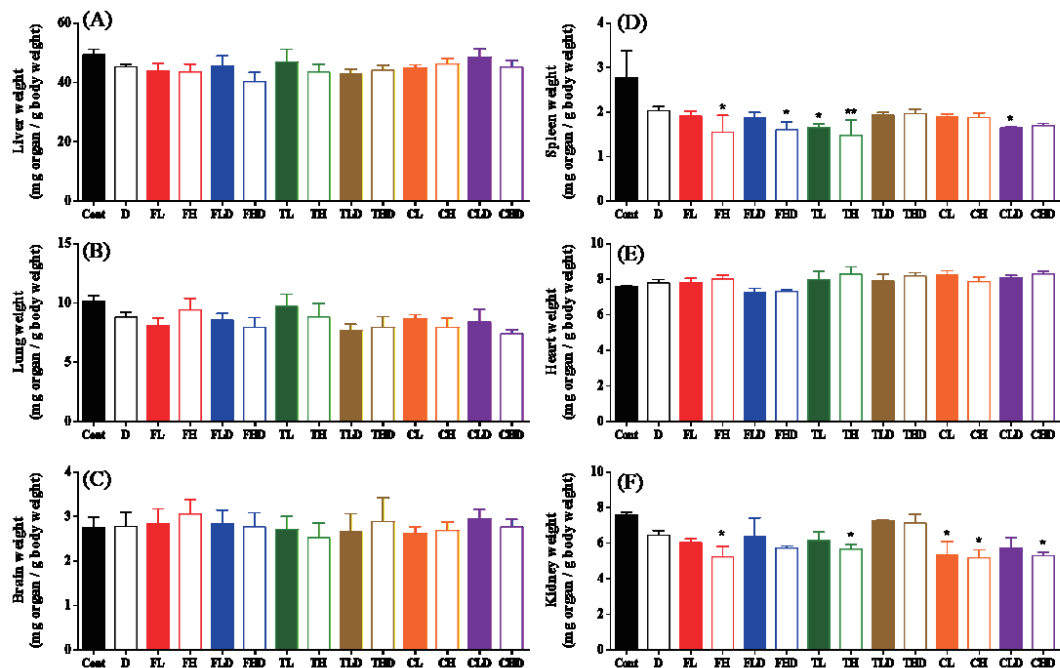
Supplementary Figure 10. Effects of ARBs and dapagliflozin on p38MAPK expression in aged SHR.

Male spontaneously hypertensive rats (SHRs) over 60 weeks of age received oral administration of the drugs for one week. After one week of drug administration, the experimental animals were euthanized using CO₂ gas, and aorta proteins were extracted for performing western blotting. Western blot images were visualized using the ChemiDoc system. The expression levels of p38 MAPK were normalized by β-actin. The relative ratio was calculated based on the control group. All data are expressed as mean ± standard error mean.



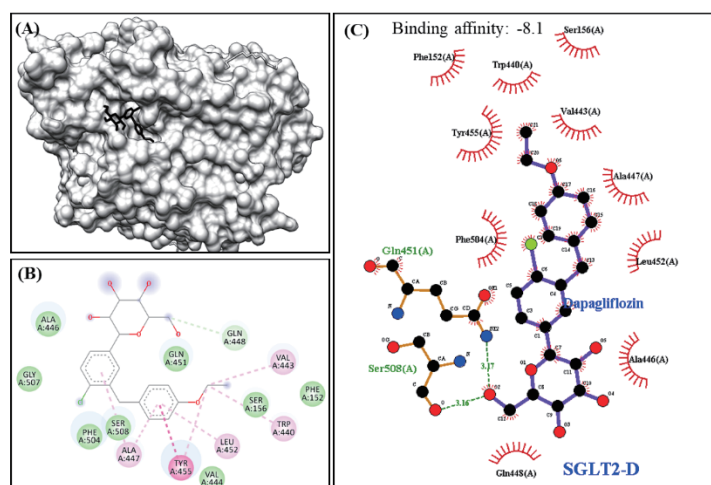
Supplementary Figure 11. Effects of ARBs and dapagliflozin on Water intake, food intake and body weight in aged SHR.

Male SHRs over 60 weeks were placed in metabolic cages of age and received oral administration of the drugs for one week. Water intake (A), food intake (B), and body weight (C) were measured one week after drug administration. All data are expressed as mean \pm standard error mean. *, **, *** means a significant difference at the $p < 0.05$, 0.01, and 0.001 levels compared to the control group. && means a significant difference at the $p < 0.01$ level compared to the dapagliflozin alone group



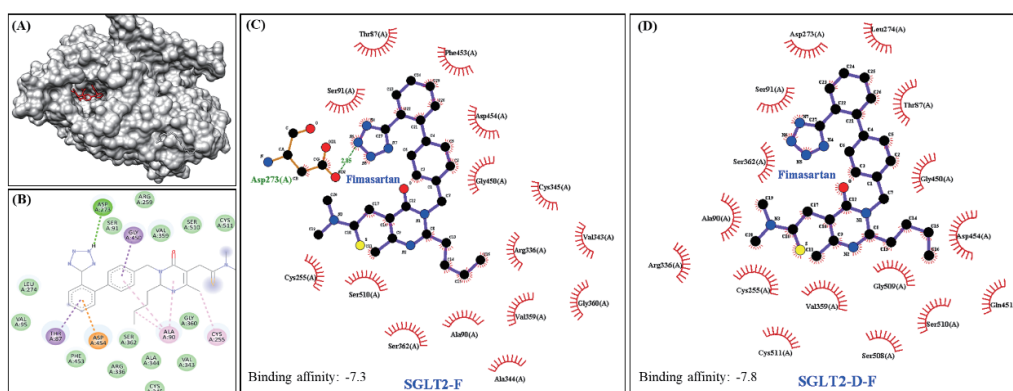
Supplementary Figure 12. Effects of ARBs and dapagliflozin on organ index in aged SHR.

Male SHRs over 60 weeks were placed in metabolic cages and received oral administration of the drugs for one week. After one week of drug administration, the experimental animals were euthanized using CO₂ gas. The organ index was calculated by dividing the weight of the liver (A), lung (B), brain (C), spleen (D), heart (E), and kidney (F) by the body weight of the animal. All data are expressed as mean ± standard error mean. *, ** means a significant difference at the $p < 0.05$ and 0.01 levels compared to the control group.



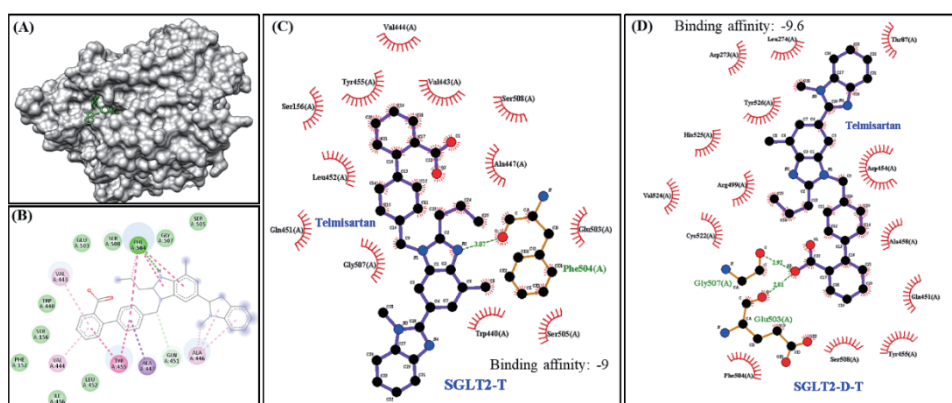
Supplementary Figure 13. The binding interaction of SGLT2 and dapagliflozin

Figures presented a comprehensive visualization of molecular docking study: (A) shows the docking simulation, (B) details the ligand's binding form and site within the target protein, and (C) highlights the hydrogen and hydrophobic bonds contributing to the stability of the complex.



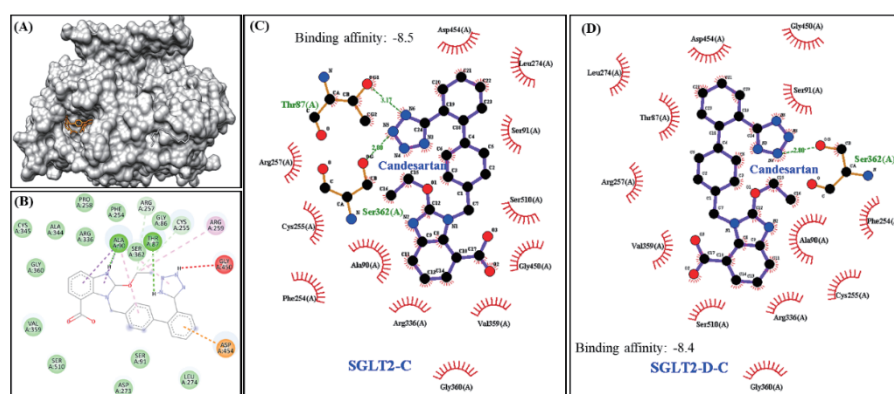
Supplementary Figure 14. The binding interaction of SGLT2 and fimasartan

Figures presented a comprehensive visualization of molecular docking study: (A) shows the docking simulation, (B) details the ligand's binding form and site within the target protein, and (C) highlights the hydrogen and hydrophobic bonds contributing to the stability of the complex. (D) shows the hydrogen and hydrophobic bonds of fimasartan to SGLT2 bound to dapagliflozin.



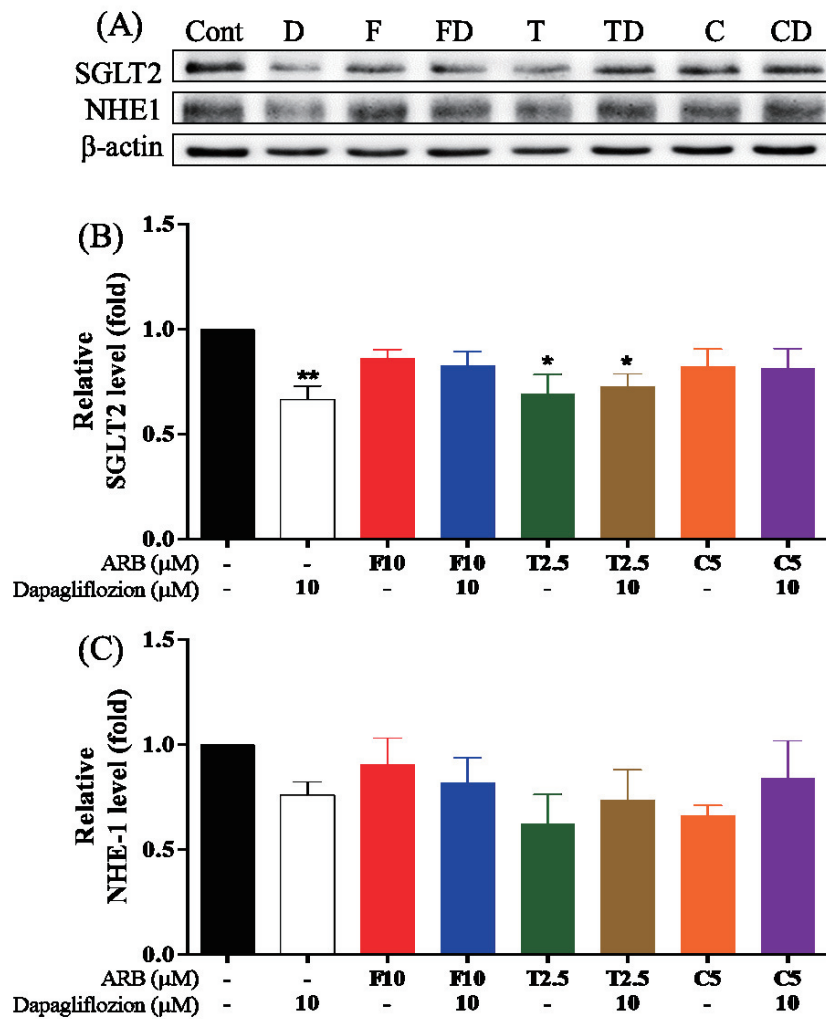
Supplementary Figure 15. The binding interaction of SGLT2 and telmisartan

Figures presented a comprehensive visualization of molecular docking study: (A) shows the docking simulation, (B) details the ligand's binding form and site within the target protein, and (C) highlights the hydrogen and hydrophobic bonds contributing to the stability of the complex. (D) shows the hydrogen and hydrophobic bonds of telmisartan to SGLT2 bound to dapagliflozin.



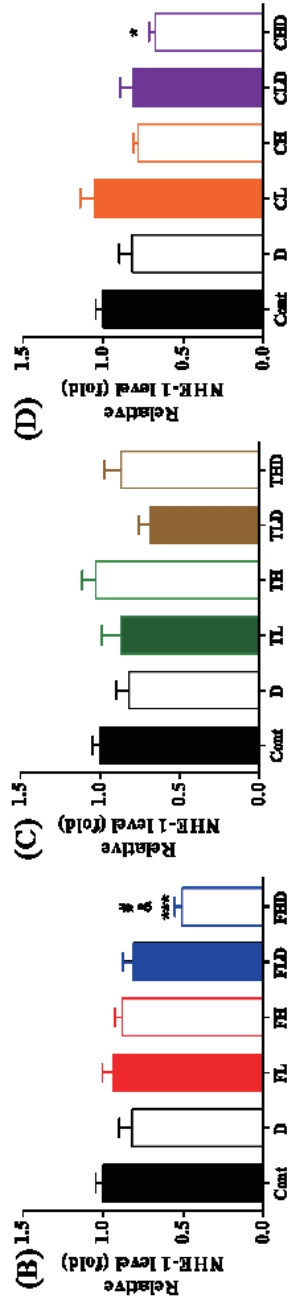
Supplementary Figure 16. The binding interaction of SGLT2 and candesaratan

Figures presented a comprehensive visualization of molecular docking study: (A) shows the docking simulation, (B) details the ligand's binding form and site within the target protein, and (C) highlights the hydrogen and hydrophobic bonds contributing to the stability of the complex. (D) shows the hydrogen and hydrophobic bonds of candesaratan to SGLT2 bound to dapagliflozin.



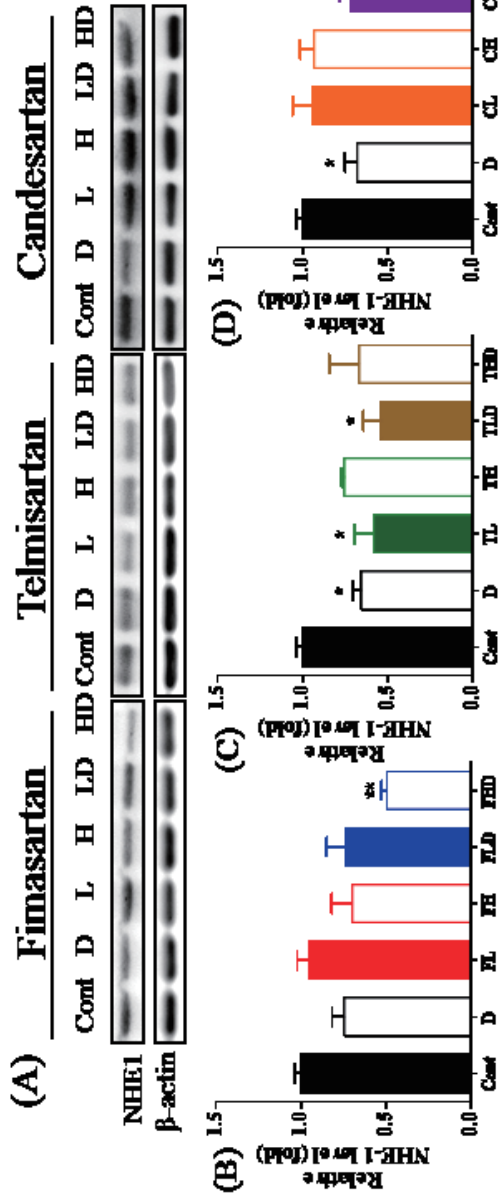
Supplementary Figure 17. Effects of ARBs and dapagliflozin on SGLT2 and NHE-1 expression in ACHN cells.

ACHN cells were treated with drugs for 24 hours, and protein was extracted for western blotting. Western blot images of SGLT2 and NHE-1 were visualized using the ChemiDoc system (A). The expression levels of SGLT2 (B) and NHE-1 (C) were normalized by β -actin. The relative ratio was calculated using the control (-/-). All data are expressed as mean \pm standard error mean. *, ** means there is a significant difference at the $p < 0.05$ and 0.01 levels compared to the control group.



Supplementary Figure 18. Effects of ARBs and dapagliflozin on NHE-1 expression in aorta of aged SHR.

Male spontaneously hypertensive rats (SHRs) over 60 weeks of age were placed in metabolic cages and received oral administration of the drugs for a week. After one week of drug administration, the experimental animals were euthanized using CO₂ gas, and aorta proteins were extracted for western blotting. Western blot images of NHE-1 were visualized using the ChemiDoc system (A). The expression levels of NHE-1 in fimasartan (B), telmisartan (C), and candesartan (C) administered groups were normalized by β-actin. The relative ratio was calculated based on the control group. All data are expressed as mean ± standard error mean. * **** means there is a significant difference at the $p < 0.05$ and 0.001 levels compared to the control group. # means that there is a significant difference at the $p < 0.05$ level compared to the dapagliflozin alone group. # means that there is a significant difference between the low and high-concentration groups at the $p < 0.05$ level.



Supplementary Figure 19. Effects of ARBs and dapagliflozin on NHE-1 expression in heart of aged SHR.

Male spontaneously hypertensive rats (SHRs) over 60 weeks of age were placed in metabolic cages and received oral administration of the drugs for one week. After one week of drug administration, the experimental animals were euthanized using CO₂ gas, and cardiac proteins were extracted for western blotting. Western blot images of NHE-1 were visualized using the ChemiDoc system (A). The expression levels of NHE-1 in fimasartan (B), telmisartan (C), and candesartan (C) administered groups were normalized by β -actin. The relative ratio was calculated based on the control group. All data are expressed as mean \pm standard error mean. * ** means there is a significant difference at the $p < 0.05$ and 0.01 levels compared to the control group.

REFERENCES

1. Elliott, W.J., *Systemic hypertension*. *Curr Probl Cardiol*, 2007. **32**(4): p. 201-59.
2. Folkow, B., "*Structural factor*" in *primary and secondary hypertension*. *Hypertension*, 1990. **16**(1): p. 89-101.
3. Mills, K.T., A. Stefanescu, and J. He, *The global epidemiology of hypertension*. *Nat Rev Nephrol*, 2020. **16**(4): p. 223-237.
4. Kurtz, T.W. and M.A. Spence, *Genetics of essential hypertension*. *Am J Med*, 1993. **94**(1): p. 77-84.
5. Hamet, P., et al., *Hypertension: genes and environment*. *J Hypertens*, 1998. **16**(4): p. 397-418.
6. Caulfield, M., et al., *Angiotensinogen in human essential hypertension*. *Hypertension*, 1996. **28**(6): p. 1123-5.
7. Fuchs, F.D. and P.K. Whelton, *High Blood Pressure and Cardiovascular Disease*. *Hypertension*, 2020. **75**(2): p. 285-292.
8. Artom, N., A. Vecchie, and A. Pende, *Effects of Blood Pressure Control in Cardiovascular Prevention*. *Curr Pharm Des*, 2016. **22**(37): p. 5649-5661.
9. Williams, B., et al., *British Hypertension Society guidelines for hypertension management 2004 (BHS-IV): summary*. *BMJ*, 2004. **328**(7440): p. 634-40.
10. *Different antihypertensive drugs as first line therapy in patients with essential hypertension: Executive summary of final report A05-09, Version 1.0*, in *Institute for Quality and Efficiency in Health Care: Executive Summaries*. 2005: Cologne, Germany.
11. Tsioufis, C. and C. Thomopoulos, *Combination drug treatment in hypertension*. *Pharmacol Res*, 2017. **125**(Pt B): p. 266-271.
12. Moller, J., et al., *Blockade of the renin-angiotensin-aldosterone system prevents growth hormone-induced fluid retention in humans*. *Am J Physiol*, 1997. **272**(5 Pt 1): p. E803-8.
13. Pieruzzi, F., Z.A. Abassi, and H.R. Keiser, *Expression of renin-angiotensin system components in the heart, kidneys, and lungs of rats with experimental heart failure*. *Circulation*, 1995. **92**(10): p. 3105-12.
14. Ghazi, L. and P. Drawz, *Advances in understanding the renin-angiotensin-aldosterone system (RAAS) in blood pressure control and recent pivotal trials of RAAS blockade in heart failure and diabetic nephropathy*. *F1000Res*, 2017. **6**.
15. Yang, T. and C. Xu, *Physiology and Pathophysiology of the Intrarenal Renin-Angiotensin System: An Update*. *J Am Soc Nephrol*, 2017. **28**(4): p. 1040-1049.
16. Miyazaki, M. and S. Takai, *Tissue angiotensin II generating system by angiotensin-converting enzyme and chymase*. *J Pharmacol Sci*, 2006. **100**(5): p. 391-7.

17. Feng, Y.H., et al., *The docking of Arg2 of angiotensin II with Asp281 of AT1 receptor is essential for full agonism*. J Biol Chem, 1995. **270**(21): p. 12846-50.
18. Crowley, S.D. and T.M. Coffman, *Recent advances involving the renin-angiotensin system*. Exp Cell Res, 2012. **318**(9): p. 1049-56.
19. Gubler, M.C. and C. Antignac, *Renin-angiotensin system in kidney development: renal tubular dysgenesis*. Kidney Int, 2010. **77**(5): p. 400-6.
20. Rush, J.W. and C.D. Aultman, *Vascular biology of angiotensin and the impact of physical activity*. Appl Physiol Nutr Metab, 2008. **33**(1): p. 162-72.
21. Crowley, S.D., et al., *Role of AT(1) receptor-mediated salt retention in angiotensin II-dependent hypertension*. Am J Physiol Renal Physiol, 2011. **301**(5): p. F1124-30.
22. Pendergrass, K.D., et al., *The angiotensin II-AT1 receptor stimulates reactive oxygen species within the cell nucleus*. Biochem Biophys Res Commun, 2009. **384**(2): p. 149-54.
23. Ding, J., et al., *Angiotensin II Decreases Endothelial Nitric Oxide Synthase Phosphorylation via AT(1)R Nox/ROS/PP2A Pathway*. Front Physiol, 2020. **11**: p. 566410.
24. Seifarth, C., et al., *Influence of antihypertensive medication on aldosterone and renin concentration in the differential diagnosis of essential hypertension and primary aldosteronism*. Clin Endocrinol (Oxf), 2002. **57**(4): p. 457-65.
25. Strauss, M.H., A.S. Hall, and K. Narkiewicz, *ACEI and ARB - Each Unique RAAS Inhibitors: The Importance of Impact on Inflammation*. Mayo Clin Proc, 2023. **98**(2): p. 350-351.
26. Buffolo, F., et al., *Aldosterone as a Mediator of Cardiovascular Damage*. Hypertension, 2022. **79**(9): p. 1899-1911.
27. Araujo-Castro, M. and P. Parra-Ramirez, *Diagnosis of primary hyperaldosteronism*. Med Clin (Barc), 2022. **158**(9): p. 424-430.
28. Oktaviono, Y.H. and N. Kusumawardhani, *Hyperkalemia Associated with Angiotensin Converting Enzyme Inhibitor or Angiotensin Receptor Blockers in Chronic Kidney Disease*. Acta Med Indones, 2020. **52**(1): p. 74-79.
29. Raebel, M.A., *Hyperkalemia associated with use of angiotensin-converting enzyme inhibitors and angiotensin receptor blockers*. Cardiovasc Ther, 2012. **30**(3): p. e156-66.
30. Goyal, R. and I. Jialal, *Type 2 Diabetes*, in *StatPearls*. 2023: Treasure Island (FL).
31. Ogurtsova, K., et al., *IDF diabetes Atlas: Global estimates of undiagnosed diabetes in adults for 2021*. Diabetes Res Clin Pract, 2022. **183**: p. 109118.
32. de Boer, I.H., et al., *Diabetes Management in Chronic Kidney Disease: A Consensus Report by the American Diabetes Association (ADA) and Kidney Disease: Improving Global Outcomes (KDIGO)*. Diabetes Care, 2022. **45**(12): p. 3075-3090.
33. Huang, D., et al., *Macrovascular Complications in Patients with Diabetes and Prediabetes*. Biomed Res Int, 2017. **2017**: p. 7839101.

34. Garofolo, M., et al., *Microvascular complications burden (nephropathy, retinopathy and peripheral polyneuropathy) affects risk of major vascular events and all-cause mortality in type 1 diabetes: a 10-year follow-up study*. Cardiovasc Diabetol, 2019. **18**(1): p. 159.
35. Alicic, R.Z., M.T. Rooney, and K.R. Tuttle, *Diabetic Kidney Disease: Challenges, Progress, and Possibilities*. Clin J Am Soc Nephrol, 2017. **12**(12): p. 2032-2045.
36. Gembillo, G., et al., *Kidney Disease in Diabetic Patients: From Pathophysiology to Pharmacological Aspects with a Focus on Therapeutic Inertia*. Int J Mol Sci, 2021. **22**(9).
37. Xin, S., et al., *Association between hemoglobin glycation index and diabetic kidney disease in type 2 diabetes mellitus in China: A cross-sectional inpatient study*. Front Endocrinol (Lausanne), 2023. **14**: p. 1108061.
38. Ren, J., et al., *Prediction and Risk Stratification of Cardiovascular Disease in Diabetic Kidney Disease Patients*. Front Cardiovasc Med, 2022. **9**: p. 923549.
39. Patel, D.M., M. Bose, and M.E. Cooper, *Glucose and Blood Pressure-Dependent Pathways-The Progression of Diabetic Kidney Disease*. Int J Mol Sci, 2020. **21**(6).
40. Jha, J.C., et al., *Diabetes and Kidney Disease: Role of Oxidative Stress*. Antioxid Redox Signal, 2016. **25**(12): p. 657-684.
41. Tong, L.L. and S.G. Adler, *Diabetic kidney disease treatment: new perspectives*. Kidney Res Clin Pract, 2022. **41**(Suppl 2): p. S63-S73.
42. Tian, B., et al., *Efficacy and safety of combination therapy with sodium-glucose cotransporter 2 inhibitors and renin-angiotensin system blockers in patients with type 2 diabetes: a systematic review and meta-analysis*. Nephrol Dial Transplant, 2022. **37**(4): p. 720-729.
43. Krzesinski, J.M. and L. Weekers, *[Hypertension and diabetes]*. Rev Med Liege, 2005. **60**(5-6): p. 572-7.
44. Sowers, J.R. and S. Khoury, *Diabetes and hypertension: a review*. Prim Care, 1991. **18**(3): p. 509-24.
45. Petrie, J.R., T.J. Guzik, and R.M. Touyz, *Diabetes, Hypertension, and Cardiovascular Disease: Clinical Insights and Vascular Mechanisms*. Can J Cardiol, 2018. **34**(5): p. 575-584.
46. Park, K.H. and W.J. Park, *Endothelial Dysfunction: Clinical Implications in Cardiovascular Disease and Therapeutic Approaches*. J Korean Med Sci, 2015. **30**(9): p. 1213-25.
47. Madonna, R., et al., *Diabetic microangiopathy: Pathogenetic insights and novel therapeutic approaches*. Vascul Pharmacol, 2017. **90**: p. 1-7.
48. Guzik, T.J. and R.M. Touyz, *Oxidative Stress, Inflammation, and Vascular Aging in Hypertension*. Hypertension, 2017. **70**(4): p. 660-667.
49. Grossman, A. and E. Grossman, *Blood pressure control in type 2 diabetic patients*. Cardiovasc Diabetol, 2017. **16**(1): p. 3.
50. Mahler, R.J., *Diabetes and hypertension*. Horm Metab Res, 1990. **22**(12): p. 599-

607.

51. Cryer, M.J., T. Horani, and D.J. DiPette, *Diabetes and Hypertension: A Comparative Review of Current Guidelines*. J Clin Hypertens (Greenwich), 2016. **18**(2): p. 95-100.
52. Kooter, A.J. and Y.M. Smulders, *[Chlorthalidone better than hydrochlorothiazide in hypertension]*. Ned Tijdschr Geneesk, 2010. **154**: p. A1608.
53. Hagen, M.D., W. Sumner, and H. Fu, *Diuretic of choice in ABFM hypertension self-assessment module simulations*. J Am Board Fam Med, 2012. **25**(6): p. 805-9.
54. Cooke, J.P., *The endothelium: a new target for therapy*. Vasc Med, 2000. **5**(1): p. 49-53.
55. Ghiadoni, L., S. Taddei, and A. Viridis, *Hypertension and endothelial dysfunction: therapeutic approach*. Curr Vasc Pharmacol, 2012. **10**(1): p. 42-60.
56. Tabit, C.E., et al., *Endothelial dysfunction in diabetes mellitus: molecular mechanisms and clinical implications*. Rev Endocr Metab Disord, 2010. **11**(1): p. 61-74.
57. Jacobs, M.D. and S.C. Harrison, *Structure of an IkappaBalpha/NF-kappaB complex*. Cell, 1998. **95**(6): p. 749-58.
58. Malekmohammad, K., R.D.E. Sewell, and M. Rafieian-Kopaei, *Antioxidants and Atherosclerosis: Mechanistic Aspects*. Biomolecules, 2019. **9**(8).
59. Zhu, Y.-P., et al., *Astragalus polysaccharides suppress ICAM-1 and VCAM-1 expression in TNF- α -treated human vascular endothelial cells by blocking NF- κ B activation*. Acta Pharmacologica Sinica, 2013. **34**(8): p. 1036-1042.
60. Kim, Y.M., et al., *Compound C independent of AMPK inhibits ICAM-1 and VCAM-1 expression in inflammatory stimulants-activated endothelial cells in vitro and in vivo*. Atherosclerosis, 2011. **219**(1): p. 57-64.
61. Miwa, K., A. Igawa, and H. Inoue, *Soluble E-selectin, ICAM-1 and VCAM-1 levels in systemic and coronary circulation in patients with variant angina*. Cardiovasc Res, 1997. **36**(1): p. 37-44.
62. Bai, B., et al., *NLRP3 inflammasome in endothelial dysfunction*. Cell Death & Disease, 2020. **11**(9).
63. Franchi, L., et al., *The inflammasome: a caspase-1-activation platform that regulates immune responses and disease pathogenesis*. Nat Immunol, 2009. **10**(3): p. 241-7.
64. Al-Qazazi, R., et al., *Macrophage-NLRP3 Activation Promotes Right Ventricle Failure in Pulmonary Arterial Hypertension*. Am J Respir Crit Care Med, 2022. **206**(5): p. 608-624.
65. Avolio, E., et al., *Role of Brain Neuroinflammatory Factors on Hypertension in the Spontaneously Hypertensive Rat*. Neuroscience, 2018. **375**: p. 158-168.
66. Higashi, Y., et al., *Endothelial function and oxidative stress in cardiovascular diseases*. Circ J, 2009. **73**(3): p. 411-8.

67. Kundu, J.K. and Y.J. Surh, *Inflammation: gearing the journey to cancer*. Mutat Res, 2008. **659**(1-2): p. 15-30.
68. Forstermann, U. and T. Munzel, *Endothelial nitric oxide synthase in vascular disease: from marvel to menace*. Circulation, 2006. **113**(13): p. 1708-14.
69. Papaconstantinou, J., *The Role of Signaling Pathways of Inflammation and Oxidative Stress in Development of Senescence and Aging Phenotypes in Cardiovascular Disease*. Cells, 2019. **8**(11).
70. Griendling, K.K. and G.A. FitzGerald, *Oxidative stress and cardiovascular injury: Part I: basic mechanisms and in vivo monitoring of ROS*. Circulation, 2003. **108**(16): p. 1912-6.
71. Galkina, E. and K. Ley, *Immune and inflammatory mechanisms of atherosclerosis (*)*. Annu Rev Immunol, 2009. **27**: p. 165-97.
72. Forte, M., et al., *Pharmacological restoration of autophagy reduces hypertension-related stroke occurrence*. Autophagy, 2020. **16**(8): p. 1468-1481.
73. Long, J., et al., *Dimerisation of the UBA domain of p62 inhibits ubiquitin binding and regulates NF-kappaB signalling*. J Mol Biol, 2010. **396**(1): p. 178-94.
74. Levine, B. and G. Kroemer, *Autophagy in the pathogenesis of disease*. Cell, 2008. **132**(1): p. 27-42.
75. Jiang, F., *Autophagy in vascular endothelial cells*. Clin Exp Pharmacol Physiol, 2016. **43**(11): p. 1021-1028.
76. Hua, Y., et al., *The Induction of Endothelial Autophagy and Its Role in the Development of Atherosclerosis*. Front Cardiovasc Med, 2022. **9**: p. 831847.
77. Khong, T.K. and E. Adeyeye, *First-line drugs for hypertension*. Drug Ther Bull, 2019. **57**(9): p. 135-136.
78. Barreras, A. and C. Gurk-Turner, *Angiotensin II receptor blockers*. Proc (Bayl Univ Med Cent), 2003. **16**(1): p. 123-6.
79. Bhardwaj, G., *How the antihypertensive losartan was discovered*. Expert Opin Drug Discov, 2006. **1**(6): p. 609-18.
80. Taylor, A.A., H. Siragy, and S. Nesbitt, *Angiotensin receptor blockers: pharmacology, efficacy, and safety*. J Clin Hypertens (Greenwich), 2011. **13**(9): p. 677-86.
81. Timmermans, P.B., *Angiotensin II receptor antagonists: an emerging new class of cardiovascular therapeutics*. Hypertens Res, 1999. **22**(2): p. 147-53.
82. Lee, H.Y. and B.H. Oh, *Fimasartan: A New Angiotensin Receptor Blocker*. Drugs, 2016. **76**(10): p. 1015-22.
83. Kim, J.H., et al., *Fimasartan, a novel angiotensin II receptor antagonist*. Arch Pharm Res, 2012. **35**(7): p. 1123-6.
84. Takezako, T., et al., *The non-biphenyl-tetrazole angiotensin AT(1) receptor antagonist eprosartan is a unique and robust inverse agonist of the active state of the AT(1) receptor*. Br J Pharmacol, 2018. **175**(12): p. 2454-2469.
85. Bakheit, A.H., et al., *Telmisartan*. Profiles Drug Subst Excip Relat Methodol,

2015. **40**: p. 371-429.
86. Goebel, M., et al., *Characterization of new PPARgamma agonists: benzimidazole derivatives - the importance of position 2*. ChemMedChem, 2009. **4**(7): p. 1136-42.
 87. Yamagishi, S., K. Nakamura, and T. Matsui, *Potential utility of telmisartan, an angiotensin II type 1 receptor blocker with peroxisome proliferator-activated receptor-gamma (PPAR-gamma)-modulating activity for the treatment of cardiometabolic disorders*. Curr Mol Med, 2007. **7**(5): p. 463-9.
 88. Devan, A.R., et al., *An insight into the role of telmisartan as PPAR-gamma/alpha dual activator in the management of nonalcoholic fatty liver disease*. Biotechnol Appl Biochem, 2022. **69**(2): p. 461-468.
 89. Nishikawa, K., et al., *Candesartan cilexetil: a review of its preclinical pharmacology*. J Hum Hypertens, 1997. **11 Suppl 2**: p. S9-17.
 90. Gleiter, C.H. and K.E. Morike, *Clinical pharmacokinetics of candesartan*. Clin Pharmacokinet, 2002. **41**(1): p. 7-17.
 91. Pfeffer, M.A., et al., *Effects of candesartan on mortality and morbidity in patients with chronic heart failure: the CHARM-Overall programme*. Lancet, 2003. **362**(9386): p. 759-66.
 92. Singh, K.D., et al., *Divergent Spatiotemporal Interaction of Angiotensin Receptor Blocking Drugs with Angiotensin Type 1 Receptor*. J Chem Inf Model, 2018. **58**(1): p. 182-193.
 93. Schmieder, R.E., *Mechanisms for the clinical benefits of angiotensin II receptor blockers*. Am J Hypertens, 2005. **18**(5 Pt 1): p. 720-30.
 94. Fujino, M., et al., *A small difference in the molecular structure of angiotensin II receptor blockers induces AT(1) receptor-dependent and -independent beneficial effects*. Hypertens Res, 2010. **33**(10): p. 1044-52.
 95. Gavras, H.P., *Issues in hypertension: drug tolerability and special populations*. Am J Hypertens, 2001. **14**(7 Pt 2): p. 231S-236S.
 96. Sekine, T., et al., *Children's toxicology from bench to bed--Drug-induced renal injury (1): The toxic effects of ARB/ACEI on fetal kidney development*. J Toxicol Sci, 2009. **34 Suppl 2**: p. SP245-50.
 97. Choi, W.J., et al., *Incidence and Pattern of Aminotransferase Elevation During Anti-Hypertensive Therapy With Angiotensin-II Receptor Blockers*. J Korean Med Sci, 2022. **37**(33): p. e255.
 98. Gillette, M., et al., *Reflections of the Angiotensin Receptor Blocker Recall by the FDA and Repercussions on Healthcare*. Cardiovasc Drugs Ther, 2020. **34**(4): p. 579-584.
 99. Charoo, N.A., et al., *Lesson Learnt from Recall of Valsartan and Other Angiotensin II Receptor Blocker Drugs Containing NDMA and NDEA Impurities*. AAPS PharmSciTech, 2019. **20**(5): p. 166.
 100. Gunasekaran, P.M., et al., *Current Status of Angiotensin Receptor Blocker Recalls*. Hypertension, 2019. **74**(6): p. 1275-1278.

101. Neldam, S., D. Zhu, and H. Schumacher, *Efficacy of Telmisartan Plus Amlodipine in Nonresponders to CCB Monotherapy*. Int J Hypertens, 2013. **2013**: p. 627938.
102. Ogihara, T., et al., *ARB candesartan and CCB amlodipine in hypertensive patients: the CASE-J trial*. Expert Rev Cardiovasc Ther, 2008. **6**(9): p. 1195-201.
103. de la Sierra, A. and V. Barrios, *Blood pressure control with angiotensin receptor blocker-based three-drug combinations: key trials*. Adv Ther, 2012. **29**(5): p. 401-15.
104. Sinha, A.D. and R. Agarwal, *Thiazide Diuretics in Chronic Kidney Disease*. Curr Hypertens Rep, 2015. **17**(3): p. 13.
105. Kjeldsen, S.E., et al., *Telmisartan and hydrochlorothiazide combination therapy for the treatment of hypertension*. Curr Med Res Opin, 2010. **26**(4): p. 879-87.
106. Takahashi, T., et al., *[Effects of the combination of angiotensin receptor blockers and thiazide diuretics on laboratory values (levels of serum potassium, sodium, and uric acid)]*. Yakugaku Zasshi, 2014. **134**(6): p. 767-74.
107. Rhee, M.Y., et al., *Efficacy of fimasartan/hydrochlorothiazide combination in hypertensive patients inadequately controlled by fimasartan monotherapy*. Drug Des Devel Ther, 2015. **9**: p. 2847-54.
108. Shimosawa, T., et al., *Effectiveness of add-on low-dose diuretics in combination therapy for hypertension: losartan/hydrochlorothiazide vs. candesartan/amlodipine*. Hypertens Res, 2007. **30**(9): p. 831-7.
109. Fogari, R., et al., *Efficacy and tolerability of candesartan cilexetil/hydrochlorothiazide and amlodipine in patients with poorly controlled mild-to-moderate essential hypertension*. J Renin Angiotensin Aldosterone Syst, 2007. **8**(3): p. 139-44.
110. Triplitt, C.L., *Understanding the kidneys' role in blood glucose regulation*. Am J Manag Care, 2012. **18**(1 Suppl): p. S11-6.
111. Sano, R., Y. Shinozaki, and T. Ohta, *Sodium-glucose cotransporters: Functional properties and pharmaceutical potential*. J Diabetes Investig, 2020. **11**(4): p. 770-782.
112. Andrianesis, V. and J. Doupis, *The role of kidney in glucose homeostasis--SGLT2 inhibitors, a new approach in diabetes treatment*. Expert Rev Clin Pharmacol, 2013. **6**(5): p. 519-39.
113. Deshmukh, A.B., M.C. Patel, and B. Mishra, *SGLT2 inhibition: a novel prospective strategy in treatment of diabetes mellitus*. Ren Fail, 2013. **35**(4): p. 566-72.
114. Lee, P.C., S. Ganguly, and S.Y. Goh, *Weight loss associated with sodium-glucose cotransporter-2 inhibition: a review of evidence and underlying mechanisms*. Obes Rev, 2018. **19**(12): p. 1630-1641.
115. Maliha, G. and R.R. Townsend, *SGLT2 inhibitors: their potential reduction in blood pressure*. J Am Soc Hypertens, 2015. **9**(1): p. 48-53.
116. Salvatore, T., et al., *An Overview of the Cardiorenal Protective Mechanisms of*

- SGLT2 Inhibitors*. Int J Mol Sci, 2022. **23**(7).
117. Zhang, Y., et al., *Network meta-analysis on the effects of finerenone versus SGLT2 inhibitors and GLP-1 receptor agonists on cardiovascular and renal outcomes in patients with type 2 diabetes mellitus and chronic kidney disease*. Cardiovasc Diabetol, 2022. **21**(1): p. 232.
 118. Dhillon, S., *Dapagliflozin: A Review in Type 2 Diabetes*. Drugs, 2019. **79**(10): p. 1135-1146.
 119. Komoroski, B., et al., *Dapagliflozin, a novel, selective SGLT2 inhibitor; improved glycemc control over 2 weeks in patients with type 2 diabetes mellitus*. Clin Pharmacol Ther, 2009. **85**(5): p. 513-9.
 120. Bailey, C.J., et al., *Effect of dapagliflozin in patients with type 2 diabetes who have inadequate glycaemic control with metformin: a randomised, double-blind, placebo-controlled trial*. Lancet, 2010. **375**(9733): p. 2223-33.
 121. Chertow, G.M., et al., *Effects of Dapagliflozin in Stage 4 Chronic Kidney Disease*. J Am Soc Nephrol, 2021. **32**(9): p. 2352-2361.
 122. Saeed, M.A. and P. Narendran, *Dapagliflozin for the treatment of type 2 diabetes: a review of the literature*. Drug Des Devel Ther, 2014. **8**: p. 2493-505.
 123. Akinci, B., *Dapagliflozin and Cardiovascular Outcomes in Type 2 Diabetes*. N Engl J Med, 2019. **380**(19): p. 1881.
 124. Ye, Y., et al., *Dapagliflozin Attenuates Na(+)/H(+) Exchanger-1 in Cardiofibroblasts via AMPK Activation*. Cardiovasc Drugs Ther, 2018. **32**(6): p. 553-558.
 125. Lin, K., et al., *Direct cardio-protection of Dapagliflozin against obesity-related cardiomyopathy via NHE-1/MAPK signaling*. Acta Pharmacol Sin, 2022. **43**(10): p. 2624-2635.
 126. Slepkov, E. and L. Fliegel, *Structure and function of the NHE-1 isoform of the Na⁺/H⁺ exchanger*. Biochem Cell Biol, 2002. **80**(5): p. 499-508.
 127. Fliegel, L., *Regulation of the Na(+)/H(+) exchanger in the healthy and diseased myocardium*. Expert Opin Ther Targets, 2009. **13**(1): p. 55-68.
 128. Malo, M.E. and L. Fliegel, *Physiological role and regulation of the Na⁺/H⁺ exchanger*. Can J Physiol Pharmacol, 2006. **84**(11): p. 1081-95.
 129. LaPointe, M.S., et al., *Na⁺/H⁺ antiporter (NHE-1 isoform) in cultured vascular smooth muscle from the spontaneously hypertensive rat*. Kidney Int, 1995. **47**(1): p. 78-87.
 130. Garcandia, A., et al., *Enhanced Na(+)-H⁺ exchanger activity and NHE-1 mRNA expression in lymphocytes from patients with essential hypertension*. Hypertension, 1995. **25**(3): p. 356-64.
 131. Aviv, A., *The links between cellular Ca²⁺ and Na⁺/H⁺ exchange in the pathophysiology of essential hypertension*. Am J Hypertens, 1996. **9**(7): p. 703-7.
 132. Wu, D. and J.A. Kraut, *Potential role of NHE-1 (sodium-hydrogen exchanger 1) in the cellular dysfunction of lactic acidosis: implications for treatment*. Am J

- Kidney Dis, 2011. **57**(5): p. 781-7.
133. Parker, M.D., E.J. Myers, and J.R. Schelling, *Na⁺-H⁺ exchanger-1 (NHE-1) regulation in kidney proximal tubule*. Cell Mol Life Sci, 2015. **72**(11): p. 2061-74.
 134. Medina, A.J., et al., *Silencing of the Na⁽⁺⁾/H⁽⁺⁾ exchanger 1(NHE-1) prevents cardiac structural and functional remodeling induced by angiotensin II*. Exp Mol Pathol, 2019. **107**: p. 1-9.
 135. Holthouser, K.A., et al., *Ouabain stimulates Na-K-ATPase through a sodium/hydrogen exchanger-1 (NHE-1)-dependent mechanism in human kidney proximal tubule cells*. Am J Physiol Renal Physiol, 2010. **299**(1): p. F77-90.
 136. Singh, M. and A. Kumar, *Risks Associated with SGLT2 Inhibitors: An Overview*. Curr Drug Saf, 2018. **13**(2): p. 84-91.
 137. Sen, T., et al., *Effects of dapagliflozin on volume status and systemic haemodynamics in patients with chronic kidney disease without diabetes: Results from DAPASALT and DIAMOND*. Diabetes Obes Metab, 2022. **24**(8): p. 1578-1587.
 138. Shen, L., et al., *Dapagliflozin in HFrEF Patients Treated With Mineralocorticoid Receptor Antagonists: An Analysis of DAPA-HF*. JACC Heart Fail, 2021. **9**(4): p. 254-264.
 139. Fischmann, T.O., et al., *Structural characterization of nitric oxide synthase isoforms reveals striking active-site conservation*. Nat Struct Biol, 1999. **6**(3): p. 233-42.
 140. Kondo, K., et al., *Comparison of telmisartan/amlodipine and telmisartan/hydrochlorothiazide in the treatment of Japanese patients with uncontrolled hypertension: the TAT-Kobe study*. Blood Press Monit, 2016. **21**(3): p. 171-7.
 141. van Ruiten, C.C., et al., *Mechanisms underlying the blood pressure lowering effects of dapagliflozin, exenatide, and their combination in people with type 2 diabetes: a secondary analysis of a randomized trial*. Cardiovasc Diabetol, 2022. **21**(1): p. 63.
 142. Weber, M.A., et al., *Effects of dapagliflozin on blood pressure in hypertensive diabetic patients on renin-angiotensin system blockade*. Blood Press, 2016. **25**(2): p. 93-103.
 143. Mancia, G., et al., *Impact of Empagliflozin on Blood Pressure in Patients With Type 2 Diabetes Mellitus and Hypertension by Background Antihypertensive Medication*. Hypertension, 2016. **68**(6): p. 1355-1364.
 144. Lambers Heerspink, H.J., et al., *Dapagliflozin a glucose-regulating drug with diuretic properties in subjects with type 2 diabetes*. Diabetes Obes Metab, 2013. **15**(9): p. 853-62.
 145. Cherney, D.Z., et al., *Renal hemodynamic effect of sodium-glucose cotransporter 2 inhibition in patients with type 1 diabetes mellitus*. Circulation, 2014. **129**(5): p. 587-97.
 146. Papadopoulou, E., et al., *Dapagliflozin Does Not Affect Short-Term Blood*

- Pressure Variability in Patients With Type 2 Diabetes Mellitus*. Am J Hypertens, 2021. **34**(4): p. 404-413.
147. Cai, Y., W. Shi, and G. Xu, *The efficacy and safety of SGLT2 inhibitors combined with ACEI/ARBs in the treatment of type 2 diabetes mellitus: A meta-analysis of randomized controlled studies*. Expert Opin Drug Saf, 2020. **19**(11): p. 1497-1504.
 148. Shin, S.J., et al., *Effect of Sodium-Glucose Co-Transporter 2 Inhibitor, Dapagliflozin, on Renal Renin-Angiotensin System in an Animal Model of Type 2 Diabetes*. PLoS One, 2016. **11**(11): p. e0165703.
 149. Santos, E.L., et al., *Mutagenesis of the AT1 receptor reveals different binding modes of angiotensin II and [Sar1]-angiotensin II*. Regul Pept, 2004. **119**(3): p. 183-8.
 150. Gruber, S. and F. Beuschlein, *Hypokalemia and the Prevalence of Primary Aldosteronism*. Horm Metab Res, 2020. **52**(6): p. 347-356.
 151. Kramers, B.J., et al., *Effects of Hydrochlorothiazide and Metformin on Aquaresis and Nephroprotection by a Vasopressin V2 Receptor Antagonist in ADPKD: A Randomized Crossover Trial*. Clin J Am Soc Nephrol, 2022. **17**(4): p. 507-517.
 152. Kennedy, G.C., E. Skadhauge, and P. Hague, *THE EFFECT OF HYDROCHLOROTHIAZIDE ON WATER INTAKE AND PLASMA OSMOLALITY IN DIABETES INSIPIDUS IN THE RAT*. Q J Exp Physiol Cogn Med Sci, 1964. **49**: p. 417-23.
 153. Masuda, T., et al., *Unmasking a sustained negative effect of SGLT2 inhibition on body fluid volume in the rat*. Am J Physiol Renal Physiol, 2018. **315**(3): p. F653-f664.
 154. Verma, S. and J.J.V. McMurray, *SGLT2 inhibitors and mechanisms of cardiovascular benefit: a state-of-the-art review*. Diabetologia, 2018. **61**(10): p. 2108-2117.
 155. Chen, L., et al., *Effect of Dapagliflozin Treatment on Fluid and Electrolyte Balance in Diabetic Rats*. Am J Med Sci, 2016. **352**(5): p. 517-523.
 156. Yerino, G.A., et al., *Pharmacokinetics of a new fixed-dose combination of candesartan cilexetil, hydrochlorothiazide, and rosuvastatin in healthy adult subjects*. Int J Clin Pharmacol Ther, 2022. **60**(4): p. 192-206.
 157. Vitovec, J. and J. Sliva, *[A fixed dose combination of telmisartan, and a thiazide diuretic in the treatment of hypertension]*. Vnitr Lek, 2013. **59**(5): p. 397-401.
 158. Wang, X.N., et al., *Evaluation of influence of telmisartan on the pharmacokinetics and tissue distribution of canagliflozin in rats and mice*. Ann Palliat Med, 2021. **10**(3): p. 3086-3096.
 159. Tsopelas, F., C. Giaginis, and A. Tsantili-Kakoulidou, *Lipophilicity and biomimetic properties to support drug discovery*. Expert Opin Drug Discov, 2017. **12**(9): p. 885-896.
 160. Trbojevic, J., et al., *Relationship between the bioavailability and molecular properties of angiotensin ii receptor antagonists*. Archives of Biological Sciences, 2016.

161. Angeli, F., et al., *PK/PD evaluation of fimasartan for the treatment of hypertension Current evidences and future perspectives*. Expert Opin Drug Metab Toxicol, 2018. **14**(5): p. 533-541.
162. Gupta, S.P., *Quantitative structure-activity relationships of antihypertensive agents*. Prog Drug Res, 1999. **53**: p. 53-87.
163. Cappetta, D., et al., *Amelioration of diastolic dysfunction by dapagliflozin in a non-diabetic model involves coronary endothelium*. Pharmacol Res, 2020. **157**: p. 104781.
164. Zhang, N., et al., *Dapagliflozin improves left ventricular remodeling and aorta sympathetic tone in a pig model of heart failure with preserved ejection fraction*. Cardiovasc Diabetol, 2019. **18**(1): p. 107.
165. Giacco, F. and M. Brownlee, *Oxidative stress and diabetic complications*. Circ Res, 2010. **107**(9): p. 1058-70.
166. Devaraj, S., M.R. Dasu, and I. Jialal, *Diabetes is a proinflammatory state: a translational perspective*. Expert Rev Endocrinol Metab, 2010. **5**(1): p. 19-28.
167. Yan, L.J., *Redox imbalance stress in diabetes mellitus: Role of the polyol pathway*. Animal Model Exp Med, 2018. **1**(1): p. 7-13.
168. Martinez-Quinones, P., et al., *Hypertension Induced Morphological and Physiological Changes in Cells of the Arterial Wall*. Am J Hypertens, 2018. **31**(10): p. 1067-1078.
169. Humphrey, J.D., *Mechanisms of Vascular Remodeling in Hypertension*. Am J Hypertens, 2021. **34**(5): p. 432-441.
170. Giles, T.D., et al., *Impaired Vasodilation in the Pathogenesis of Hypertension: Focus on Nitric Oxide, Endothelial-Derived Hyperpolarizing Factors, and Prostaglandins*. The Journal of Clinical Hypertension, 2012. **14**(4): p. 198-205.
171. Sena, C.M., et al., *Methylglyoxal promotes oxidative stress and endothelial dysfunction*. Pharmacol Res, 2012. **65**(5): p. 497-506.
172. Gallo, G., M. Volpe, and C. Savoia, *Endothelial Dysfunction in Hypertension: Current Concepts and Clinical Implications*. Front Med (Lausanne), 2021. **8**: p. 798958.
173. Zoccali, C., et al., *Uric acid and endothelial dysfunction in essential hypertension*. J Am Soc Nephrol, 2006. **17**(5): p. 1466-71.
174. Ferner, R.E., et al., *The effects of intradermal bradykinin are potentiated by angiotensin converting enzyme inhibitors in hypertensive patients*. Br J Clin Pharmacol, 1989. **27**(3): p. 337-42.
175. Sposito, A.C., et al., *Dapagliflozin effect on endothelial dysfunction in diabetic patients with atherosclerotic disease: a randomized active-controlled trial*. Cardiovasc Diabetol, 2021. **20**(1): p. 74.
176. Zhi-ping, L., *The change of peripheral vascular function in patients with hypertension and the effect of candesartan intervention*. Medical Journal of Chinese People's Health, 2010.
177. Kim, I., C.S. Park, and H.Y. Lee, *Angiotensin II Type 1 Receptor Blocker*,

- Fimasartan, Reduces Vascular Smooth Muscle Cell Senescence by Inhibiting the CYR61 Signaling Pathway.* Korean Circ J, 2019. **49**(7): p. 615-626.
178. Mollnau, H., et al., *Effects of telmisartan or amlodipine monotherapy versus telmisartan/amlodipine combination therapy on vascular dysfunction and oxidative stress in diabetic rats.* Naunyn Schmiedebergs Arch Pharmacol, 2013. **386**(5): p. 405-19.
 179. Kagota, S., et al., *Telmisartan provides protection against development of impaired vasodilation independently of metabolic effects in SHRSP.Z-Lepr(fa)/IzmDmcr rats with metabolic syndrome.* Can J Physiol Pharmacol, 2011. **89**(5): p. 355-64.
 180. Nakagiri, A., et al., *Evidence for the involvement of NADPH oxidase in ischemia/reperfusion-induced gastric damage via angiotensin II.* J Physiol Pharmacol, 2010. **61**(2): p. 171-9.
 181. Takai, S., et al., *Candesartan and amlodipine combination therapy provides powerful vascular protection in stroke-prone spontaneously hypertensive rats.* Hypertens Res, 2011. **34**(2): p. 245-52.
 182. Sato-Horiguchi, C., et al., *Telmisartan attenuates diabetic nephropathy by suppressing oxidative stress in db/db mice.* Nephron Exp Nephrol, 2012. **121**(3-4): p. e97-e108.
 183. Ko, S.F., et al., *Combined therapy with dapagliflozin and entresto offers an additional benefit on improving the heart function in rat after ischemia-reperfusion injury.* Biomed J, 2022. **46**(3): p. 100546.
 184. Hejazian, S.M., et al., *Nrf-2 as a therapeutic target in acute kidney injury.* Life Sci, 2021. **264**: p. 118581.
 185. Huang, C.Y., et al., *Attenuation of Lipopolysaccharide-Induced Acute Lung Injury by Hispolon in Mice, Through Regulating the TLR4/PI3K/Akt/mTOR and Keap1/Nrf2/HO-1 Pathways, and Suppressing Oxidative Stress-Mediated ER Stress-Induced Apoptosis and Autophagy.* Nutrients, 2020. **12**(6).
 186. Adoga, J.O., M.L. Channa, and A. Nadar, *Type-2 diabetic rat heart: The effect of kolaviron on mTOR-1, P70S60K, PKC- α , NF- κ B, SOD-2, NRF-2, eNOS, AKT-1, ACE, and P38 MAPK gene expression profile.* Biomed Pharmacother, 2022. **148**: p. 112736.
 187. Nordgren, K.K. and K.B. Wallace, *Keap1 redox-dependent regulation of doxorubicin-induced oxidative stress response in cardiac myoblasts.* Toxicol Appl Pharmacol, 2014. **274**(1): p. 107-16.
 188. Wu, J., et al., *The role of oxidative stress and inflammation in cardiovascular aging.* Biomed Res Int, 2014. **2014**: p. 615312.
 189. Arab, H.H., M.Y. Al-Shorbagy, and M.A. Saad, *Activation of autophagy and suppression of apoptosis by dapagliflozin attenuates experimental inflammatory bowel disease in rats: Targeting AMPK/mTOR, HMGB1/RAGE and Nrf2/HO-1 pathways.* Chem Biol Interact, 2021. **335**: p. 109368.
 190. Kim, S., et al., *Fimasartan, a Novel Angiotensin-Receptor Blocker, Protects against Renal Inflammation and Fibrosis in Mice with Unilateral Ureteral*

- Obstruction: the Possible Role of Nrf2*. Int J Med Sci, 2015. **12**(11): p. 891-904.
191. Kabel, A.M. and S.A. Salama, *Effect of taxifolin/dapagliflozin combination on colistin-induced nephrotoxicity in rats*. Hum Exp Toxicol, 2021. **40**(10): p. 1767-1780.
 192. Nathan, C. and A. Ding, *Nonresolving inflammation*. Cell, 2010. **140**(6): p. 871-82.
 193. Xia, F., et al., *Luteolin protects HUVECs from TNF- α -induced oxidative stress and inflammation via its effects on the Nox4/ROS-NF- κ B and MAPK pathways*. J Atheroscler Thromb, 2014. **21**(8): p. 768-83.
 194. Vallega, K.A., et al., *Macrophage-Conditioned Media Promotes Adipocyte Cancer Association, Which in Turn Stimulates Breast Cancer Proliferation and Migration*. Biomolecules, 2022. **12**(12).
 195. Dos Santos, T.C., et al., *Effect of Photobiomodulation on C2C12 Myoblasts Cultivated in M1 Macrophage-conditioned Media*. Photochem Photobiol, 2020. **96**(4): p. 906-916.
 196. Toba, H., et al., *Telmisartan inhibits vascular dysfunction and inflammation via activation of peroxisome proliferator-activated receptor-gamma in subtotal nephrectomized rat*. Eur J Pharmacol, 2012. **685**(1-3): p. 91-8.
 197. Dohi, Y., et al., *Candesartan reduces oxidative stress and inflammation in patients with essential hypertension*. Hypertens Res, 2003. **26**(9): p. 691-7.
 198. Cho, J.H., et al., *Fimasartan attenuates renal ischemia-reperfusion injury by modulating inflammation-related apoptosis*. Korean J Physiol Pharmacol, 2018. **22**(6): p. 661-670.
 199. Liu, Z., et al., *Impact of sodium glucose cotransporter 2 (SGLT2) inhibitors on atherosclerosis: from pharmacology to pre-clinical and clinical therapeutics*. Theranostics, 2021. **11**(9): p. 4502-4515.
 200. Gaspari, T., et al., *Dapagliflozin attenuates human vascular endothelial cell activation and induces vasorelaxation: A potential mechanism for inhibition of atherogenesis*. Diab Vasc Dis Res, 2018. **15**(1): p. 64-73.
 201. Qiang, L., *Effect of telmisartan on plasma levels of inflammatory cytokine in unstable angina patients complicated with diabetes mellitus and hypertensive after percutaneous coronary intervention*. Chinese Journal of Rehabilitation Theory and Practice, 2005.
 202. Ren-quan, Z., *The effects of telmisartan on serum cytokine levels and left ventricular function in patients with chronic heart failure*. Hainan Medical Journal, 2008.
 203. Song, K.H., et al., *Telmisartan attenuates hyperglycemia-exacerbated VCAM-1 expression and monocytes adhesion in TNF α -stimulated endothelial cells by inhibiting IKK β expression*. Vascul Pharmacol, 2016. **78**: p. 43-52.
 204. Kim, J.H., et al., *Fimasartan reduces neointimal formation and inflammation after carotid arterial injury in apolipoprotein E knockout mice*. Mol Med, 2019. **25**(1): p. 33.

205. Jang, Y.N., et al., *Fimasartan Ameliorates Deteriorations in Glucose Metabolism in a High Glucose State by Regulating Skeletal Muscle and Liver Cells*. Yonsei Med J, 2022. **63**(6): p. 530-538.
206. Ryu, S., et al., *Fimasartan, anti-hypertension drug, suppressed inducible nitric oxide synthase expressions via nuclear factor-kappa B and activator protein-1 inactivation*. Biol Pharm Bull, 2013. **36**(3): p. 467-74.
207. Rosei, E.A., et al., *Effects of candesartan cilexetil and enalapril on inflammatory markers of atherosclerosis in hypertensive patients with non-insulin-dependent diabetes mellitus*. J Hypertens, 2005. **23**(2): p. 435-44.
208. Kimura, H., et al., *Telmisartan, a possible PPAR- δ agonist, reduces TNF- α -stimulated VEGF-C production by inhibiting the p38MAPK/HSP27 pathway in human proximal renal tubular cells*. Biochem Biophys Res Commun, 2014. **454**(2): p. 320-7.
209. Ahmed, H.I. and E.A. Mohamed, *Candesartan and epigallocatechin-3-gallate ameliorate gentamicin-induced renal damage in rats through p38-MAPK and NF- κ B pathways*. Journal of Biochemical and Molecular Toxicology, 2019. **33**(3): p. e22254.
210. Montezano, A.C., et al., *Angiotensin II and vascular injury*. Curr Hypertens Rep, 2014. **16**(6): p. 431.
211. Hernandez, G.E. and M.L. Iruela-Arispe, *The many flavors of monocyte/macrophage--endothelial cell interactions*. Curr Opin Hematol, 2020. **27**(3): p. 181-189.
212. Helmke, A., et al., *Endothelial-to-mesenchymal transition shapes the atherosclerotic plaque and modulates macrophage function*. Faseb j, 2019. **33**(2): p. 2278-2289.
213. Abdollahi, E., et al., *Dapagliflozin exerts anti-inflammatory effects via inhibition of LPS-induced TLR-4 overexpression and NF-kappaB activation in human endothelial cells and differentiated macrophages*. Eur J Pharmacol, 2022. **918**: p. 174715.
214. Xiong, S., et al., *The effect of dapagliflozin on myocardial ischemia-reperfusion injury in diabetic rats*. Can J Physiol Pharmacol, 2023. **101**(2): p. 80-89.
215. Pang, T., et al., *Telmisartan directly ameliorates the neuronal inflammatory response to IL-1 β partly through the JNK/c-Jun and NADPH oxidase pathways*. J Neuroinflammation, 2012. **9**: p. 102.
216. Yang, X.L., et al., *Anti-inflammatory effects of fimasartan via Akt, ERK, and NF κ B pathways on astrocytes stimulated by hemolysate*. Inflamm Res, 2016. **65**(2): p. 115-23.
217. Theofilis, P., et al., *Inflammatory Mechanisms Contributing to Endothelial Dysfunction*. Biomedicines, 2021. **9**(7).
218. Yu, Y.-W., et al., *Sodium-Glucose Co-transporter-2 Inhibitor of Dapagliflozin Attenuates Myocardial Ischemia/Reperfusion Injury by Limiting NLRP3 Inflammasome Activation and Modulating Autophagy*. Frontiers in Cardiovascular Medicine, 2022. **8**.

219. Faridvand, Y., et al., *Dapagliflozin attenuates high glucose-induced endothelial cell apoptosis and inflammation through AMPK/SIRT1 activation*. Clin Exp Pharmacol Physiol, 2022. **49**(6): p. 643-651.
220. Lin, D. and Y. Song, *Dapagliflozin Presented Nonalcoholic Fatty Liver Through Metabolite Extraction and AMPK/NLRP3 Signaling Pathway*. Horm Metab Res, 2023. **55**(1): p. 75-84.
221. Lin, W.Y., et al., *Repositioning of the Angiotensin II Receptor Antagonist Candesartan as an Anti-Inflammatory Agent With NLRP3 Inflammasome Inhibitory Activity*. Front Immunol, 2022. **13**: p. 870627.
222. Liu, W., et al., *Protective effect of telmisartan on neurovascular unit and inflammasome in stroke-resistant spontaneously hypertensive rats*. Neurol Res, 2015. **37**(6): p. 491-501.
223. Kwon, H.S., et al., *Telmisartan Inhibits the NLRP3 Inflammasome by Activating the PI3K Pathway in Neural Stem Cells Injured by Oxygen-Glucose Deprivation*. Mol Neurobiol, 2021. **58**(4): p. 1806-1818.
224. Yang, X., et al., *Pretreatment with low-dose fimasartan ameliorates NLRP3 inflammasome-mediated neuroinflammation and brain injury after intracerebral hemorrhage*. Exp Neurol, 2018. **310**: p. 22-32.
225. Eskelinen, E.L. and P. Saftig, *Autophagy: a lysosomal degradation pathway with a central role in health and disease*. Biochim Biophys Acta, 2009. **1793**(4): p. 664-73.
226. Salazar, G., et al., *SQSTM1/p62 and PPARGC1A/PGC-1alpha at the interface of autophagy and vascular senescence*. Autophagy, 2020. **16**(6): p. 1092-1110.
227. Zhang, X.B., et al., *Telmisartan attenuates kidney apoptosis and autophagy-related protein expression levels in an intermittent hypoxia mouse model*. Sleep Breath, 2019. **23**(1): p. 341-348.
228. Mondaca-Ruff, D., et al., *Angiotensin II-Regulated Autophagy Is Required for Vascular Smooth Muscle Cell Hypertrophy*. Front Pharmacol, 2018. **9**: p. 1553.
229. Zhou, L., B. Ma, and X. Han, *The role of autophagy in angiotensin II-induced pathological cardiac hypertrophy*. J Mol Endocrinol, 2016. **57**(4): p. R143-R152.
230. Qian, M., X. Fang, and X. Wang, *Autophagy and inflammation*. Clin Transl Med, 2017. **6**(1): p. 24.
231. Rasheduzzaman, M. and S.Y. Park, *Antihypertensive drug-candesartan attenuates TRAIL resistance in human lung cancer via AMPK-mediated inhibition of autophagy flux*. Exp Cell Res, 2018. **368**(1): p. 126-135.
232. Li, L., et al., *Dapagliflozin Alleviates Hepatic Steatosis by Restoring Autophagy via the AMPK-mTOR Pathway*. Front Pharmacol, 2021. **12**: p. 589273.
233. Jaikumkao, K., et al., *Dapagliflozin ameliorates pancreatic injury and activates kidney autophagy by modulating the AMPK/mTOR signaling pathway in obese rats*. J Cell Physiol, 2021. **236**(9): p. 6424-6440.
234. O'Neill, H.M., *AMPK and Exercise: Glucose Uptake and Insulin Sensitivity*. Diabetes Metab J, 2013. **37**(1): p. 1-21.

235. Matzinger, M., et al., *AMPK leads to phosphorylation of the transcription factor Nrf2, tuning transactivation of selected target genes*. Redox Biol, 2020. **29**: p. 101393.
236. Gong, H., et al., *Nrf2-SHP Cascade-Mediated STAT3 Inactivation Contributes to AMPK-Driven Protection Against Endotoxic Inflammation*. Front Immunol, 2020. **11**: p. 414.
237. Salminen, A., J.M. Hyttinen, and K. Kaarniranta, *AMP-activated protein kinase inhibits NF-kappaB signaling and inflammation: impact on healthspan and lifespan*. J Mol Med (Berl), 2011. **89**(7): p. 667-76.
238. Ding, J., et al., *Structural and functional characterization of transmembrane segment VII of the Na⁺/H⁺ exchanger isoform 1*. J Biol Chem, 2006. **281**(40): p. 29817-29.
239. Hill, J., D.M. Gothard, and M.M. McLean, *Prehospital Blood Glucose Testing as a Predictor of Impending Hypotension in Adult Trauma Patients*. Air Med J, 2020. **39**(1): p. 20-23.
240. Moore, M.J., et al., *Predictors for glucose change in hypertensive participants following short-term treatment with atenolol or hydrochlorothiazide*. Pharmacotherapy, 2014. **34**(11): p. 1132-40.
241. Gillespie, E.L., et al., *The impact of ACE inhibitors or angiotensin II type 1 receptor blockers on the development of new-onset type 2 diabetes*. Diabetes Care, 2005. **28**(9): p. 2261-6.
242. Lindholm, L.H., B. Carlberg, and O. Samuelsson, *Should beta blockers remain first choice in the treatment of primary hypertension? A meta-analysis*. Lancet, 2005. **366**(9496): p. 1545-53.
243. Huen, S.C. and D.S. Goldfarb, *Adverse metabolic side effects of thiazides: implications for patients with calcium nephrolithiasis*. J Urol, 2007. **177**(4): p. 1238-43.
244. Roumie, C.L., et al., *Blood Pressure Control and the Association With Diabetes Mellitus Incidence: Results From SPRINT Randomized Trial*. Hypertension, 2020. **75**(2): p. 331-338.
245. Furukawa, H., et al., *Telmisartan increases localization of glucose transporter 4 to the plasma membrane and increases glucose uptake via peroxisome proliferator-activated receptor γ in 3T3-L1 adipocytes*. Eur J Pharmacol, 2011. **660**(2-3): p. 485-91.
246. Lee, C.J., et al., *Effects of high-intensity statin combined with telmisartan versus amlodipine on glucose metabolism in hypertensive atherosclerotic cardiovascular disease patients with impaired fasting glucose: A randomized multicenter trial*. Medicine (Baltimore), 2022. **101**(36): p. e30496.
247. Liu, T., et al., *Telmisartan Potentiates Insulin Secretion via Ion Channels, Independent of the AT1 Receptor and PPARgamma*. Front Pharmacol, 2021. **12**: p. 739637.
248. Ayza, M.A., et al., *Anti-Diabetic Effect of Telmisartan Through its Partial PPARgamma-Agonistic Activity*. Diabetes Metab Syndr Obes, 2020. **13**: p. 3627-

3635.

249. Tojo, A., et al., *Angiotensin receptor blocker telmisartan suppresses renal gluconeogenesis during starvation*. *Diabetes Metab Syndr Obes*, 2015. **8**: p. 103-13.
250. Lee, Y.J. and H.J. Han, *Troglitazone ameliorates high glucose-induced EMT and dysfunction of SGLTs through PI3K/Akt, GSK-3 β , Snail1, and β -catenin in renal proximal tubule cells*. *Am J Physiol Renal Physiol*, 2010. **298**(5): p. F1263-75.
251. Kim, M., et al., *The effect of PPAR γ agonist on SGLT2 and glucagon expressions in alpha cells under hyperglycemia*. *J Endocrinol Invest*, 2017. **40**(10): p. 1069-1076.
252. Zeng, S., et al., *142-LB: Very Low Dose SGLT2 Inhibition Is as Effective as Angiotensin II Receptor Blockage for Cardiac and Renal Fibrosis in High Salt 5/6 Nephrectomized Rats*. *Diabetes*, 2020. **69**(Supplement_1).
253. Biemesderfer, D., et al., *Immunocytochemical characterization of Na(+)-H+ exchanger isoform NHE-1 in rabbit kidney*. *Am J Physiol*, 1992. **263**(5 Pt 2): p. F833-40.
254. Liu, C.L., et al., *Na(+)-H(+) exchanger 1 determines atherosclerotic lesion acidification and promotes atherogenesis*. *Nat Commun*, 2019. **10**(1): p. 3978.
255. Mraiche, F., et al., *Activated NHE-1 is required to induce early cardiac hypertrophy in mice*. *Basic Res Cardiol*, 2011. **106**(4): p. 603-16.
256. Wu, K.L., et al., *Renal tubular epithelial cell apoptosis is associated with caspase cleavage of the NHE-1 Na+/H+ exchanger*. *Am J Physiol Renal Physiol*, 2003. **284**(4): p. F829-39.
257. Yamashita, J., et al., *Role of Na+/H+ exchanger in the pathogenesis of ischemic acute renal failure in mice*. *J Cardiovasc Pharmacol*, 2007. **49**(3): p. 154-60.
258. Wu, K.L., et al., *The NHE-1 Na+/H+ exchanger recruits ezrin/radixin/moesin proteins to regulate Akt-dependent cell survival*. *J Biol Chem*, 2004. **279**(25): p. 26280-6.
259. Morahan, G., et al., *Genetic and physiological association of diabetes susceptibility with raised Na+/H+ exchange activity*. *Proc Natl Acad Sci U S A*, 1994. **91**(13): p. 5898-902.
260. Okuda, S., et al., *Increased expression of Na+/H+ exchanger in the injured renal tissues of focal glomerulosclerosis in rats*. *Kidney Int*, 1994. **46**(6): p. 1635-43.
261. Zhang, M., et al., *Aldosterone promotes fibronectin synthesis in rat mesangial cells via ERK1/2-stimulated Na-H+ exchanger isoform 1*. *Am J Nephrol*, 2010. **31**(1): p. 75-82.
262. Zhang, M., et al., *The role of Na+-H+ exchanger isoform 1 in aldosterone-induced glomerulosclerosis in vivo*. *Ren Fail*, 2009. **31**(8): p. 726-35.
263. Yan, P., B. Ke, and X. Fang, *Ion channels as a therapeutic target for renal fibrosis*. *Front Physiol*, 2022. **13**: p. 1019028.
264. Morigiwa, K. and N. Vardi, *Differential expression of ionotropic glutamate receptor subunits in the outer retina*. *J Comp Neurol*, 1999. **405**(2): p. 173-84.

265. van der Aart-van der Beek, A.B., et al., *Evaluation of the Pharmacokinetics and Exposure-Response Relationship of Dapagliflozin in Patients without Diabetes and with Chronic Kidney Disease*. Clin Pharmacokinet, 2021. **60**(4): p. 517-525.
266. Cherney, D.Z.I., et al., *Effects of the SGLT2 inhibitor dapagliflozin on proteinuria in non-diabetic patients with chronic kidney disease (DIAMOND): a randomised, double-blind, crossover trial*. Lancet Diabetes Endocrinol, 2020. **8**(7): p. 582-593.
267. Cassis, P., et al., *SGLT2 inhibitor dapagliflozin limits podocyte damage in proteinuric nondiabetic nephropathy*. JCI Insight, 2018. **3**(15).
268. Kinguchi, S., et al., *Relationship between basal sodium intake and the effects of dapagliflozin in albuminuric diabetic kidney disease*. Sci Rep, 2021. **11**(1): p. 951.
269. Abd, M.R. and A.F. Hassan, *The Ameliorative Effect of Fimasartan against Methotrexate-Induced Nephrotoxicity in Rats*. Iraqi Journal of Pharmaceutical Sciences (P-ISSN 1683-3597 E-ISSN 2521-3512), 2022. **31**(1): p. 87-94.
270. Park, J.B., et al., *Gender-specific differences in the incidence of microalbuminuria in metabolic syndrome patients after treatment with fimasartan: The K-MetS study*. PLoS One, 2017. **12**(12): p. e0189342.
271. Fandinata, S.S., et al., *Monitoring Kidney Function Through the Use of Candesartan, Telmisartan or Valsartan Antihypertensive Therapy towards Patients CKD*. Media Kesehatan Masyarakat Indonesia, 2022. **18**(1): p. 1-9.
272. Yoo, T.H., et al., *The FimAsartaN proTeinuriA SusTaIned reduCtion in comparison with losartan in diabetic chronic kidney disease (FANTASTIC) trial*. Hypertens Res, 2022. **45**(12): p. 2008-2017.
273. Zou, H., B. Zhou, and G. Xu, *SGLT2 inhibitors: a novel choice for the combination therapy in diabetic kidney disease*. Cardiovasc Diabetol, 2017. **16**(1): p. 65.
274. Cingolani, O.H., et al., *In vivo key role of reactive oxygen species and NHE-1 activation in determining excessive cardiac hypertrophy*. Pflugers Arch, 2011. **462**(5): p. 733-43.
275. Thieme, K., et al., *The effect of angiotensin II on intracellular pH is mediated by AT(1) receptor translocation*. Am J Physiol Cell Physiol, 2008. **295**(1): p. C138-45.
276. Vart, P., et al., *Estimated Lifetime Benefit of Combined RAAS and SGLT2 Inhibitor Therapy in Patients with Albuminuric CKD without Diabetes*. Clin J Am Soc Nephrol, 2022. **17**(12): p. 1754-1762.
277. Liu, C.L., et al., *Reduced NHE-1 (Na(+)-H(+)) Exchanger-1) Function Protects ApoE-Deficient Mice From Ang II (Angiotensin II)-Induced Abdominal Aortic Aneurysms*. Hypertension, 2020. **76**(1): p. 87-100.
278. Wang, S.X., et al., *Cariporide inhibits high glucose-mediated adhesion of monocyte-endothelial cell and expression of intercellular adhesion molecule-1*. Life Sci, 2006. **79**(14): p. 1399-404.
279. Wang, S., et al., *Na⁺/H⁺ exchanger is required for hyperglycaemia-induced*

- endothelial dysfunction via calcium-dependent calpain*. Cardiovasc Res, 2008. **80**(2): p. 255-62.
280. Chen, S., et al., *Direct cardiac effects of SGLT2 inhibitors*. Cardiovasc Diabetol, 2022. **21**(1): p. 45.
281. Arow, M., et al., *Sodium-glucose cotransporter 2 inhibitor Dapagliflozin attenuates diabetic cardiomyopathy*. Cardiovasc Diabetol, 2020. **19**(1): p. 7.
282. Solomon, S.D., et al., *Effect of Dapagliflozin in Patients With HFrEF Treated With Sacubitril/Valsartan: The DAPA-HF Trial*. JACC Heart Fail, 2020. **8**(10): p. 811-818.
283. Song, J., et al., *Increased renal ENaC subunit and sodium transporter abundances in streptozotocin-induced type 1 diabetes*. Am J Physiol Renal Physiol, 2003. **285**(6): p. F1125-37.
284. Al-Shamasi, A.A., et al., *Crosstalk between Sodium-Glucose Cotransporter Inhibitors and Sodium-Hydrogen Exchanger 1 and 3 in Cardiometabolic Diseases*. Int J Mol Sci, 2021. **22**(23).
285. Gajjar, K. and P. Luthra, *Euglycemic Diabetic Ketoacidosis in the Setting of SGLT2 Inhibitor Use and Hypertriglyceridemia: A Case Report and Review of Literature*. Cureus, 2019. **11**(4): p. e4384.
286. Iwanaga, T., et al., *Concentration-dependent mode of interaction of angiotensin II receptor blockers with uric acid transporter*. J Pharmacol Exp Ther, 2007. **320**(1): p. 211-7.
287. Li, Y., et al., *Effects of angiotensin II receptor blockers on renal handling of uric acid in rats*. Drug Metab Pharmacokinet, 2008. **23**(4): p. 263-70.
288. Krapf, R., et al., *Expression of rat renal Na/H antiporter mRNA levels in response to respiratory and metabolic acidosis*. J Clin Invest, 1991. **87**(2): p. 747-51.
289. Zhao, Y., et al., *Type 2 diabetic mice enter a state of spontaneous hibernation-like suspended animation following accumulation of uric acid*. J Biol Chem, 2021. **297**(4): p. 101166.
290. Cho, J.H., et al., *Aldosterone stimulates intestinal Na⁺ absorption in rats by increasing NHE3 expression of the proximal colon*. Am J Physiol, 1998. **274**(3): p. C586-94.

국문 초록

Angiotensin Receptor Blocker와 Dapagliflozin이 혈압 조절, 혈관 및 신장 기능에 미치는 영향

전 윤 아

제주대학교 대학원 수의학과

고혈압과 당뇨병은 다양한 합병증을 공유할 뿐 아니라 흔히 공존하는 만성 질환이다. 중증도에 따라 많은 경우에 단독 요법으로 목표 혈압과 혈당에 도달하지 못하고 있으며, 이를 보완하고자 다양한 병용요법이 시도되고 있다. 그럼에도 여전히 포도당 대사 장애 및 이온 불균형과 같은 약물 부작용, 혈당과 혈압의 조절에도 개선되지 않는 혈관 및 신장의 기능 부전 등이 해결되지 않은 문제로 잔존하고 있다. 이러한 이유로, 새로운 병용 약물로서 Angiotensin Receptor Blocker (ARB)와 Sodium-Glucose Cotransporter 2 (SGLT2) 억제제의 가능성을 알아보려고 하였다. 두 약물은 모두 우수한 항염 및 신장 보호 효과를 갖는 것으로 알려져 있을 뿐 아니라 ARB에 의해 유발될 수 있는 포도당 불균형 및 SGLT2 억제에 의해 유발될 수 있는 Renin-Angiotensin-Aldosterone System 활성화에 대한 상호 보완적 기능을 할 수 있을 것으로 기대된다. 따라

서 본 연구에서는 dapagliflozin과 fimasartan, telmisartan, 그리고 candesartan의 복합투여가 혈압 및 혈당 강하, 혈관과 신장 기능에 미치는 영향을 알아보고자 하였다. 본태성 고혈압 쥐(SHR)에 약물을 단기간 동안 투여하며 혈압, 혈관 기능, 혈당, 그리고 NHE-1 및 요 단백을 신장 손상 지표로서 측정하였다. 또한 혈관 기능 개선의 기전을 규명하기 위해 저 등급 염증에 노출된 EA.hy926 세포와 고령의 SHR의 대동맥에서 산화 스트레스, 염증, 그리고 자가 포식과 관련된 단백질의 발현을 평가했다. 실험 결과, dapagliflozin은 fimasartan과 telmisartan에 의한 혈압조절을 강화하여 추가적으로 혈압을 감소시키고 유지기간을 연장시켰다. Telmisartan은 또한 SGLT2의 공동 억제를 통해 포도당과 나트륨 배설에 dapagliflozin과 상승 효과를 나타냈으나, 신장 손상 지표는 telmisartan 단독군에 비해 증가되었다. Fimasartan과 candesartan은 대동맥의 내피 의존적 이완 반응을 개선했고, 그 기전은 산화스트레스와 염증의 감소, 그리고 자가 포식의 활성화로 확인되었다. 또한 fimasartan과 candesartan은 NHE-1과 단백뇨를 모두 감소시켰고, 이러한 효능은 dapagliflozin에 의해 증진되었다. 요약하면, telmisartan과 dapagliflozin은 혈압과 혈당, 그리고 나트륨의 감소에 상승 효과를 나타냈지만 SGLT2 억제라는 공동 기전을 가지는 바, 신장 부하 등의 잠재적인 부작용에 유의해야 할 것으로 판단되었다. Candesartan과 dapagliflozin은 혈관 및 신장 보호에 상승 효과를 보였으나 혈압 조절에 대한 유의미한 상호작용은 나타나지 않았다. 한편 fimasartan과 dapagliflozin은 혈압 감소, 혈관 및 신장 보호 모두에서 부분적인 상승효과를 보인 바, 가장 적합한 조합으로 판단되었다. 그러나 본 연구는 단기간동안 수행된 전임상 시험이므로, 실제 환자에서의 두 약물의 상호 작용 및 장기간 투여에 따른 잠재적인 부작용

에 대한 명확한 이해를 위해서는 추가적인 실험이 요구된다. 그럼에도 불구하고 ARB와 SGLT2 억제제는 환자 개인의 특성에 따라 다양한 조합으로 사용될 수 있으며, 혈압과 혈당 외에도 혈관 및 신장에 강력한 보호 효능을 갖는 새로운 조합 약물로서 유망할 것으로 사료된다.